Engineering of Inhalation Aerosols Combining Theophylline and Budesonide

C. Chen

PHD

2014

Engineering of Inhalation Aerosols Combining Theophylline and Budesonide

Chi CHEN

Submitted for the Degree of

Doctor of Philosophy

Faculty of Life Science

University of Bradford

2014

Abstract

Engineering of Inhalation Aerosols Combining Theophylline and Budesonide

Chi Chen

Keywords: inhalation, combination particles, inhalable theophylline, budesonide, particle engineering, experimental design.

In asthma therapy, the use of theophylline to prevent bronchial spasm and glucocorticoids to decrease inflammation is widely indicated. Apart from the acute asthma attack oral theophylline is treated for chronic therapy in order to minimize inflammation and to enhance the efficiency of corticosteroids and recover steroids' anti-inflammatory actions in COPD treatment. The preferred application route for respiratory disease treatment is by inhalation, such as dry powder inhalers (DPI) being the delivery systems of first choice. As shown recently, there is an advantageous effect if the drugs are given simultaneously which is caused by a synergistic effect at the same target cell in the lung epithelia. Therefore, it seems rational to combine both substances in one particle. This type of particle has the advantage over a combination product containing both drugs in a physical mixture which occurs rather randomly deposition leading to API segregation and non-dose-uniformity.

Dry powder inhalers (DPIs) is a type of therapeutic pharmaceutical formulations usually present in the solid form. Due to the nature of the solid-state, an understanding of chemical and physical properties must be established for acquiring optimum performance of the active pharmaceutical ingredients (APIs).

In recent year, generation of DPIs is a destructive procedure to meet the micron size. Such processes are inefficient and difficult to control. Moreover, according to current researches on combination APIs formulation, this type of DPIs performed a greater variability in does delivery of each active, leading to poor bioavailability and limit clinical efficient. This result suggest that combination formulations require advanced quality and functionality of particles with suitable physicochemical properties. Hence, in order to production of binary and combination DPIs products, the aim of this study was to develop the spray drying and ultrasonic process for engineering of combination drug particles that will be delivered more efficiently and independently of dose variations to the lung.

Microparticles were produced by spray drying or/and ultrasonic technique. The processing parameters and addition of excipients (polymers) were optimized using a full factorial design such that microparticles were produced in a narrow size range suitable for inhalation. Employing excipients resulted in high saturation environment leading to minimized sphere particles when compared to conventional solvent. Solid state characterization of microparticles using powder x-ray diffraction and differential scanning calorimetry indicated that the particles contained crystalline but no cocrystal. The combination particles comparable to or better than micronized drug when formulated as a powder blended with lactose. It was concluded that the use of HPMC enhanced crystallinity suitable for inhalation; and combination particles improved uniform distribution on the stage of NGI.

Acknowledgements/ Dedications

I would like to express my gratitude to Professor Anant Paradkar, Dr. Ian Grimsey, and Dr. Qun Shao for their supervision of this work, and also thank Dr. Victoria Silkstone and Dr. Marcel de Matas for their support during the first two years. I feel honoured to have benefited from their supervision, support, encouragement and unflappable belief in my ability. I thank you all sincerely for your admirable academic and personal integrity.

I thank Dr. Khaled Assi and his students for allowing me to use their inhalation analytical equipment and laboratories. I would like to acknowledge Mr Andrew Healey and Mr Dennis Farwell for their technical support and assistance. I also thank the staff from Centre for Chemical and Structural Analysis, past and present, for their support, assistance, and scientific advice in analytical laboratory.

I would like to thank all the students of the Centre for Pharmaceutical Engineering Science for their moral support, company and friendship over the last four years. Thanks to all my family for their support, tolerance and encouragement throughout the last four years and their challenges and pleasures.

Table of Contents

List of Figures

List of Tables

List of Equations

Chapter 1 : Introduction

1.1 Chronic obstructive pulmonary disease (COPD)

Chronic obstructive pulmonary disease (COPD) is a syndrome of progressive airflow limitation caused by chronic inflammation of the airways and lung parenchyma (Sutherland and Cherniack, 2004). It is characterized by airflow obstruction. The airflow obstruction is usually progressive and not fully reversible(NHS, 2004). The term of COPD includes two main conditions- chronic bronchitis and emphysema (NHS, 2010). Chronic bronchitis is a chronic inflammation of bronchi in the lung; and emphysema is a long-term, progressive disease of the lungs, which can cause physical damage to the shape and function of lungs. Both of two diseases can be caused by smoking tobacco, which is the one of risk factors of COPD. In addition, gene, airway hyperresponsiveness, lung growth, occupational dust and chemicals, air pollutions and infections all are related to the causes of COPD(NHS, 2010).

Current treatments for COPD are aimed at increasing airflow, decreasing respiratory symptoms, decreasing exacerbations, and improving the quality of life (Bateman et al., 2008). The antimuscarinics, methylxanthines, short-acting and long-acting bronchodilators and corticosteroids are commonly used as single therapeutic or in combination to treat patients with COPD (Albert and Calverley, 2008, Lasseter et al., 2011).

The methylxanthines, such as theophylline, have been used in the treatment of COPD for many years. Recent studies suggest that theophylline can improve lung

and diaphragmatic muscle function, thereby reducing COPD symptoms (Barnes, 2006).

Bronchodilators also can be grouped into long/short acting β_2-adrenergic-receptor agonists, and muscarinic receptor antagonist (Albert and Calverley, 2008, Moulton and Fryer, 2011). Their primary therapeutic effects are increase of lung function and decrease of dyspnoea and other COPD symptoms. In a clinical study, it was found that β_2- agonists significantly reduced exacerbations and improved a health-related quality of life (HRQOL) in patients with COPD (Cazzola et al., 2010). Recently , long acting β_2-agonists, for example salmeterol xinafoate and formoterol fumarate, have been recommended as first-line maintenance therapy in the treatment of COPD (Bateman et al., 2008). Recent studies also suggested that combination therapy of a corticosteroid and a long acting β_2-agonist have been very successful in managing asthma and COPD (Wouters et al., 2005, Miller-Larsson and Selroos, 2006, Greening et al., 1994, Calverley et al., 2003, Szafranski et al., 2003, Cazzola and Hanania, 2006).

Corticosteroids are recommended in step 2 of the British Thoracic Society's (BTS) guidelines for the treatment of chronic asthma (Bateman et al., 2008, BTS, 2011), but their role in COPD is controversial. A number of studies have shown steroids alleviate patients' symptoms, reduce the exacerbation rate, and improve health status in patients with COPD or asthma (Vestbo et al., 1999, Sutherland et al., 2003). However, it has also been reported (Sutherland et al., 2003, Wouters et al., 2005) that steroids do not substantially modify airway inflammation in COPD; and compared to placebo, there is no appreciable improvement of lung function with steroid therapy. In addition, corticosteroids provide less benefit to the

patients who smoke (Chaudhuri et al., 2003, Ito et al., 2001, Vestbo et al., 1999). This suggests that there could be corticosteroid-resistance in some patients with COPD. Recently, studies have reported that a combination of corticosteroid with theophylline is superior to placebo or steroid monotherapy with regard to lung function, anti-inflammation in airway, symptoms, frequency of exacerbation and health status in COPD (Spears et al., 2009, Lim et al., 2000, Barnes, 2003, Ford et al., 2010). This may suggest that theophylline can help reduce steroid resistance and enhance anti-inflammatory activity in COPD.

1.2 Treatment of COPD

1.2.1 Methylxanthines

Theophylline is a xanthine, which has been recognized as third-line agent in asthma and COPD therapy according to international guidelines (Bateman et al., 2008). This is because of its unacceptable side effects. Many patients treated with theophylline experience nausea, headaches, vomiting, abdominal discomfort, restless, seizure and cardiac arrhythmias (Kirsten et al., 1993). Theophylline has been used as bronchodilator for several decades, however, it has a narrow therapeutic index (10-20 mg/L) (Zhou et al., 2006, Kobayashi et al., 2004, McKay et al., 1993). Patients of the oral taking theophylline must therefore have plasma concentration monitored (Barnes, 2006).

Recently, theophylline is marketed under several brand names such as Uniphyl and Theochron, which comes as a tablet, capsule, solution, and syrup to take by mouth. Its dose is from 80mg to 600mg (DrugBank). Among of them, capsule and tablet are extended-release formulation. In clinical studies, they are used as bronchodilator in COPD (Barnes, 2003). The mixture of theophylline with

ethylenediamine can be given by injection, which is called as aminophylline, but this injection is needed rarely for severe asthma.

1.2.2 Selective beta$_2$ (β_2) agonists

The selective β_2 agonists selectively stimulate β_2 adrenoceptors in the airway. They produce bronchodilation either short or long acting. The short-acting β_2 agonists can immediately relief of asthma symptoms within 5 min by inhalation, and is generally at its maximum within 30 min (Rennard, 2004). Salbutamol and terbutaline belong to this group. The long-acting β_2 agonists, such as formoterol and salmeterol, have duration of action, which can be lasted at least 12 h.

Both short and long acting agonists have inhalation and oral formulations. Inhaled medicines can be delivered by pressurized-metered dose inhalators, nebulizer, and dry powder inhaler. Particularly, the nebulizer can be used to deliver solutions of salbutamol and terbutaline for the treatment of severe acute symptoms.

The oral preparations of β_2 agonists may be beneficial in patients who cannot manage the inhaled route, for instance, children and elderly. However the inhaled β_2 agonists are more effective and less side-effects than oral administration. There is a report that have indicated that reduces of oral deposition can be able to decrease the systemic effects (Dahl et al., 2001). The side-effects of β_2 agonists include fine tremor, nervous tension, headache, muscle cramps, palpitation, and so on (NHS, 2010).

1.2.3 Anticholinergics bronchodilators

Anticholinergics also are named as antimuscarinic. They are effective bronchodilators because they block the action of acetylcholine on M3 muscarinic

receptors that induce contraction on airway smooth muscle (Rennard, 2004). Short and long-acting bronchodilators are available.

Ipratropium can provide short-term relief in COPD, but its action is relatively slower than short-acting β_2 agonists. Its maximal effect occurs 30-60 min after inhaled and continue the action for 3 to 6 hours. The long-acting anticholinergics is tiotropium, which is effective for the management of COPD. It reduces exacerbation frequency in COPD patients. Currently, only inhaled anticholinergics are used for clinical treatment.

1.2.4 Corticosteroids

Corticosteroids (or glucorticosteroids) are widely used in the treatment of inflammatory and immune diseases, which have been used for the management of reversible and irreversible airway disease. Inhaled steroids have been recommended in the BTS guidelines for the prophylaxis of asthma (BTS, 2011). In COPD treatment, inhaled corticosteroids also may reduce exacerbations.

Steroids can be formulated as inhaled, oral and parenteral dosage forms. The inhaled steroids could help to distinguish asthma form COPD by using 3-4 weeks (BTS, 2011). The combination inhalation therapy (steroids and bronchodilator) have been proved to improved forced expiratory volume in 1 second (Cazzola and Hanania, 2006). Beclomethasone dipropionate, budesonide, and fluticasone propionate have been widely developed for COPD treatment.

1.3 Inhalation aerosols

Local delivery of medication to lungs is highly desirable, because of the large surface area, the abundance of capillaries and the thinness of the air-blood

barrier (Winkler et al., 2004). Therefore, inhaled drugs are delivered to the respiratory tract for the treatment of airways diseases, which can result in a rapid onset of activity. Additionally, smaller doses can be administered locally compared to delivery by oral or parenteral routes (Sutherland and Cherniack, 2004), thereby, reducing the potential adverse systemic effects and drug costs. Furthermore, the pulmonary route can avoid first-pass metabolism in liver (Winkler et al., 2004), as well as issues associated with limited absorption via the GI tract and local tolerability issues Thus this approach has been utilized as a portal for entry of peptides and proteins (Hussain et al., 2004).

1.3.1 Inhalation devices

Inhaled drug delivery devices are divided into three categories: pressurized metered-dose inhalers (pMDIs), dry powder inhalers (DPIs), and nebulizers. A good delivery device can provide physical and chemical stability of drug formulations (Pilcer and Amighi, 2010). Additionally, it can generate a homogeneous aerosol and provide reproducible drug dosing. For drug deposition purposes, the inhaler should discharge 0.5-5µm particles. Moreover, the ideal device must be simple, convenient, inexpensive, and portable.

The pMDIs also referred to as metered-dose inhalers (MDIs) are the most commonly used inhalation drugs delivery devices (Aulton, 2009). In pMDIs, drug is either dissolved or suspended in liquid propellants with other excipients. Upon activation, a predetermined volume of liquid (drug and propellant) is released. The gas is produced by evaporation of propellants. The propellants used in pMDI formulations are liquefied gas, usually chlorofluorocarbons (CFCs) and hydrofluoroalkanes (HFAs). The liquefied propellants establish a saturation vapor

pressure in the head space of the aerosol canister. On spraying, the propellants evaporate, leading to constant and consistent pressure. This high-speed gas flow helps to break up the liquid into a fine spray of droplets. Additionally, pMDIs are portable, low cost and disposable devices. However, they also demonstrate a number of disadvantages. Owning to their high velocity of propellant droplets, most of drug is lost through impaction of these droplets in the oropharynx. Meanwhile, propellants may not evaporate sufficiently rapidly for droplet size to decrease; and the mean droplet size may exceed 40μm which makes it difficult for drug to reach the deep lung. An additional problem with pMDIs is their correct use by patients. For vital for effective drug deposition and action, that inhalers are used in accordance with the manufactures instructions (Crompton, 1982). pMDIs should be actuated followed by slow and deep inhalation, followed by a period of breath-holding, which is very difficult to control, especially in children and the elderly. However, it should be noted that even the correct use of this inhaler, pMDIs can result in only 10-20% of the emitted dose being deposited at the site of action.

In DPIs, drug is emitted as a cloud of fine particles. The drugs can be preloaded into an inhaler or filled into hard gelatin capsules and foil blister discs (Aulton, 2009). DPIs have a number of advantages over pMDIs. These advantages are (i) delivery of DPI formulations does not rely on propellant, (ii) formulations do not contain other excipients except carriers, (iii) usage of DPIs does not require inhalation/actuation synchronization, (iv) the normal deep breath can actuate DPIs, and result in better lung delivery, (v) DPIs are suitable for delivery of large dosages of drugs, and (vi) the volume and concentration of drug is markedly restricted by valve in pMDIs. However, there are a number of disadvantages for

DPIs, for instance, emission of particles from the pMDIs device and deaggregation of particles is affected by the patients' ability to inhale, and DPIs are exposed to ambient atmospheric conditions which may reduce formulation stability.

Nebulizers are the first commercial inhaler for inhalation therapy. They have subsequently been evolved into three different devices. These include jet nebulizers, ultrasonic nebulizers, and vibrating-mesh devices (Aulton, 2009). Some studies have indicated that nebulizer always demonstrate low efficient, poor reproducibility, and great variability (Pilcer and Amighi, 2010). Nevertheless, nebulizers have a number of advantages over pMDIs and DPIs. These are (i) nebulizer systems can be used to deliver the formulations which cannot be formulated into pMDIs and DPIs, such as large volume solutions and suspensions, (ii) nebulizers can emit larger therapeutic doses than pMDIs and DPIs, and (iii) drugs can be discharged from nebulizers via normal tidal breathing, thus this kind of device is suitable for children, and the elderly.

1.3.2 Formulation of pulmonary drugs: particle engineering

Pulmonary deposition performance of the aerosol is predominantly dependent upon aerodynamic particle size which is influenced by powder flow, shape, surface properties, drug carriers, inhalation devices, and inspiratory flow rate (Usmani et al., 2003). Thereby, the balance between inhalation devices, drug formulation and patients' inspiratory flow rate is very important for inhaled drug design (Pilcer and Amighi, 2010). To reach this balance, the ideal strategy involves particle engineering with the intent to achieve controlled and suitable properties such as narrow particle-size distribution and improved dispersibility.

The physicochemical characteristics of particles, such as morphology, granulometry, stability, can influence dispersive performance of inhaled drugs. Particle engineering can control particle size, morphology, and crystal structure to meet the requirements of inhaler design and drug delivery. It can narrow the particle-size distribution, improve dispersibility, enhance chemical and physical stability, and bioavailability. A number of methods have been developed to produce particles with desirable characteristics for inhalation.

1.3.2.1 Milling

Inhalation products such as pMDIs, suspension nebulizers and DPIs, consist of micronized APIs in either agglomerated or blended form. Such particles are generally produced by batch crystallization, followed by filtering, drying and micronization (Shekunov et al., 2003). Milling is a well-established method for particle engineering. It can yield micron size particles for inhaled drugs. One of the well-validated methods for manufacture dry powder inhalation is jet mill.

Jet milling reduces particle size via high velocity particle-particle collision. The unmilled particles are fed into milling chamber. The high pressure air from the nozzles accelerates the particles. The particles collide and fracture in the chamber. Particles are projected around the mill; the larger particles are subject to higher centrifugal forces and are therefore forced to the outer perimeter of the chamber. The smaller particles drop into the central discharge stream (Aulton, 2009).

This technology has been used successfully for producing very fine products. However, the fluidized particles may suffer some degree of surface damage, leading to generally undesirable breakage (Bentham et al., 2004). Therefore, jet

milling may be unpredictable to control of important product characteristics such as size, shape, morphology, surface properties, and electrostatic charge (Bentham et al., 2004, Pilcer and Amighi, 2010). In addition, the jet-milled particles have a high interparticle cohesive forces (Fukunaka et al., 2005). This micronized powder are grown by the crystals cleave at the cleavage plane, which leads to a broad particle size distribution. The micronization method using mills is a high-energy input process. It also has been suggested that it could induce crystal disorder (Chikhalia et al., 2006) and can enhance chemical degradation (Shoyele and Cawthome, 2006). Thus, those milled powders have an unstable and controllable physical and chemical properties influence the performance in processing and formulations, particularly in DPI delivery. The poor flow properties caused by higher energetic surface decrease the delivery efficiency of DPIs. This was shown for supercritically produced (volume mean diameter 3.55 μm) and milled (1.7 μm) salmeterol xinafoate (Shekunov et al., 2003). However the milled sample exhibits a higher bulk density, specific free energy and aerodynamic shape factor. The milled particles have a higher tensile strength of the aggregates and indicated a two-fold decrease of fine particle fraction deposited in a cascade impactor (Shekunov et al., 2003). Milling techniques, in general, show several disadvantages, but the advantages of milling include limited metal contamination, easy cleaning, simple operation and relativity low cost. However, new techniques which produce the drug directly in the required small particle size are desirable, and more research is needed.

Wet milling can achieve nano-size particles (Peltonen and Hirvonen, 2010). Micron size drug crystals are media milled in a water-based solution and reduced to nanometer-sized particles. This technology has been identified as a useful

procedure to develop formulations of poorly-water-soluble compounds. Wet milling can be operated in re-circulation mode (Van Eerdenbrugh et al., 2008, Peltonen and Hirvonen, 2010). A suspension (Telko and Hickey, 2005) consisting of drug, water and excipients is fed into the milling chamber that is charged by milling media. In the mill chamber, the suspension is processed into a nanocrystalline dispersion. The typical residence time required to generate a nanometer-sized dispersion with a mean diameter <200nm is 30-60min.

During the wet-milling process, the grinding between glass beads and particles or particles and particles break up the crystalline lattice for particle size reduction (Van Eerdenbrugh et al., 2008). The particle size distribution is related to the milling time and size of glass beads (Yang et al., 2008). In Yang's research, it used 0.50–0.75 mm diameters of glass beads and milled for 24 hours to reach a crystalline form, potency and homogeneity, and stability nanosuspension of budesonide and fluticasone. It should be noted that using glass beads has been the possible formation of glass particles from the milling process, which could potentially cause lung irritation and influence study results (Yang et al., 2008). In nano-crystalline suspensions of naproxen, thermodynamically unstable amorphous materials could be created on the surface of particles (Kumar and Burgess, 2014). In addition, the presence of aqueous medium could facilitate crystalline form conversion or formation of hydrates. The potential solid form changes could lead to stability or processing issues for nanosuspensions and ultimately impact their performance in lung delivery.

Wet milling is an advanced technique to generate physically stable dispersions. However, this technology may also lead to chemical degradation. It is not suitable

for water soluble and the nano-size particles are subject to agglomeration and crystal growth.

1.3.2.2 Spray drying

Spray drying is a one-step process that converts a liquid feed into a dried particle (Aulton, 2009). There are four stages in spray drying: (i) atomization of the feed solution, (ii) droplets-air contact, (iii) drying droplet, and (iv) separation of the dried particles from the gas stream. The feed solutions can be solution, slurry, suspension, and colloidal dispersion.

The particles produced by spray drying can be manipulated by changing the parameters of spray drying (Pilcer and Amighi, 2010, Tong.H. H. Y and Chow.A. H. L, 2006, Shoyele, 2008). The design of the nozzle can affect the atomization of droplet and control the size of particles. Once the droplets leave the nozzle, they make contact with hot gas in the drying chamber. Thus, the inlet and outlet temperatures are the most important variables for drying. Additionally, the retention time of droplets, drying gas medium, gas humidly, and gas flow rate may affect particle shape, size and density. The properties of particles are also related to the character of the API solution. The different concentrations, solutes, solvents and pH values of solutions can also lead to variations in particle forms.

There are many COPD medications processing by spray drying, which could be injected as solutions, emulsions, and suspensions. In the articles of formulation of salbutamol sulfate, the shell-like, ultra-light particles could be generated from emulsion (Steckel and Brandes, 2004). If the sample was pre-treated by ultrasonic methods, the particles would be needle-like after spray drying (Dhumal et al., 2009). Spraying drying the composite solution of salbutamol sulfate, the

obtained particles have a modified surface morphology (Seville et al., 2007). The corticosteroid drug, budesonide was spray dried to gain nano-scale particles. Nolan et al. (Nolan et al., 2009) found that spray dried budesonide is low density and porous-like particle with amorphous content, but the powder is thermodynamically stable for up to 12 months.

Compared to milling, spray drying is easier to generate small spherical particles with more homogeneous size distribution (Tong.H. H. Y and Chow.A. H. L, 2006). These particles can result in higher respirable fraction than micronized particles obtained from mechanical milling. Because spray drying is a fast and high temperature process (Shoyele, 2008), the particles generated from solution using spray drying are usually amorphous. However, it should be noted that spray drying can maintain crystalline state of APIs, when it is drying suspensions and slurries.

1.3.2.3 Spray freeze drying

Spray freeze drying is a technique to spray drug solution into a vessel filling with a cryogenic liquid, such as nitrogen, oxygen, or argon (Aulton, 2009), meanwhile the droplets are quickly frozen. Lyophilization of frozen droplets results in porous particles suitable for inhalation. Although the porous spherical particles are low density, the particles are usually amorphous and high aggregation. Spray freeze dried particles can reach to the desired respiratory size range <5 μm or even down to nanoscale (Ali and Lamprecht, 2014). Parathyroid hormone particles (Shoyele et al., 2011) are spray freeze dried which have mass medium diameter 12μm and tapped density 0.007 g/cm^3. In addition, particles of kanamycin for inhalation delivery were produced with the spray freeze-drying method (Her et al.,

2010). The diameters of particles are from 13.5μm to 21.8μm and their aerodynamic diameters were between 3.58μm and 6.39μm. Those researches suggested that spray freeze drying process delivers very strongly porous structures.

Spray freeze drying is conducted at sub-ambient temperature, thus it can be used for processing heat sensitive compounds. It has been widely used in formulation of protein and peptide, including anti-IgE monoclonal antibody, deoxyribonucleases, insulin, and cetrorelix acetate (Pilcer and Amighi, 2010, Sadrzadeh et al., 2007).

1.3.2.4 Supercritical fluid crystallization

In recent years, supercritical fluid crystallization (SFC) technologies have gained increasing attention in the pharmaceutical industry due to their capability and versatility of producing micro-fine particles to predetermined specifications. Supercritical fluids (SCFs) technology is a methodology that utilizes carbon dioxide (CO_2) at temperatures and pressures above its critical point to effuse through solids like a gas, and dissolve materials like a liquid, Fig. 1-1.

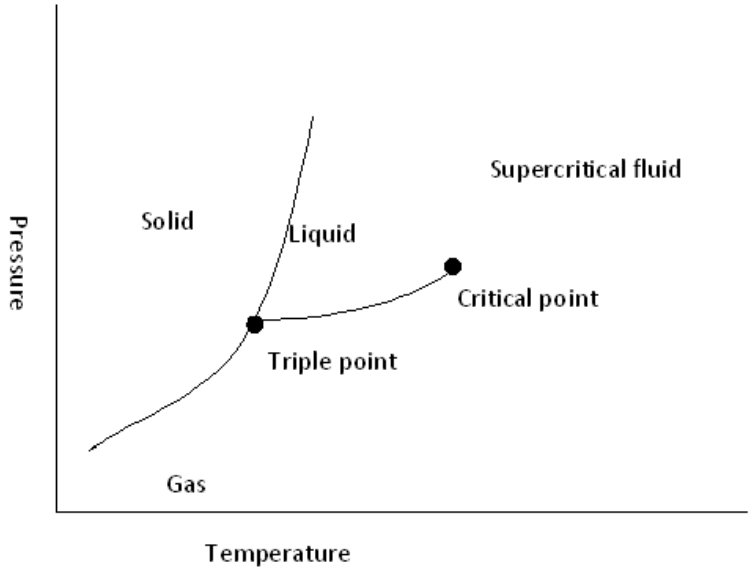

Fig. 1-1. Phase diagram of CO_2

There are three main SCF processes (York P. et al., 2004): (a) precipitation from supercritical solutions composed of supercritical fluid and solutions (RESS); (b) precipitation from gas saturated solutions (PGSS) and; (c) precipitation from saturated solutions using supercritical fluid as anti-solvent (SAS).

Using RESS drug is firstly dissolved in SCF followed by rapid expansion of the fluid solution across a heated orifice to cause a reduction in the density of the solution. This leads to a decrease in the solvation power of the fluid which leads to precipitation of the drug (York P. et al., 2004). In PGSS, the drug is molten and then the SCF is dissolved in the molten solute. The supercritical solution is then fed into a chamber via an orifice leading to a rapid expansion under ambient condition (Pilcer and Amighi, 2010). However, application of these techniques is limited by particle aggregation, nozzle blockage and limited solubility of solutes in supercritical CO_2 (York P. et al., 2004). Under these circumstances, the third method, SAS, becomes the most common method, although a range of different

variants have been involved. Each process relies on the capability of SCF to act as an anti-solvent (York P. et al., 2004, Pilcer and Amighi, 2010, Tong.H. H. Y and Chow.A. H. L, 2006). CO_2 can easily dissolve in organic solvents leading to volume expansion. Thereby, when SCF makes contact with drug solutions, it results in reduction of solvent density and solvation capability. Such decreases lead to increasing levels of supersaturation, solute nucleation and particle formation. Finally, the drug particles precipitate during dissolution of SCF into the drug solution. Once the solute has precipitated out, the SCF-solvent can be removed. However, due to the extremely fast precipitation in SCF, this induces amorphicity in same materials (Tong.H. H. Y and Chow.A. H. L, 2006).

The benefit of SCF technologies is that various particle shapes and morphologies can be obtained (compact crystals, needles, dendritic aggregates, balloon-like structures, porous aggregates) depending on the controlled supersaturation and kinetics of precipitation(York P. et al., 2004). Particles can be produced as single-components or composites. SCF methods allow designing particle morphology and size by several factors: precursor composition and concentration, nozzle geometry, spraying distance, operating conditions (T, p, flows, pre-expansion pressure)(York P. et al., 2004). Selective precipitation with a control of crystallinity and crystalline forms is possible.

1.3.2.5 Sonocrystallization

Ultrasound can affect the nucleation and crystal growth during crystallization (Mullin and William J., 2001). The application of ultrasound can induce cavitation in the liquid. The cavitation effects produce bubbles (Virone et al., 2006, Narducci et al., 2011), which collapse in the liquid. Transient bubble collapse cause local

regions of extreme excitation, temperature (5000K) and pressure (2000atm) (Keller and Miksis, 1980), and consistent shock waves (Storey and Szeri, 2001). These regions lead to an increasing supersaturation, and a decreasing temperature of crystallization (Narducci et al., 2011).

Theoretically, short bursts of ultrasound can produce lower supersaturation and continuous sonication would be able to facilitate crystallization at a higher level of supersaturation (Ruecroft et al., 2005). In this regard, it is possible to tailor a crystal size distribution using different wave frequencies of ultrasound (Kordylla et al., 2009). In addition, particle morphology are influenced by ultrasound-generated temperature and pressure gradients, which reduce particle aggregation (Ruecroft et al., 2005).

Therefore, ultrasound can be able to alter and improve in the physical properties associated with solids such as;

a) Morphologies like particle size, shape, crystal habit, density, porosity etc.

b) Physical properties which are associated with morphology, such as flowablity, compatibility and compressibility. Efficient production of small particles with uniform size is required in the pharmaceutical industry due to their impact on performance while processing and impact on patients after consumption.

In recent years, researchers at the University of Bath developed a sonocrystallization technology called solution atomization and crystallization by sonication (SAX) (Kaerger and Price, 2004), which has been shown to be extremely useful in preparation of nano- and micro- size particles. This technology consists of four major processes, including (I) formation of API

solution, (II) atomization of solution into a chamber, (III) collection of aerosol droplet in a nonsolvent, and (IV) application of ultrasound to induce crystallization (Ruecroft et al., 2005). SAXS is capable of reproducibly generating particles with micro- or nano-size (Bucar and MacGillivray, 2007, Kaerger and Price, 2004) , and formation of particles containing multiple drugs (Pitchayajittipong et al., 2009).

1.5 Combination particles for pulmonary delivery

Combination particle is a particle containing multiple substances. These particles can be imaged to be formed like as in Fig. 1-2. For DPI formulation, it has been reported that nanoparticles have been designed to form Trojan, strawberry and nanoparticles aggregates (Sofia Silva et al., 2014).

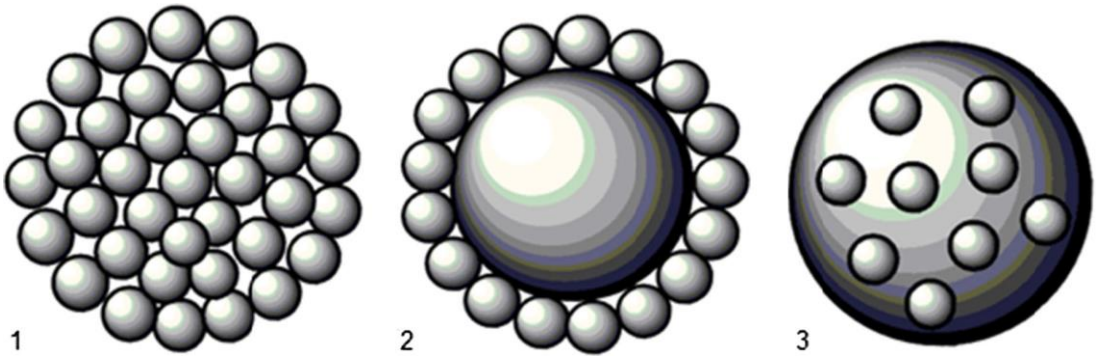

Fig. 1-2. Nanoparticle-based dry powders for inhalation: 1 Trojan particles; 2 Strawberry particles; 3 Particles with nanofeatures (Sofia Silva et al., 2014)

Trojan particles are micron-sized large porous particles, which were composed by plenty of nano-size particles. The strawberry particle designation first appeared during the 2005 Aerosol Society meeting (Sofia Silva et al., 2014), and it is associated with micro-carriers coated with active nanoparticles connected. This structure is advantageous because it improves flowability and prevents aggregation. On the surface, the coated nanoparticles work as spacers between

the microparticles, the adhesion between particles is diminished, making the handling easier. Moreover, this structure has a potentiality to be used to formulate high does DIPs, which can prevent from poor flowability and increase the FPF. Finally, particle with nanofeatures is a nano-embedded microparticles. It is a type of microcapsules with solid domains. These particles are fabricated from macromolecular and/or molecular assemblies, polymers or lipids, in which the active principle is either dissolved, entrapped, encapsulated, adsorbed or attached to the external interface.

Combination particles can be formed by different shapes of particles, but the spherical particles are the ideal structure for inhalation. Combination particles has advantages over a combination product containing both drugs in a physical mixture where codeposition of APIs occurs rather randomly when codepositing from the same cloud (Westmeier and Steckel, 2008). It is predictable and controllable, which can be detected if adhesion of one API over the other on the lactose, or along with self-agglomeration of one or both drugs, or will cause content segregation, or dose uniformity. All particles have uniform drug composition.

Co-precipitation or co-spray drying a solution containing two APIs is recent strategy used to formulate combination particles. Spray drying is a well published technology used for formulation of combination particles. In 2006, Corrigan and his colleagues (Corrigan et al., 2006) formed salbutamol sulphate/ipratropium bromide and salbutamol sulphate/excipient combinations particles by spray drying. They reported the fine particle fractions (FPF) of combination particles were greater than that of micronized salbutamol sulphate alone. The particles

were spherical and diameters range from 1µm to 7µm, which improved their flowability and deposition. However, the particles were amorphous, resulting in cohesiveness and physically instability. This method was also demonstrated by Tajber in 2009 (Tajber et al., 2009a). Tajbar and co-workers formulated budesonide/formoterol fumarate particles by spray drying. They also compared combination particles with a physical mix of micronized powder in *in vitro* deposition studies (Tajber et al., 2009b), indicating that there was 2.6-fold increase in respirable fraction and better dose uniformity. Additionally, drugs spray dried with certain excipients can provide crystalline particles. Kumon and his co-workers (Kumon et al., 2010) produced a combination particles by spray drying solution containing corticosteroids, β_2-agonist and mannitol. The particles obtained from this solution were crystalline and stable and showed excellent aerosol performance.

Co-precipitation seems a seldom used methodology for producing combination particles. There are a few published papers about this process. Pachuau and his co-workers (Pachuau et al., 2008) produced microspheres containing theophylline, salbutamol sulphate and polymer via evaporation of emulsions. However, the size of microspheres was not suitable for pulmonary delivery. Thereby, in order to better control precipitation of particles, there are several novel technologies that can potentially be used. Westmeier formulated salmeterol xinafoate/fluticasone propionate combination particles using an interdigital slit micromixer (MMA, Mainz, Germany) (Westmeier and Steckel, 2008). He firstly obtained suspensions from the micromixer; and then spray dried these to obtain a dry powder. The shape of particles was needle-like, and thickness of particles depended on the solvent composition used. Moreover geometrical dimensions of

all particles were less than 10μm. In the aerodynamic assessment, the FPF of particles was around 22%. A lactose blend with combined particles resulted in an FPF of 36%. Meanwhile, APIs were uniformly distributed throughout the stages of the NGI. The other novel formulation used solution atomization and crystallization by sonication (SAX), which is developed by University of Bath, UK. This technology can be used to form combination particles containing multiple substances. So far, they have formulated particles comprising two (theophylline/fluticasone propionate (Dhillon A et al.), budesonide/formotrol fumarate (Pitchayajittipong C et al.) and fluticasone propionate/salmeterol xinafoate (Pitchayajittipong et al., 2009). Three APIs (Dhillon A., 2009) (Ipratropium bromide/salmeterol xinafoate/fluticasone propionate and salmeterol xinafoate/fluticasone propionate/theophylline) have also been implanted in to dry powder aerosols. The volume median diameters of the particles were less than 5μm. In NGI experiments, the ratio of individual APIs was similar at each stage, indicating that combination formulations delivery consistently.

According to the above described studies, combination particles appear to be an ideal formulation method for administering multiple drugs to be delivered in to the lung. It has a number of advantages over physical mixtures, for instance, combination particles overcome un-evenly delivery caused by physical mixtures, leading to better aerodynamic performance and bioavailability. However, formation of combination particles is a complicated physical process with high energy input. Thereby, it is easy to obtain amorphous particles, which are physically unstable. Thus, the selection of process parameters is very important to control the physical and chemical characteristics of APIs particles. Therefore, in order to obtain consistent deposition of theophylline and corticosteroids in the

targeted site of lung, theophylline and corticosteroids can be combined into individual particles in accordance with the studies describing in this report.

1.4 Combination therapy of theophylline with corticosteroids for COPD

Combination inhalation therapy has the potential to provide notable benefits to patients through synergistic pharmacological action, resulting in fewer side effects, better compliance and improved therapeutic outcomes.

Since the 1990s, there have been a number of studies investigating combination therapies of theophylline and steroids or β_2-agnoist for the treatment of COPD and asthma. There is known to be limited clinical effect for combination therapy using theophylline and β_2-agnoist (Cazzola et al., 2000). However, combinations of low dose oral-theophylline and low dose inhaled-steroid produced similar benefits to monotherapy with high dose steroids in COPD (Van Andel et al., 1999, Lim et al., 2000, Evans et al., 1997).

Thus combination therapy has the potential to provide inexpensive and clinical efficient treatment in the patients who are not adequately controlled on steroid therapy, whilst avoiding the side effects caused by high theophylline concentration. However, some studies have reported no clinical improvements in combination therapy in COPD (Van Andel et al., 1999). One explanation could be that these patients were treated with inhaled steroid plus oral rather than inhaled theophylline, which may cause relatively slower absorption and fewer interactions with the inhaled steroid in lung. Therefore, simultaneous inhalation of theophylline and steroids may enhance the reproducibility of combination therapy.

1.4.1 Combination inhalation in COPD treatment

Commercially available combination formulations are either mixed solutions or blends of the active pharmaceutical ingredients (APIs) with lactose carrier particles. Commonly used compound bronchodilator prescribed in COPD are combination short-acting β_2 agonist and anticholinergic, and combination long-acting β_2 agonist and corticosteroid. The combination short-acting β_2 agonist and anticholinergic, which is Combivent® (Boehringer Ingelheim). It is a nebulizer solution. One spray of Combivent® contains ipratropium and salbutamol. The commercial products of combination long-acting β_2 agonist and corticosteroid include Symbicort® (AstraZeneca) and Seretide® (A & H). Symbicort® is a blended with budesonide and formoterol fumarate. Seretide® contains fluticasone propionate and salmeterol.

Both of formulation are physical mixture of APIs and carriers. In the recent the articles, the researchers have found there the deposition of APIs are not consistent in NGI from these products. In the aerodynamic properties study of Seretide® Accuhaler®, it observed that content of salmeterol was decreased in the lower stages. The research of Symbicort® pMDI found significantly differences in the stage deposition of budesonide and formoterol fumarate and suggested that the two drugs were deposited as separate entities.

This kind of formulation is made homogeneity depends upon the mixing process. However, blending performance is uncontrolled and unpredicted (Kumon et al., 2010), due to different sizes and amounts of powders and different surface energies, leading to API segregation and non-dose-uniformity. Thereby, the possible solution is to combine the APIs in one particle, providing differential the

advantage over other combination inhalation products produced by physical mixing.

1.6 Aim and scope of the thesis

Technologies for modifying combination particles in order to achieve a greater control of size and surface properties of particles for DPI formulations have been investigated for a few years. However, these processes are inefficient to control physical and aerodynamic properties of combination particles which contain APIs with +20 folds difference. In addition, there is limited researches about theophylline DPI and formulation of high dose inhaler.

The aim of this study is to develop an alternative strategy that is a constructive approach for combination particle generation to achieve a successful control of the physical characteristics and geometry of active drug materials.

The scope of this thesis are therefore to:

1. Produce theophylline particles for use in inhaled formulation by micronization processes.
2. Produce combination particles of theophylline and steroids for inhalation purpose by co-spray drying and co-precipitation
3. Determine the operational parameters of generation process which affect the particle size and uniformity of combination particles of theophylline and the model drug budesonide.
4. Investigate the effects on crystallinity and crystal form of particles caused by excipients.
5. Investigate the aerodynamic properties of particles delivered from DPIs.

Chapter 2 : Materials and Methodologies

2.1 Introduction

In Chapter 1, the importance of the physicochemical properties of components of inhalation dosage forms was highlighted. Physicochemical properties such as particle size, shape and crystallinity can have a dramatic effect on interparticle forces within inhalation dosage forms and drug product performance. This chapter, therefore, describes the methodologies of characterisation used in this study.

2.2 Materials

2.2.1 Active drugs

Micronized budesonide (JAI RADHE SALES, India), anhydrous theophylline (Sigma, UK) were used for this study.

Steroids are highly effective in reducing inflammation in the airways, however, they might be less effective in some patients (Wouters et al., 2005) who have a broad spectrum of anti-inflammatory effects in asthma. At a cellular level, corticosteroids reduce the number of inflammatory cells in the airways (Barnes, 1998). They can suppress the production of chemotactic mediators and adhesion molecules, leading to inhibition of the recruited inflammatory cells in the airways (Barnes, 2005). Due to these reactions of corticosteroids, the inflammatory cells such as eosinophils, T lymphocytes, mast cells, and dendritic cells, reduce in the airways.

A previous article reviewed the cellular transportation of corticosteroids (Barnes and Adcock, 2003), which indicate the mechanism of transportation. This

mechanism is that corticosteroids diffuse across cell membrane by binding to glucocorticoid receptors on the cytoplasm. The cytoplasmic glucocorticoid receptors are normally bound to proteins, known as molecular chaperone proteins. After corticosteroids have bound to glucocorticoid receptors, the receptors dissociate with chaperones, leading to the exposure of nuclear localization signals on glucocorticoid receptors and translation of the activated glucocorticoid receptor-corticosteroid complex into the nucleus. In the nucleus, the activated receptor-corticosteroid complex binds to DNA sequence, leading to changes in gene transcription, such as increased small number of anti-inflammatory genes and reduced inflammatory gene expression (Winkler et al., 2004). For example, the activated receptor-corticosteroid complexes involved in histone acetylation (Barnes, 2010, Barnes and Adcock, 2003). Glucocorticoids bind to glucocorticoid receptors leading to recruit histone deascetylase 2 (HDAC2). This suppresses histone acetylation and results in a reduction of transcription of genes encoding inflammatory proteins.

Theophylline has been used for many years, however its molecular mechanisms are still uncertain (Ito et al., 2002). Several molecular mechanisms of action have been discussed including inhibition of phosphodiesterases, transcription factor, antiapoptotic protein, and adenosine receptor antagonism, and stimulation of IL-10 and HDACs, but among of them, most seem to occur with higher concentrations than those recommended for the clinical situation.

According to recent articles, theophylline provides anti-inflammatory effects within its therapeutically relevant concentration (Barnes, 2006, Kobayashi et al., 2004). The anti-inflammatory mechanism of theophylline has been described in

terms of histone deascetylase (HDACs) activation (Ito et al., 2002). HDACs which is related to inflammatory gene transcription (Barnes et al., 2005) and is usually decreased in COPD (Ito et al., 2005). This reduction of HDACs leads to an increase of inflammatory gene expression. The anti-inflammatory mechanism of theophylline in COPD appears to directly activate HDACs to suppress inflammatory gene transcription by using low dose of theophylline (about 5 mg/L) (Ito et al., 2002, Hansel et al., 2004, Cosio et al., 2004). This interaction occurs at therapeutic concentration of theophylline (2 mg/L-2 mg/L), and is diminished at higher concentration (20 mg/L), which suggests that using low dosage of theophylline as anti-inflammatory substance will benefit the COPD, minimize the side effects caused by high dose and will also potentially avoid the requirement to monitor plasma concentration very closely (Rossi et al., 2002).

Mechanism of corticosteroid has been well explained in (Barnes and Adcock, 2003). Interestingly, it was found that steroids activate HDACs activity by recruitment of HDACs to activated transcription site. However, in the patients with COPD, there is an extreme reduction of HDAC activity and HDAC2 expression (Ito et al., 2005), which is the main cause of steroid resistance. On the other hand, the effect of theophylline is different from that of corticosteroids. It appears that theophylline is related directly to the activation of HDACs and switches inflammatory gene transcription (Ito et al., 2002). This reaction independent of the level of HDACs can be detected at the low levels of these enzymes. In this regard, theophylline can enhance HDAC activity in COPD patients. Combination therapy with theophylline and corticosteroids may therefore be able to enhance the efficiency of corticosteroids and recover their anti-inflammatory actions in COPD treatment (Lim et al., 2000, Spears et al., 2009, Ford et al., 2010).

2.2.2 Excipients

2.2.2.1 Lactose

Lactose ML001 (Respitose® ML001, DFE Pharma, Germany) was used as carrier. Lactose is by far the most important carrier used for inhalants (Pilcer and Amighi, 2010). It is one of the very few substances accepted by all medical and regulatory authorities as being ideal for inhaled medicines. Every type of inhaler requires a different grade and blend of lactose to ensure the best possible performance. Therefore, the various grade of lactose were used for aerosolization performance study to select the desired grade of carrier. The results of this experiment were illustrated in Appendix's Figure A1. With regard to this study, ML001 (Respitose® ML001, DFE Pharma, Germany) was selected in which particle size distribution was indicated in Table 2-1.

Table 2-1 Particle size distribution of Respitose® ML001 (cited from DFE Pharma product certificate)

	Typical (µm)	
d10	4	
d50	55	
d90	170	
	Specification	Typical
<45µm	40-60%	45%
<100µm	75-100%	82%
<150µm	90-100%	96%
<315µm	99.5-100%	100%

2.2.2.2 Polymers

Polymers applied in this study were used to inhibit crystal growth (Xia et al., 2012), improve the structure of particles (Singh et al., 2010) and stabilize uniformity of

nanosuspension (Verma et al., 2009). Due to the sensitivity of lung tissue, a limit number of excipients are currently approved by the Food and Drug Administration (FDA) for inhalation. Among them, the safe polymeric excipients are polyvinylpyrrolidone(PVP), polyvinyl alcohol(PVA), hydroxypropyl methyl cellulose(HPMC), hydroxypropylcellulose(HPC), chitosan, cyclodextrins, hyaluronan, and polymeric surfactant (Tween 20 and Tween 80) (Dumitriu and Popa, 2013).

In order to obtain particles with inhalable size range and controllable morphology, HPMC can directly inhibit crystal growth and control particle size in antisolvent precipitation procedure (Smyth and Hickey, 2011). Along with PVP, HPMC–PVP interactions accumulate at the boundary layer around the drug particles thus leading to growth inhibition and additional prolonged stability (Ali et al., 2009). In nano-suspension, the neutral HPMC and PVP were used, because their stabilizing ability is less dependent than ionic polymers or surfactants, which are upon changes in the chemical environment, such as changes in pH (Sepassi et al., 2007). Moreover, a published work has demonstrated that HPMC miscible with PVP enhanced the mucoadhesive properties of copolymer (Karavas et al., 2006) that improve the ability to trap nanoparticles of active drugs.

In this study, Polyvinylpyrrolidone PVP (Kollidon 25, BASF, Ludwigshafen, Germany), hydroxypropylmethyl cellulose (HPMC, Metolose 60 SH 50, Shin-EtsuChemical,Tokyo, Japan) were employed.

2.2.3 Chemicals for inverse gas chromatography (IGC)

Probes used for IGC including non-polar and polar probes.

The non-polar probes used (n-alkanes) in ICG for this project are listed as below:

(i) Hexane, 95% HPLC grade, Batch No.-1072208, Fisher scientific, England

(ii) Heptane, 99+% purity, Lot No.-50228042, Sigma-Aldrich, Gillingham, England

(iii) Octane, 99+% purity, Lot No.-CO04654BO, Aldrich Chemical Company, W1, USA

(iv) Nonane, 99+% purity, Lot No.-EO08280AO, Aldrich Chemical Company, W1, USA

The polar probes used in inverse gas chromatography (GC) for this project are given as follows:

(i) Chloroform, HPLC grade, Batch No.-0565673, Fisher scientific, England

(ii) Acetone, 99+%, Lot No.-9307A, Sigma-Aldrich, England

(iii) Ethylacetate, 99+% purity, HPLC grade, Sigma-Aldrich, England

(iv) Tetrahydrofuran, 99+% purity, Lot No.-13540, Rathburn Chemical Ltd., Scotland

The Materials were used for IGC column preparation are those in the following items:

(i) Glass columns, 1.27m length (1.5 loops), 3mm i.d., 6mm o.d., Glass blowing workshop, University of Bradford, UK.

(ii) Glass column, 0.68m length (single U shape), 3mm i.d., 6mm o.d., Glass blowing workshop, University of Bradford, UK.

(iii) Methanol, 99+% purity, HPLC grad, Batch No.- 092356

(iv) Tolune, 99+% purity, Laboratory grad, Bach No.- 0814374

(v) Dimethylchlorosilane, Lot No.-55H1218, Aldrich, England

(vi) Silanised glass wool, Lot No.-592, Jones Chromatography, Scotland

Moreover, the compressed gasses also used for IGC analysis. These gasses are hydrogen, nitrogen and air, and all from BOC Ltd., England.

2.3 Particle engineering

2.3.1 Jet milling

The FPS spiral fluid jet mill was used to reduce the particle size distribution of theophylline. The particle size can be controlled through changing the feed rate alongside with grinding and injection pressures. In this study, the grinding pressure and injection pressure were set 5 bar and 8 bar, respectively. Theophylline was loaded into grinding chamber at speed of 231 mg/ml.

2.3.2 Spray drying

The samples was spray dried from a saturated solution using a LU – 228 ADVANCED Spray Dryer (Labultima, Maharashtra, India) fitted with a standard FLU-P-4.01 spray nozzle. Because there an article has proved that process temperatures did not have significant effects on physical properties of particles (Nandiyanto and Okuyama, 2011, Tong.H. H. Y and Chow.A. H. L, 2006, Asada et al., 2004), in this study, the atomising air pressure at which the spray dryer operated was set to 2 Kg/cm^2. The process parameters are given as follows: (1) inlet temperature: 75-80 ◦C; (2) airflow rate: 60 Nm3/h; (3) feed pump flow rate: 2ml/min. These parameters resulted in the outlet temperature of 37-40 ◦C. The processed solutions were prepared by ultrasonication at room temperature (20 ◦C), in which the solvent contains 80% (v/v) ethanol and 20% (v/v) deionised water, and the concentration of APIs at about 2.9% W/V. The solutions were prepared with and without polymers.

2.3.3 Wet milling

The wet mill has the ability to reduce the particle size distribution to submicron size. In this study, the impacts on wet milling on the size of theophylline particles was assessed using only distilled water in the absence of stabilizer. The basic operation is described as follows:

Firstly, theophylline was dispersed in distilled water to produce a 10% theophylline suspension. Following this, 250ml of homogenized suspension was poured into sample holder and then fed into milling chamber. After that, the bulk populations of the nanosuspension were analysed by photon correlation spectroscopy. Finally, samples of suspension were analysed at 5, 15, 30, 45, 60, and 75 minutes. The suspension obtained at 45 minutes was used as final sample of wet milling and for the characterization of particle properties.

2.3.4 Ultrasonic production

The ultrasound equipment consists of a probe and high intensity ultrasonic processor/sonifier (Sonics and Materials Inc., Vibra Cell, Model VCX 500, Connecticut, USA) with temperature controller microprocessor. A high intensity solid probe (tip diameter 13mm) was immersed (tip 5 mm in process liquid in a jacketed flow cell) in the processing liquid(Muhammad et al., 2013). The device was operated at a fixed wavelength of 20 kHz and capable of producing a maximum power output of 500 W.

2.4 Particle characterisation

2.4.1 Determination of particle size distribution

2.4.1.1 Laser diffraction

The particles size distribution of samples were analysed using laser diffraction. The technique of laser diffraction is based around the principle that particles

passing through a laser beam which scatters light at an angle that is directly related to their size. As the particle size decreases, the observed scattering angle increases logarithmically. In this study, micro-particle sizing was carried out by laser diffraction through using Malvern Mastersizer Sirocco 2000 (Malvern Instruments Ltd., UK).

2.4.1.1.1 Analysis of raw materials

Measurements of particle size distributions of particle were obtained by using a laser diffraction particle sizer HELOS (Sympatec GmbH, System-Partikel-Technik, Germany). For each batch, the measurement was conducted and repeated in triplicate time adopting three individual samples.

Table 2-2 is the inspection of the particle size distribution of the raw materials, which shows the cumulative distribution of raw theophylline (TH00) and budesonide (BU00).

Table 2-2 Summary particle size statistics of the raw drugs

Samples	Particle Size Distribution		
	D10 (µm) (±SD)	D50 (µm) (±SD)	D90 (µm) (±SD)
TH00	11.18 (0.2)	27.74 (2.4)	67.85 (7.12)
BU00	0.57 (0.04)	1.38 (0.01)	0.04)

2.4.1.2 Dynamic light scattering

The Zetasizer Nano uses dynamic light scattering. Dynamic light scattering is based on Brownian motion of molecules or particles in suspension, which is the

motion induced by the bombardment from solvent molecules. The particles or molecules in suspension are illuminated with a laser which changes the intensity of the scattered light fluctuates. This change dependent upon the size of the particles as smaller particles create more fluctuations (Sartor). It is possible to compute the particle size distribution and give a description of the particle's motion in the medium, and measuring the diffusion coefficient of the particle.

2.4.1.2.1 Analysis of wet milling theophylline

The theophylline nanoscale suspension was evaluated using Zetasizer Nano (Malvern Instruments Ltd) to determine particle size distribution of theophylline suspension that was made by wet milling. Table 2-3 illustrate the average particles size of theophylline suspension at different time points.

Table 2-3 the average particles size of theophylline submicron suspension produced by wet milling (none stabilizer)

Time Point (minutes)	Particle diameter (nm)	Width of Size distribution (nm)
5	310.4	71.67
15	359.7	76.40
45	383.7	86.21
60	588.6	118.8
75	757.1	256.9

2.4.2 Power x-ray diffraction (PXDR)

PXDR is an application to detect the changes in the intensity of reflected beams relating to the crystal structure of samples. It works on the principle of keeping the wavelength constant and varying the angle of incidence, θ towards to the samples. The reflections of incidences obey the Bragg equation (Equation 2-1)(C.

Suryanarayana and Norton, 1998). The resultant diffracted X-Rays are detected and processed producing a diffraction pattern.

$$n\lambda = 2d_{hkI} \sin\theta \qquad \text{(Equation 2-1)}$$

where n is the order of diffraction, λ is the wavelength, d_{hkl} is the space between two lattice planes and θ is the angle of incidence (and reflection) of beam to the planes.

In this work, powder XRD analysis was conducted using nickel filtered Cu Kα, λ=1.542Å monochromatic radiation on a Bruker D-8 powder x-ray diffractometer (Bruker, Kahlsruhl, Germany). The anode X-ray tube was operated at 40 kV and 30mA. Measurements were taken at 2θ=5°-35° at a step size of 2θ=1° per min. Low background silicon mounts (Bruker AXS, UK) were used to support the sample during measurements.

2.4.2.1 Analysis of raw materials

The raw APIs were analysed by XRD to discover if there contained any amorphous content. As shown in Fig. 2-1, the samples were highly crystalline. The observed diffraction patterns are in accordance with published articles (Toropainen et al., 2006, Otsuka and Kinoshita, 2010), which demonstrate that the raw materials comply with the expected crystalline structures.

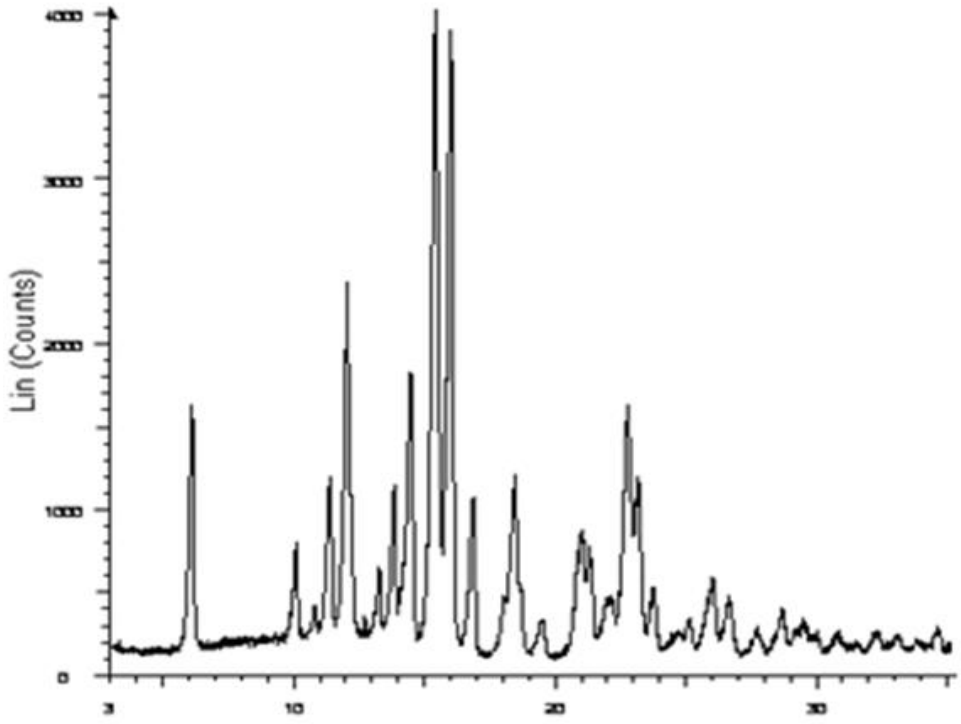

A

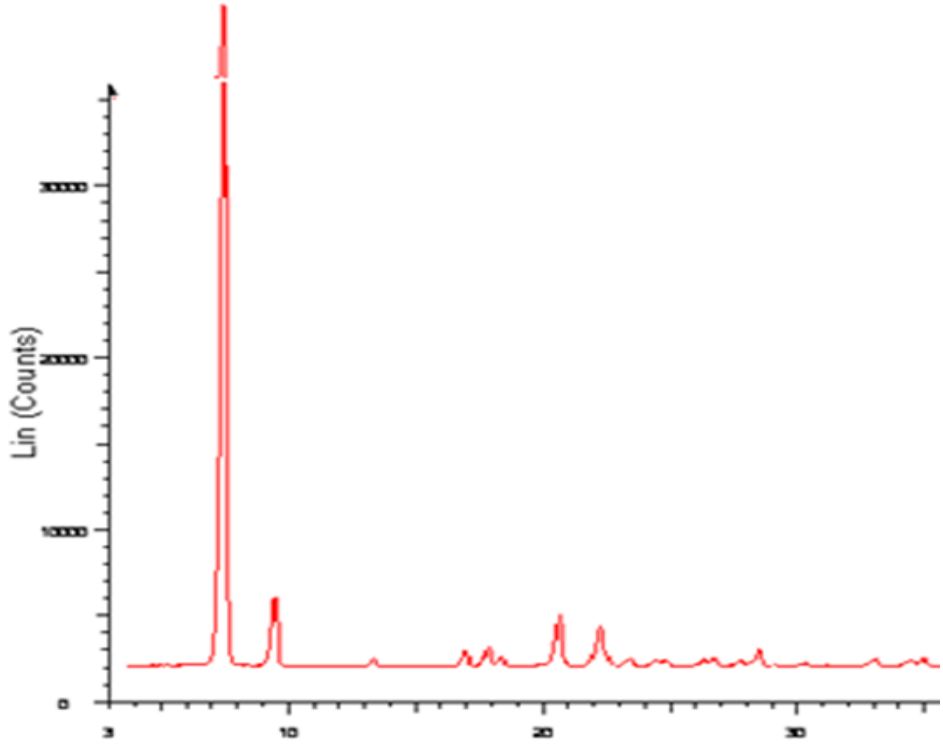

B

Fig. 2-1. XRPD patterns: A. Budesonide BU00; B. Theophylline TH00

2.4.3 Thermal gravimetric analysis (TGA) and differential scanning calorimetry (DSC)

Thermal gravimetric analysis (TGA) is used to measure the changes in weight of a sample in relation to the change in temperature. The weight changes of theophylline or budesonide associated with the decomposition or desorption is detected using a high precision electronic microbalance in the TGA.

Differential scanning calorimetry (DSC) thermograms were obtained using the TA instruments Q2000. It was used to detect the changes in heat flow between the sample and a reference, which is related to physical transformation, such as material melting, glass transition and fusion. Each of these parameters can be used to make an assessment of the degree of crystallinity or physical properties of polymer or hydrate of a sample.

Differential scanning calorimetry (DSC) experiments were conducted using TA instruments Q2000 (TA Instruments, UK). Hermetically sealed aluminium pans were used throughout the study. Moreover, Thermogravimetric Analysis (TGA) was performed using TA instrument Q5000 (TA Instruments, West Sussex, UK). It should be noted that a heating rate of 10 ◦C/min was set in all DSC and TGA measurements.

2.4.3.1 Analysis of raw materials

The result of thermal analysis for TH00 and BU00 are displayed in Fig. 2-2. According to the result, TH00 is stable up to approximately 200 ◦C and then loss weight dramatically. As for the BU00, it was found that it decompose at a temperature of approximately 280 ◦C. DSC confirms that both raw materials are crystalline with melting points of 260 ◦C and 270 ◦C, respectively.

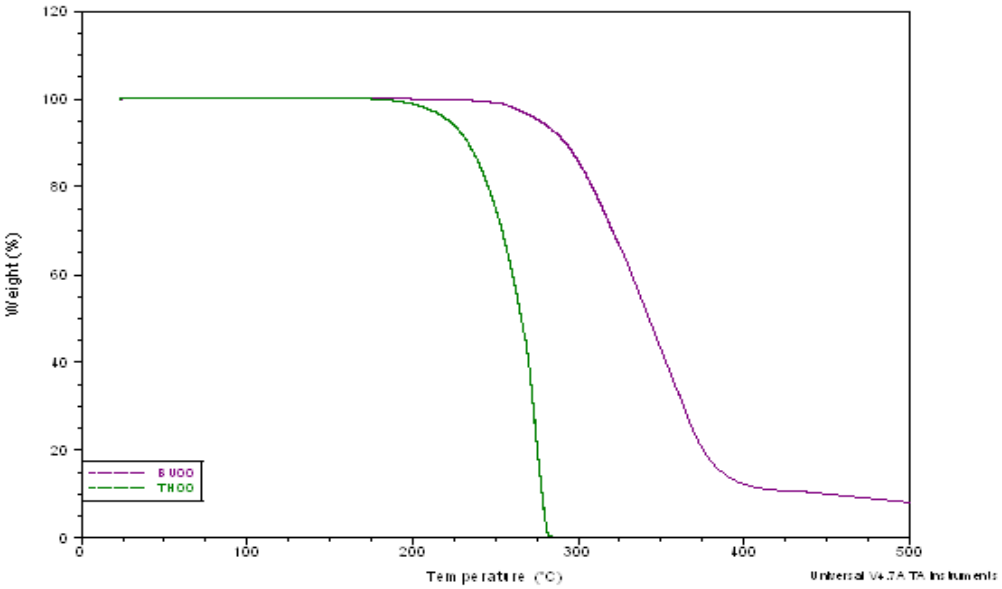

A

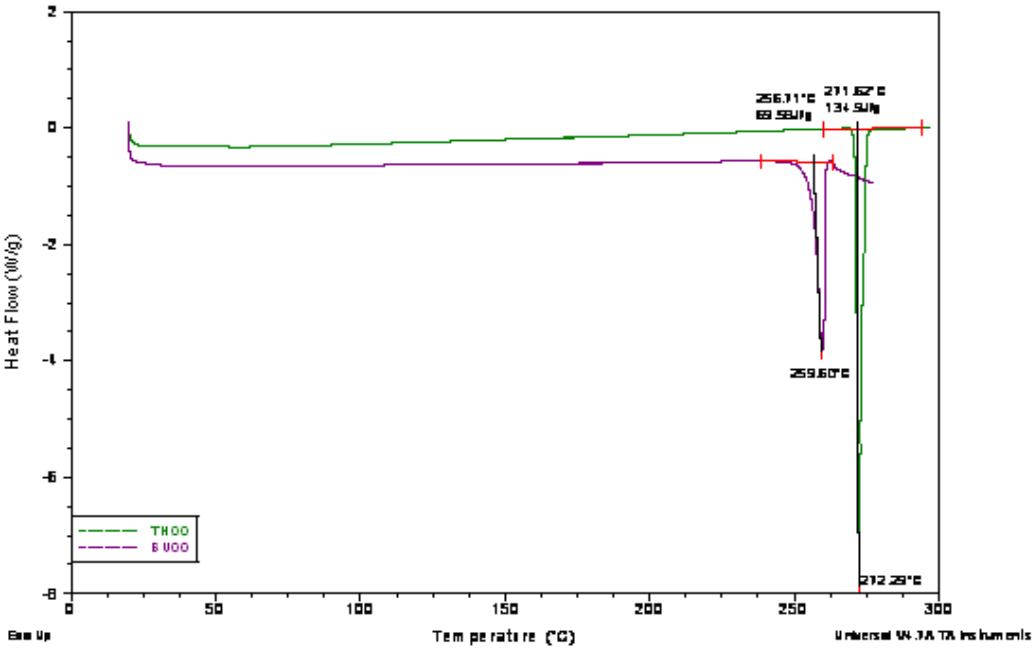

B

Fig. 2-2. Figure of thermal analysis for raw theophylline (TH00) and raw budesonide (BU00). A: TGA plots for TH00 and BU00; B: DCS plots for TH00 and BU00.

2.4.4 Scanning electron microscopy (SEM)

Scanning electron microscopy (SEM) is a type of electron microscope, which consists of a tungsten cathode, which emits a high energy electron beam. The electron beam is then accelerated towards an anode, and focused by condenser lenses. The focused electron beam is deflected horizontally and vertically by a pair of scanning coils. The electron beam exchanges the energy with the sample and emits the electrons and electromagnetic radiation, which are ultimately detected and imaged.

SEM analysis was performed using a Quanta 400 SEM (FEI Company, UK) variable pressure scanning electron microscope. Samples were glued onto aluminium stubs and sputter coated with gold prior to analysis.

2.4.4.1 Analysis of raw materials

All materials were analysed by SEM at a range of magnifications. The obtained images are shown in Fig. 2-3. As illustrated in Fig. 2-3, the size of TH00 is over ten times larger than BU00. The raw theophylline is needle-like shape with the particle size more than 50μm. In the Fig. 2-3-B, particle size of BU00 is about 5μm and particles bind together.

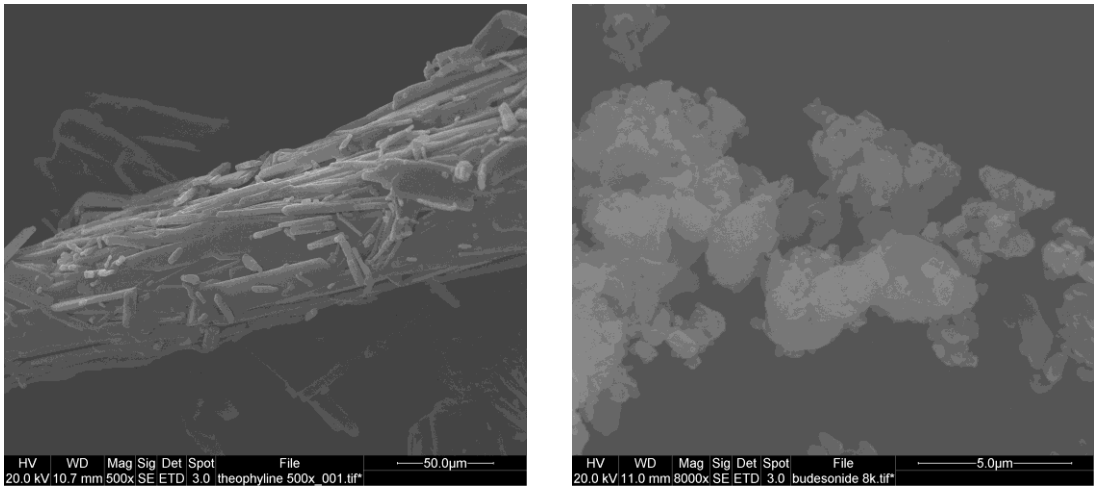

A **B**

Fig. 2-3. SEM of raw materials. A=TH00 x500, B=BU00 x8000

2.4.5 Dynamic vapour sorption (DVS)

Dynamic vapour sorption is a technique to measure changes in the mass of a sample at different relative humidities (RH). It is able to detect amorphous content down to a level of 0.5%.

The weight change of sample associated with the water vapour sorption and desorption was monitored using an IGAsorp moisture sorption analyser (Hiden Analyticals, UK). Each sample was loaded in a meshed sample basket and exposed to dry air until a constant weight was obtained. The relative humidity was then increased from 0% to 95% in 10% increments per step. Thereafter, the sample was exposed to RH of 95%. The humidity was then reduced in a stepwise down to 0%. All experiments were run at 25 ◦C (room temperature).

The result of DVS is illustrated in Appendix's Figure A2.

2.4.6 Inverse gas chromatography (IGC)

Inverse gas chromatography is a technique employed to detect the surface free energy of an unknown solid using a number of volatile probes. These probes include polar and non-polar probes, which bind to the surface of the sample and are eluted using nitrogen. Its retention time and volume can be detected via flame ionization detector(Buckton and Gill, 2007). The retention time and volumes then are utilised to calculate the surface free energy and specific energy, which influence moisture adsorption and desorption, wetting, dissolution, gas absorption, cohesion and adhesion. The dispersive component of the solid surface free energy (γ_s^{d}) is calculated by following relationships (Equation 2-2) (Gamble et al., 2011):

$$RT\ lnV_N = 2N\sqrt{\gamma_s^d a}\sqrt{\gamma_1^d + c} \qquad \text{(Equation 2-2)}$$

Where R is the gas constant, T is the temperature, N is the Avogadro's number, α is the projected surface are of the sample probe, $\gamma_1^{\mathrm{d}}$is the dispersive component of the probe, and $\mathrm{V_N}$ is the net volume of carrier gas. The surface free energy is determined from the slop of retention volume ($\mathrm{RT\ lnV_n}$) against $\mathrm{a}(\gamma_1^{\mathrm{d}})^{0.5}$.

In the experiment, IGC was run on a Hewlett Packard 5710A gas chromatograph. Nitrogen was used as the carrier gas while Air and hydrogen was adopted to enable the flame ionization detector at flow rate of 240 and 30 $cm^3\ min^{-1}$. The temperature of the injection port and the detector were set at 100 and 150 ◦C respectively. The injection volume was set at 0 ml to satisfy the requirement of infinite dilution and speed was set to NORM. The sample was loaded into a pre-silanised glass column which was deactivated by methanol, toluene and 5%

deimethychlorosilane and then the end of the column plugged with silanised glass wool.

2.4.6.1 Analysis of raw materials

The IGC analysis was carried out on samples of TH00 and BU00. The results from the analysed data shows that TH00 has similar dispersive energy to budesonide, which is (45.8±1.9 mJ/m^2) and (45±0.1 mJ/m^2) respectively. Also as can be noticed in Fig. 2-4, THF and ethyl acetate probes have a greater affinity for the TH than BU. These results suggest that acidic domains are exposed in theophylline rather than in budesonide. TH00 is considered to be more polar than BU00. This could be able to explain why theophylline has higher solubility in water than budesonide.

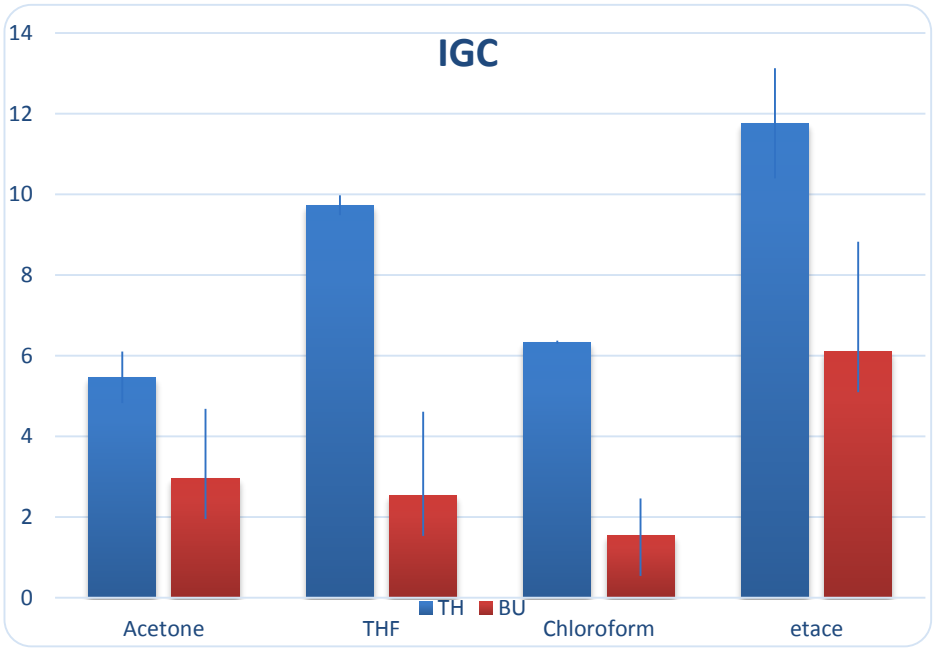

Fig. 2-4. Specific surface energies obtained for the TH00 and BU00. Energy values are in mJ/m^2. The number in graph is average result with error bars denoting SD.

2.4.7 Characterization of aerosols

Deposition of aerosols within the respiratory tract is dependent upon inertial impaction, gravitational sedimentation and Brownian diffusion (Yeh et al., 1976). Therefore, particle size, morphology and surface properties have the potential to affect pulmonary performances of aerosols. Among these parameters, particle size is an important factor in determining aerosol deposition and also in aerosol formulation.

2.4.7.1 Particle diameter

Drug particles in an aerosol are normally characterized for size using the parameter aerodynamic diameter (d_{ae}). The aerodynamic diameter is the diameter of a sphere with a unit density that has the same terminal settling velocity in still air as the particle in consideration (de Boer et al., 2002). It is measured by sizing techniques that are based on inertial impaction. The aerodynamic diameter (d_{ae}) is defined by the Equation 2-3 (de Boer et al., 2002, Hinds, 1982):

$$dae = dgeo\sqrt{\frac{\rho p}{\rho o \chi}} \qquad \text{(Equation 2-3)}$$

(dgeo: geometric diameter, ρp: particle density, ρo: unit densities, χ: dynamic shape factor)

Owing to this equation is generated by determination of sedimentation velocity of particles with unit shape, therefore, this equation is not suitable for the particle that varies across a size distribution. A descriptor of the particle size distribution is mass median aerodynamic diameter (MMAD) (Usmani et al., 2003). MMAD is a calculated aerodynamic diameter that is particle size distribution of half mass

of particles, and is a term along with the geometric standard deviation (GSD) to describe an aerosol. GSD is a parameter of polydispersity of an aerosol. It should be mentioned that Monodisperse and heterodisperse aerosols have a GSD of 1 and greater than 1.2 respectively (Musante et al., 2002).

For pulmonary drug delivery, the optimum particle size is required between 0.5 and 5µm to reach the lower respiratory tract for optimal pulmonary drug deposition. If the size of particles is outside of this range, it would either deposit in the oropharynx or be subject to exhaustion (Byron, 1986, Moren, 1987, Zanen et al., 1996).

2.4.7.2 *In vitro* assessment

In vitro methods are used to assess the uniformity of dose and particle size distribution of an aerosol. The main method of *in vitro* assessment is by inertial impaction. Inertial impaction is a precise and sensitive technique able to predict pulmonary performance of an aerosol. Currently the BP (2014) recommends the use of Apparatus A (glass impinger), Apparatus C (multi-stage liquid impinger) Apparatus D (Andersen cascade impactor) and Apparatus E (next generation impactor) for the sizing of aerosols (Agency, 2014).

2.4.7.2.1 Glass impinger (Twin stage impinger)

Fig. 2-5 illustrates a typical twin stage impinge (Agency, 2014). As can be seen, the glass impinger consists of two chambers, i.e. upper and lower. An aerosol is discharged from mouthpiece adaptor, and is fractionated according to particle size. The larger size would hypothetically impact in the upper respiratory tract. This fraction size would deposit in upper chamber. The respirable fraction should penetrate into lower chamber. This process is typically undertaken at operational

flow rate of 60±5 litres/min. The cut point of first stage is greater than 6.4µm and the second stage is less than 6.4µm. This leads to the glass impinger is not precise as other multi-stages impinger. However, for the sake of simplicity and time saving in the analysis, it is therefore usually adopted for routine quality assessment.

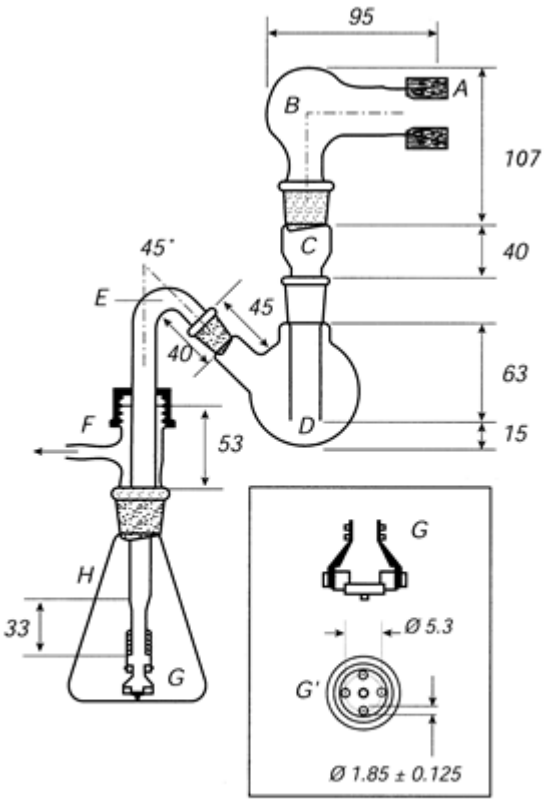

Dimensions in millimetres (tolerances ± 1 mm unless otherwise prescribed)

Component specification

Code	Item	Description	Dimensions*
A	Mouthpiece adaptor	Moulded rubber adaptor for actuator mouthpiece	
B	Throat	Modified round-bottomed flask:	50 mL
		– *ground-glass inlet socket*	29/32
		– *ground-glass outlet cone*	24/29
C	Neck	Modified glass adapter:	
		– *ground-glass inlet socket*	24/29
		– *ground-glass outlet cone*	24/29
		Lower outlet section of precision-bore glass tubing:	
		– *bore diameter*	14
		Selected bore light-wall glass tubing:	
		– *external diameter*	17
D	Upper	Modified round-bottomed flask	100 mL
	impingement	– *ground-glass inlet socket*	24/29
	chamber	– *ground-glass outlet cone*	24/29
E	Coupling tube	Medium-wall glass tubing:	
		– *ground-glass cone*	14/23
		Bent section and upper vertical section:	
		– *external diameter*	13
		Lower vertical section:	
		– *external diameter*	8
F	Screwthread,	Plastic screw cap	28/13
	side-arm	Silicone rubber ring	28/11
	adaptor	PTFE washer	28/11
		Glass screwthread:	
		– *thread size*	28
		Side-arm outlet to vacuum pump:	
		– *minimum bore diameter*	5
G	Lower jet assembly	Modified polypropylene filter holder connected to lower vertical section of coupling tube by PTFE tubing	see Figure 2.9.18.-1
		Acetal circular disc with the centres of four jets arranged on a projected circle of diameter 5.3 mm with an integral jet spacer peg:	10
		– *peg diameter*	2
		– *peg protrusion*	2
H	Lower	Conical flask	250 mL
	impingement chamber	– *ground-glass inlet socket*	24/29

* Dimensions in millimetres, unless otherwise stated.

Fig. 2-5. Apparatus of twin impinger is described by British Pharmacopeia 2014(Agency, 2014)

2.4.7.2.2 Multi-stage liquid impinger

A multi-stage liquid impinger (MSLI) consists of impaction stage 1 (pre-separator), 2, 3, and 4 and integral filter stage (stage 5), which can be shown in Fig. 2-6. As can be noticed, the cut-off diameter of each stage is 25, 13, 6.8, 3.1 and 1.7µm respectively. The outlet of impinger connects to a suitable vacuum pump, from which the flow rate of inlet is adjusted to 30 litres/min (±5 per cent). The MSLI has several advantages over the glass impinger in that the former device can classify the size distribution to greater degree. Further, the MSLI is calibrated to measure the particle size of an aerosol at flow rates ranging from 30 to 100 L/min.

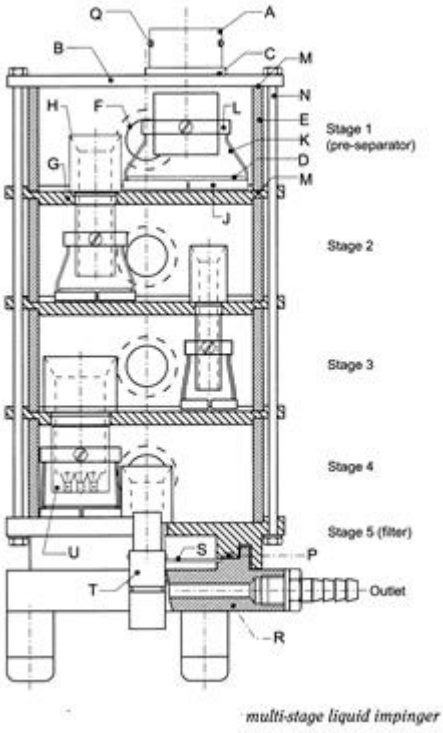

multi-stage liquid impinger

Dimensions[1] of jet tube with impaction plate

Type	Code[2]	Stage 1	Stage 2	Stage 3	Stage 4	Filter (stage 5)
Distance	1	9.5 (-.0+.5)	5.5 (-.0+.5)	4.0 (-.0+.5)	6.0 (-.0+.5)	n.a.
Distance	2	26	31	33	30.5	0
Distance	3	8	5	5	5	5
Distance	4	3	3	3	3	n.a.
Distance	5	0	3	3	3	3
Distance	6 [3]	20	25	25	25	25
Distance	7	n.a.	n.a.	n.a.	8.5	n.a.
Diameter	c	25	14	8.0 (± .1)	21	14
Diameter	d	50	30	20	30	n.a.
Diameter	e	27.9	16.5	10.5	23.9	n.a.
Diameter	f	31.75 (-.0+.5)	22	14	31	22
Diameter	g	25.4	21	13	30	21
Diameter	h	n.a.	n.a.	n.a.	2.70 (± .5)	n.a.
Diameter	j	n.a.	n.a.	n.a.	6.3	n.a.
Diameter	k	n.a.	n.a.	n.a.	12.6	n.a.
Radius[4]	r	16	22	27	28.5	0
Radius	s	46	46	46	46	n.a.
Radius	t	n.a.	50	50	50	50
Angle	w	10°	53°	53°	53°	53°
Angle	u	n.a.	n.a.	n.a.	45°	n.a.
Angle	v	n.a.	n.a.	n.a.	60°	n.a.

(1) Measures in millimetres with tolerances according to ISO 2768-m unless otherwise stated
(2) Refer to Figure 2.9.18.-5
(3) Including gasket
(4) Relative centreline of stage compartment
n.a. = not applicable

Fig. 2-6. Apparatus of MSLI is described by British Pharmacopeia 2014 (Agency, 2014)

2.4.7.2.3 Andersen cascade impactor

Fig. 2-7 describes an Andersen cascade impactor (ACI) which has been widely used in pharmaceutical aerosol characterization. It is designed to cover the size range of importance in pulmonary deposition. The ACI consists of eight stages together with a final filter. The diameter of the aperture on each stage decreases progressively. Impactor is measurements are conducted at flow rate of 28.3 litres/min; and the particles deposit on eight stages with different cut-off diameters of 9, 5.8, 4.7, 3.3, 2.1, 1.1, 0.7, and 0.4 respectively. The ACI is superior to both the twin impinger and MSLI in that the ACI can produce more detailed particle size distribution of the aerosolized drug. However, it still has some limitations including collection surface, overloading of collected particle deposits, and inter-stage loss.

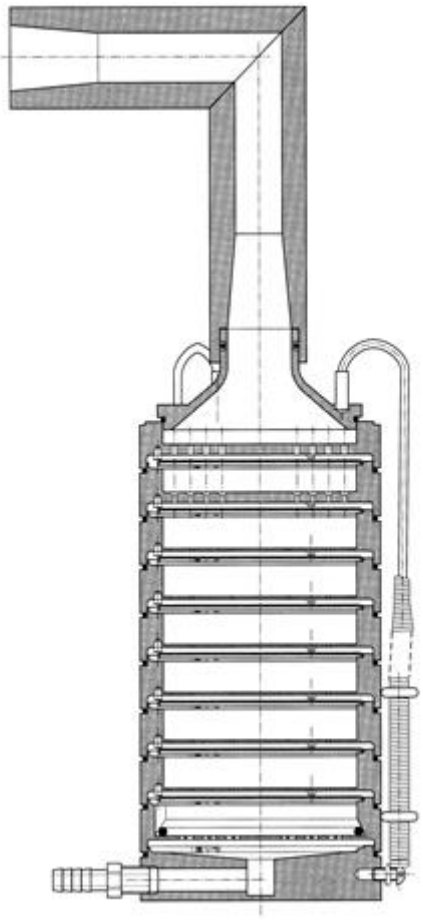

Andersen cascade impactor used for pressurised inhalers

Critical dimensions for apparatus

Description	Number	Dimension (mm)
Stage 0 nozzle diameter	96	2.55 ± 0.025
Stage 1 nozzle diameter	96	1.89 ± 0.025
Stage 2 nozzle diameter	400	0.914 ± 0.0127
Stage 3 nozzle diameter	400	0.711 ± 0.0127
Stage 4 nozzle diameter	400	0.533 ± 0.0127
Stage 5 nozzle diameter	400	0.343 ± 0.0127
Stage 6 nozzle diameter	400	0.254 ± 0.0127
Stage 7 nozzle diameter	201	0.254 ± 0.0127

Fig. 2-7. Apparatus of ACI is described by British Pharmacopeia 2014(Agency, 2014)

2.4.7.2.4 Next generation impactor (NGI)

The next generation impactor (NGI) is a seven stage cascade impactor, as depicted in Fig.2-8. It can be operated at flow rate range of 30 litres/min to 100 litres/min. The 50 percent-efficiency cut-off diameter is from 11.7 to 0.24 µm. Within this flow range, there are usually at least 5 stages with D50 values between 0.5 µm and 6.5 µm. The NGI is 50% more productive than the ACI, because a clean induction port/preseparator and set of cups can be inserted for a new test while samples from a previous test are processed. With semi-automated sample analysis provided by adjunct instruments, the NGI can handle

as many as 30 tests per day compared to the typical manual rate for an ACI of 5 per day (Copley).

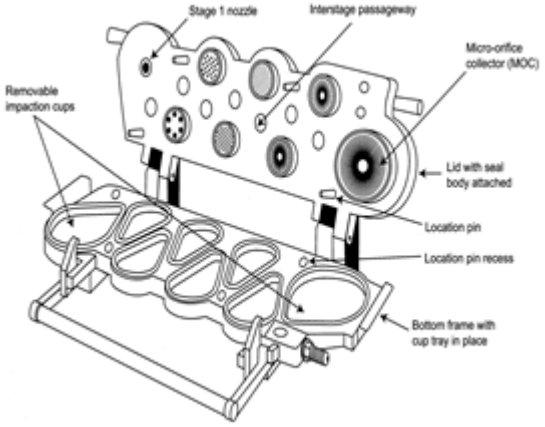

Critical dimensions

Description	Dimension (mm)
Pre-separator (dimension a - see Figure 2.9.18.-15)	12.8 ± 0.05
Stage 1* Nozzle diameter	14.3 ± 0.05
Stage 2* Nozzle diameter	4.88 ± 0.04
Stage 3* Nozzle diameter	2.185 ± 0.02
Stage 4* Nozzle diameter	1.207 ± 0.01
Stage 5* Nozzle diameter	0.608 ± 0.01
Stage 6* Nozzle diameter	0.323 ± 0.01
Stage 7* Nozzle diameter	0.206 ± 0.01
MOC*	approx. 0.070
Cup depth (dimension b - see Figure 2.9.18.-14)	14.625 ± 0.10
Collection cup surface roughness (Ra)	0.5 - 2 µm
Stage 1 nozzle to seal body distance** - dimension c	0 ± 1.18
Stage 2 nozzle to seal body distance** - dimension c	5.236 ± 0.736
Stage 3 nozzle to seal body distance** - dimension c	8.445 ± 0.410
Stage 4 nozzle to seal body distance** - dimension c	11.379 ± 0.237
Stage 5 nozzle to seal body distance** - dimension c	13.176 ± 0.341
Stage 6 nozzle to seal body distance** - dimension c	13.999 ± 0.071
Stage 7 nozzle to seal body distance** - dimension c	14.000 ± 0.071
MOC nozzle to seal body distance** - dimension c	14.429 to 14.571

* See Figure 2.9.18.-13
** See Figure 2.9.18.-14

Fig. 2-8. Apparatus of NGI is described by British Pharmacopeia 2014(Agency, 2014)

For assessment of the aerodynamic behaviour of the particles, the powder had to be dispersed into an air stream. In this assessment, the Aeroliser® device was used to test the aerosolisation of the dry powders.

The aerodynamic behaviour of the particles was assessed using a Next Generation Impactor (NGI, Copley Scientific Limited, Nottingham, UK) at a flow rate of 60 L/min, which corresponds to a run time of 4s for an inspiration flow of 4L (Agency, 2014). The powder was directly weighed into HPMC capsule (Size 3, CAPSUGEL, Germany) or an interactive mixture of particles with lactose (Respitose® ML001, DFE Pharma, Germany) as carrier was made and

subsequently weighed into capsules. In order to obtain a good quality lactose-APIs mixture and physical mixture of APIs sandwich- method was used. Theophylline:budesonide were mixed at ratio of 20 to 1. The filled capsules were stored dry until used and then individually placed in the Aeroliser® device. If the capsule was not emptied at the first discharge, a second actuation followed as described in the user instructions of the Aeroliser® device.

All capsules were collected after emptying and washed with 80% methanol to determine the amount of APIs. All NGI stages as well as the throat and the preseparator were washed with 80% methanol to dissolve the drug on the stages for HPLC analysis. All measurements were performed in triplicate. FPF was calculated as the percentage of drug particles below a size of 5μm. When the flow rate is 60 L/min, stage 4 until the MOC were utilised.

2.4.8 Drug quantification

Determination of drug content and analysis of NGI measurements was carried out using HPLC (Waters Corp., USA). A 5 μm Nucleosil C18 column (SUPELCO INC. USA) with Nucleosil® Guard Column (SUPELCO INC. USA) was used as stationary phase, which was conditioned to 37 ◦C in a column oven. As mobile phase a mixture of methanol and water (80:20) was used. Flow rate was 1 mL/min; detection wavelength was 270 nm for theophylline (tr for theophylline 2.8 min). The wavelength of 244 nm was used to detect budesonide (tr for budesonide 3.8 min).Quantification was carried out by an external standard method.

2.5 Statistic analysis

2.5.1 Design of experiments (DOE)

Design of experiments (DOE) is the design of any information-gathering exercises where variation is present (JMP, Barrentine, 1999). DOE can identify

important interactions that may be missed when experimenting with one factor at a time to determine whether the experiments are under the full control or not. It is also a process to organize the experiment properly to ensure that the amount of reliable data is available to answer the questions of interest as clear and efficient as possible.

On the other hand, DOE is the simultaneous study of several process variables. By combining several variables in one study instead of creating separate study for each, the amount of testing required will be drastically reduced and greater process understanding (Barrentine, 1999) can be attained. The objectives of the DOE here are:

1. To understand how to change a process average in desired direction
2. To learn how to reduce process variation
3. To learn how to make response controllable
4. To identify which variables are important or not

Before experimentation, a hypothesis should be made and terminology should be defined (Barrentine, 1999). According to literature (Barrentine, 1999), the following actions should be considered for better managing of an experiment.

1. Define the process to be studies
2. Determine the responses
3. Determine the measurement precision and accuracy
4. Generate candidate factors
5. Determine level of factors
6. Select the experimental design
7. Have a plan to control extraneous variables

8. Perform the experiments according to the design
9. Analyse and draw conclusions
10. Verify and documents the new process
11. Propose the next study

The screening design, full factorial deign and fractional factorial design have become popular in industry and academic research over the last decade. Screening design is typically used in the initial stages of experimentation. They examine many factors to identify those that have the greatest effect on the response or responses. The identified factors are then studied using more sensitive designs. This experimental design is popular for 2 or more factors with two-level (JMP)

A full factorial design contains all possible combinations of a set of factors. This is the most fool proof design approach, but it is also the most costly in experimental resources. Thereby, full factorial design is suitable for small data set. In full factorial designs, experiments run at every combination of the factor levels. The sample size is the product of the numbers of levels of the factors. For example, a factorial experiment with a two-level factor, a three-level factor, has 2 x 3 = 6 runs (JMP).

If full factorial design is too high to be logistically feasible, a fractional factorial design may be done, in which some of the possible combinations are meaningless. In statistics, fractional factorial designs are experimental designs consisting of a carefully chosen fraction of the experimental runs of a full factorial design (Wikipedia, 2012). The fraction is chosen experiments which are the most important features of the problem studies, while using a fraction of the effort of a

full factorial design in terms of experimental runs and resources. An important property of a fractional design is its resolution to separate main effects and low-order interactions from one another. There are six types of resolution. Among them, Resolution III, IV and V are important and common designs (SUPPORT).

The resolution III is used for the situation, which no main effects are aliased with any other main effect, but main effects are aliased with 2-factor interactions. Example can be given as: 2^{3-1} with defining relation I = ABC. As for Resolution IV, it can resolute the factors, in which no main effects are aliased with any other main effect or 2-factor interactions, but some 2-factor interactions are aliased with other 2-factor interactions and main effects are aliased with 3-factor interactions. Example can be shown as: 2^{4-1} with defining relation I = ABCD. Resolution V is suitable for the factors, which do not have main effects or 2-factor interactions are aliased with any other main effect or 2-factor interactions, but 2-factor interactions are aliased with 3-factor interactions and main effects are aliased with 4-factor interactions. Example can be elucidated as: 2^{5-1} with defining relation I = ABCDE.

2.5.2 Regression analysis

In statistics, regression analysis is a statistical process for estimating the relationships among variables. It includes many techniques for modelling and analysing several variables, when the focus is on the relationship between a dependent variable and one or more independent variables. More specifically, regression analysis helps one understand how the typical value of the dependent variable changes when any one of the independent variables is varied, while the other independent variables are held fixed. Most commonly, regression analysis estimates the conditional expectation of the dependent variable given the

independent variables. That is the average value of the dependent variable when the independent variables are fixed. Less commonly, the focus is on a quantile, or other location parameter of the conditional distribution of the dependent variable given the independent variables. In all cases, the estimation target is a function of the independent variables called the regression function. In regression analysis, it is also of interest to characterize the variation of the dependent variable around the regression function which can be described by a probability distribution.

Regression model describes relationship between a scalar dependent variable and one or more explanatory variables. It is a method of analysis for assessing the coefficients between a set of independent variables and dependent variable. Applying regression analysis to a set of data results in what are known as regression coefficients, one for each explanatory variable. Therefore, the regression model is useful for a response variable with observed values.

The mathematical expression for regression model can be described as below:

$$Y = \beta_0 + \beta_1 x_1 + \beta_2 x_2 \ldots + \beta_p x_p + \epsilon \qquad \text{(Equation 2-4)}$$

The regression coefficients, β_0, $\beta_1 \ldots \beta_p$ are generally estimated by least squares. The fit of a regression model can be judged with calculation of the correlation coefficient, R^2, defined as the correlation between the observed values of the response variable and the values predicted by the model (Paul R. Kinnear and Gray., 2008). This model was generated using SPSS software (IBM SPSS statistics 19, USA).

Analysis of variance (ANOVA) is a collection of statistical models used to analyse the differences between group means and their associated procedures, such as "variation" among and between groups (Julie, 2013). In the ANOVA setting, the observed variance in a particular variable is partitioned into components attributable to different sources of variation. In its simplest form, ANOVA provides a statistical test of whether or not the means of several groups are equal, and therefore generalizes the t-test to more than two groups. As doing multiple two-sample t-tests would result in an increased chance of committing a statistical type I error, ANOVAs are useful in comparing (testing) three or more means (groups or variables) for statistical significance. ANOVA is a special case of regression, which was implemented using SPSS software (IBM SPSS statistics 19, USA).

The mathematical model of ANOVA can be expressed as:

$$Y = \beta_0 + \beta_1 x_1 + \beta_2 x_2 \ldots + \beta_{1\ldots n} x_{1\ldots n} + \epsilon \qquad \text{(Equation 2-5)}$$

2.5.3 Artificial neural network (ANN)

Artificial neural networks are computational models inspired by animals' central nervous systems (in particular the brain) that are capable of machine learning and pattern recognition (Gevrey et al., 2003). They are usually presented as systems of interconnected "neurons" that can compute values from inputs by feeding information through the network, as depicted in Fig. 2-9. ANN provides the most flexibility for situation, in which user may not have a clear understanding of the scope of information contained within data set, and therefore may not have specific hypotheses from which to begin an analysis.

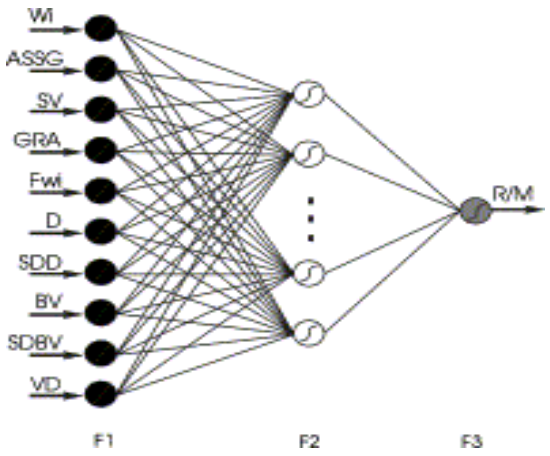

Fig. 2-9. Structure of the neural network used in this study. F1, input layer of neurons comprising as many neurons as variables at the entry of the system; F2, hidden layer of neurons whose number is determined empirically; F3, output layer of neurons with a single neuron corresponding to the single dependent variable (Gevrey et al., 2003).

Artificial neural networks are well established and many applications have been reported in pharmaceutical formulation and processing (Shao et al., 2006). The range of applications has been reviewed by Colbourn and Rowe (Colbourn and Rowe). Neural networks are useful in detecting complex non-linear relationships between a set of inputs and outputs and estimate magnitude of the relationships without requiring a mathematical description of how the output functionally depends on the input. The training process depends on the training vector and on the topology of the ANN. The ANN manages to converge if the training data are adequate to create the appropriate discriminations between the different output classes.

In this study, there was shown to be some linkages between excipients and physical properties of particles. This section describes the modelling of experimental data able to provide some reliable indication of morphology and

performing outcomes of particles from knowledge of particles properties and their characteristics. In order to discover relations between the excipients and properties of formulation, pooled data from the experiment were analysed using commercially available ANN software (INForm v3.4, Intelligensys, UK). A description of this application and its utility for modelling pharmaceutical formulation and processing data has previously been given in (de Matas et al., 2008).

For neural network training purposes, processing parameters were treated as independent variables (inputs) and physical properties and morphology of particles as the response variable (output). In order to avoid overtraining of ANN, ANN model was established by leave-one-out cross validation technique. The database was divided into a training set (k-1 data records), a test set (1 data records) and a validation set (1 data records). Training and test data were used by the ANN to learn the cause effect relationships, inherent in the data set, whilst the validation data, which were excluded from training, were used to assess the predictability of generated models.

2.5.4 Cross validation

Due to small sample size, in order to avoid the over-fitting of ANN model, k-fold cross validation was chosen to validate the quality of models. Cross-validation is a model validation technique for assessing how the results of a statistical analysis will generalize to an independent data set. It is mainly used in settings where the goal is prediction, and one wants to estimate how accurate a predictive model will perform in practice (Mirzaie et al., 2014, Afshin Maleki et al., 2014). It is worth highlighting that in a prediction problem, a model is usually given a dataset of

known data on which training is run (training dataset), and a dataset of unknown data (or first seen data) against which the model is tested (testing dataset). The goal of cross validation is to define a dataset to "test" the model in the training phase (i.e., the validation dataset), in order to limit problems like overfitting and give an insight on how the model will generalize to an independent data set (i.e., an unknown dataset, for instance from a real problem).

K-fold cross-validation is a model selection tool. The k-fold cross-validation splits the training-validation data set into k equally-sized blocks. At each stage, k-1 blocks are used for estimating the model and the remaining block is used for computing its average prediction error (mean squared error, MSE). The blocks used for estimation are called the training data and the block used for prediction diagnostics is called the validation data. The process repeats itself until each single block is used as the validation data. The results from k different validation procedures are averaged to produce the overall cross-validation score. The cross-validation score is an estimate of the true prediction error on the training-validation data set (stanfordphd).(stanfordphd)(stanfordphd)(stanfordphd)

2.6 Conclusion

The characterisation of the samples was studied using an array of analytical methods. Moreover, similarities and differences in the physical properties of such materials were also investigated. The supplied micronized drugs were similar to each other in terms of particle size and shape. The differences between materials characterised using DVS, DSC and XRPD were observed. Importantly, the physicochemical characterisation of the pharmaceutical materials shown in this chapter will be compared to those of processed particles in the following chapters.

Chapter 3 : Production of Inhalable Theophylline using Jet Milling, Wet Milling and Spray Drying

3.1 Introduction

The advantages of pulmonary delivery of drug have been reviewed and discussed in the previous chapter. From these findings, it can be estimated that inhalation of theophylline would be an ideal delivery methodology to avoid the side effects caused by high concentration of theophylline; and slower and uncontrollable metabolism yield by its oral administration, leading to better bioavailability and treatment performance (Cosio et al., 2004). Manufacturing of inhalable theophylline requires powders with desirable characteristics. Among of micronizing techniques, jet milling and spray drying were widely used in industry product, while the wet milling can achieve nano-size particles (Peltonen and Hirvonen, 2010).

In this study, jet milling, spray drying and wet milling were used to reduce the size distribution of theophylline. Jet milling reduces particle size via high velocity particle-particle collision. Spray drying is a one-step process that converts a liquid feed into a dried particle (Aulton, 2009), where feed solution is atomized from nozzle to form small droplets, and droplets contact with air and getting dry. The advantage of this technique is that it can be used for drying any type of fluid. In wet milling, micron size drug crystals are media milled in a water-based solution and reduced to nanometer-sized particles. This technique has been identified as a useful procedure to develop formulations of poorly-water-soluble compounds.

3.1.1 Aim and scope of the works

The aim of this study is to produce micronized theophylline that has suitable morphology for aerosol dispersion, using jet milling, spray drying and wet milling. The high energy input of jet milling and spray dry can cause area of powder surface to become amorphous, which can lead to poor flowability and hinder the removal of the powder from an inhaler. The extraordinary reduction of particle size distribution in wet milling can cause a high level of agglomeration. Therefore, in order to develop inhalable theophylline, firstly it needs to investigate and compare the morphology changes caused by these processes. Additionally, aerodynamic behaviour of micronized particles has to be examined. In this study, Aeroliser® is used as a model device. The batch of sample that has the best aerodynamic property is selected for physical mixture. Finally, the aerosolization performance of theophylline/budesonide physical mixture will be tested.

3.2 Materials

3.2.1 Active drugs

The active drugs used in this experiments can be found in Chapter 2.2.1.

3.2.2 Chemicals for IGC

All chemicals used for IGC have been indicated in Chapter 2.2.3.

3.3 Methodologies

3.3.1 Micronization of theophylline

3.3.1.1 Jet milling

The processing of jet milling has been illustrated in Chapter 2.3.1.

3.3.1.2 Spray drying

The processing of spray drying has been explained in Chapter 2.3.2.

This solution was prepared by ultrasonication at room temperature (20 ◦C). The solvent contains 80% (v/v) ethanol and 20% (v/v) deionised water, where the concentration is about 2.9%W/V.

3.3.1.3 Wet milling

The procedure of wet milling has been demonstrated in Chapter 2.3.3.

3.3.2 Thermal analysis

The procedure of thermal analysis (TGA and DSC) have been described in Chapter 2.4.3.

3.3.3 X-ray diffraction (XRD) analysis

The processing of XRD has been mentioned in Chapter 2.4.2.

3.3.4 Visualisation of particles

The SEM analysis has been described in Chapter 2.4.4.

3.3.5 Particle sizing

The Measurements of particle size distributions of particle have been mentioned in Chapter 2.4.4.

3.3.6 Aerodynamic assessments

The aerodynamic assessments were analysed by next generation impactor (NGI). The descriptions have been elucidated by Chapter 2.4.7.2.

3.3.7 Drug quantification

This analysis has operated by high performance liquid chromatography (HPLC). The processing has been demonstrated in Chapter 2.4.6.

3.4 Results and discussion

3.4.1 Reduction of particle size

Laser diffraction was used to analyse the size distribution of micronized theophylline. Following jet milling, theophylline caused the powder to change colour from transparent to white. It was observed that the size of powder was reduced dramatically to less than 5µm, which has been indicated in Table 3-1. Table 3-1 displays the particle size distributions of raw material and processed samples. It can be observed that the geometric particle size distribution of raw theophylline (TH00) is out of measurement range (between 0.2 and 87.5µm). The batch TH01 has a size distribution of D50=1.20µm±0.13, VMD=1.23µm±0.12, respectively. The wet milling sample has a particle size of approximately 400nm at 45 mins in suspension, but after air drying the final sample (TH03), the size distribution increases dramatically. Table 3-1 also indicates that the spray drying sample (TH02) contains big particle, which is 74.78±0.76µm of D90.

Table 3-1 Particle size distribution of TH00, TH01, TH02 and TH03 (raw theophylline: Th00; jet milling: TH01; spray drying: TH02; wet milling: TH03)

Samples	Particle Size Distribution		
	D10 (µm)	D50 (µm)	D90 (µm) (±SD)
TH00	11.18±0.2	27.74±2.4	87.5 (Maximum)
TH01	0.74±0.053	1.20±0.13	1.76±0.23
TH02	0.74±0.03	4.21±0.18	74.78±0.76
TH03	0.885±0.21	2.91±0.21	54.815±0.28

According to the size distributions of each batches, all the batches meet the requirement for the inhalable range (1-5µm) (de Boer et al., 2002). Particularly,

jet milling could produce a micro-particle with narrower size distribution, rather than wet milling and spray dry.

3.4.2 Thermal analysis (differential scanning calorimetry (DSC) and thermogravimetric analysis (TGA))

Fig. 3-1 is the DSC profile of raw theophylline and micronized samples. The micronized samples, TH01, TH02 and TH03, showed no evidence of conversion to amorphous form as observation for raw theophylline (TH00) can be seen in the DSC profile of Fig. 3-1.

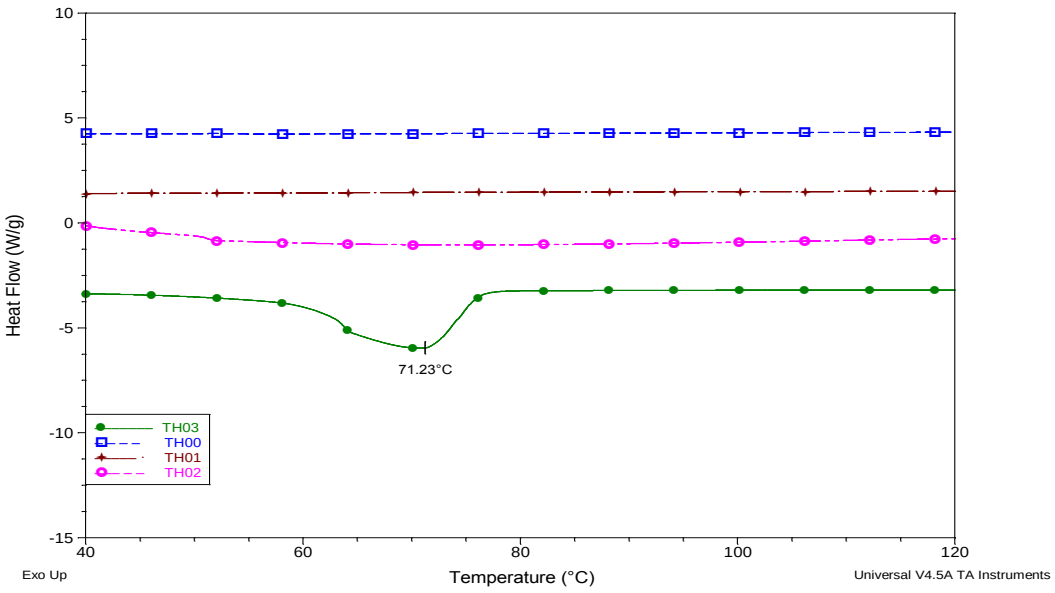

(a).Endotherm below 100 °C

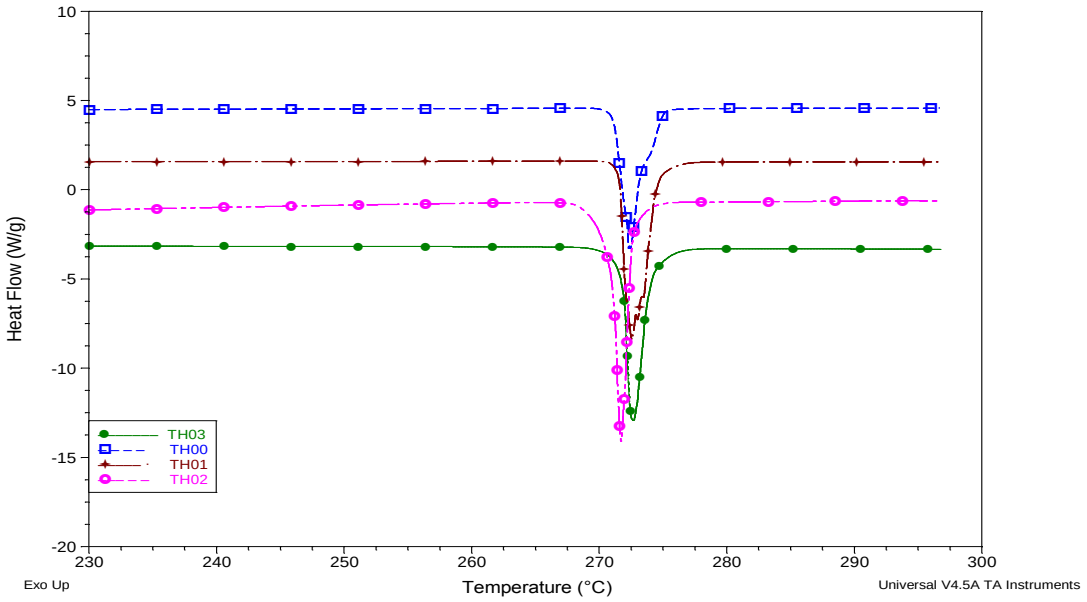

(b). Melting point of samples

Fig. 3-1. DCS plots for raw theophylline (TH00) and its samples milled using jet mill (TH01), spray drying (TH02) and wet mill (TH03). (a) is endotherm that is below 100°C, and (b) indicate the heat change over 240°C.

However, as can be found in Fig. 3-1-b, DSC data of TH03 reveals that an endotherm was observed below 100 °C. This finding is in good agreement with the figure published in the literature (Suihko et al., 1997). This endotherm is related to theophylline monohydrate, which concurs with the findings of TGA in Fig. 3-2. As can be seen in Fig. 3-2, TH03 loss approximately 9% of mass at temperature of 80 °C. This weight lost is to be the dehydration of TH03, which suggests that anhydrous theophylline is converted to monohydrate theophylline (TH03) during wet milling.

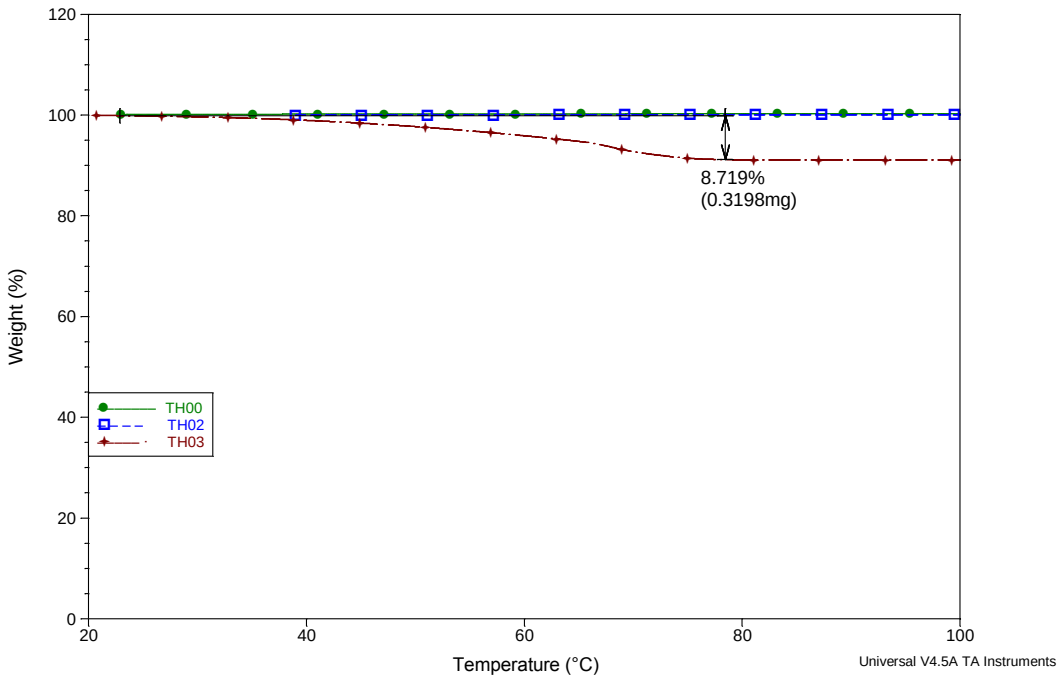

Fig. 3-2. TGA profiles of the Theophylline before and after milling using jet mill and wet mill, 8.719% of weight loss was found at temperature of 79 ◦C

3.4.3 Characterization of particles

3.4.3.1 PXRD analysis

Fig. 3-3 is the patterns of PXRD. The powder diffraction patterns obtained from the micronized theophylline (TH01, TH02, and TH03) are compared with the powder patterns of pre-milled sample (TH00). According to Fig. 3-3, no notable evidence of amorphous theophylline are observed.

As can be discovered in patterns of DSC as shown in Fig. 3-2, the peaks of micronized samples are low intensity, slightly broader and less well defined. In XRD figure, new peaks are observed at 32º and 42º, whilst all peaks accordant with the recommended sample TH00 as described in Fig.3-3. These changes are

caused by size reduction. Owing to size reduction, the fresh surfaces has been exposed.

Moreover, in pattern of TH03, there are several new peaks on 9^o, 12^o and 14^o, as described in (Suihko et al., 1997, Otsuka and Kinoshita, 2010), these peaks correspond to those known for theophylline monohydrate.

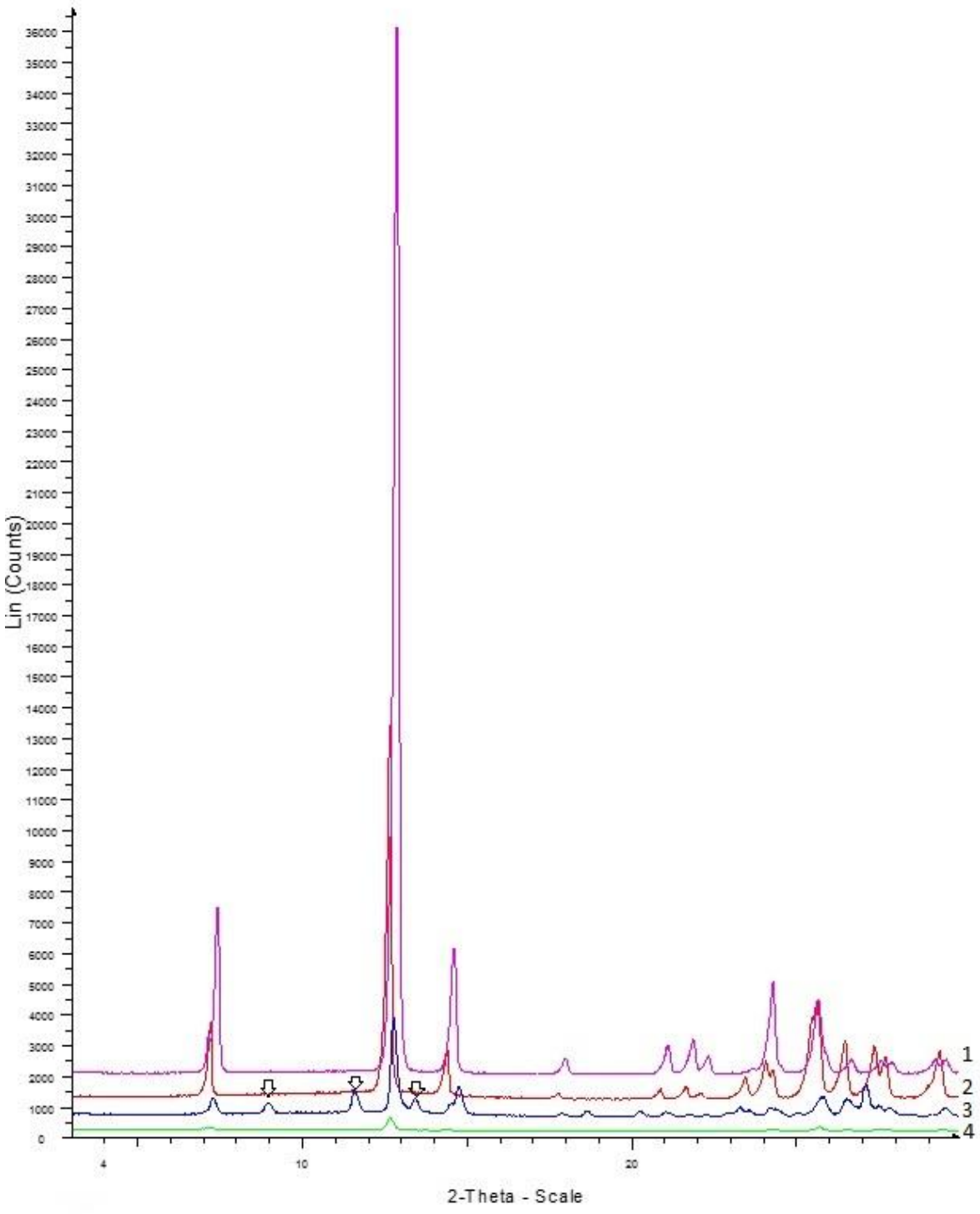

Fig. 3-3. XRPD patterns produced by Theophylline before and after micronizing using jet mill, spray drying and wet mill. 1: raw theophylline (TH00); 2: jet milling sample (TH01); 3: wet milling sample (TH03), new peaks on 9º, 12º and 14º were indicated by arrow; 4: spray dried sample (TH02)

3.4.3.2 Inverse gas chromatography (IGC)

In order to detect the surface energy change after processing, IGC analysis has been carried out on raw material and micronized samples. These are the raw material TH00, spray drying TH02; and the TH01 and TH03 forms after jet and wet milling. The obtained data shows that dispersive energies are greater for the processed samples compared with their pre-micronized counterparts (45.8±1.9 mJ/m^2). The spray drying TH01 has value of 63.83±0.52 mJ/m^2. The milled forms have values of 63.00±0.45 mJ/m^2 and 66.40±0.67 mJ/m^2 for TH01 and TH03 respectively. According to specific energies analysis of Fig. 3-4, THF and ethyl acetate probes have a greater affinity for the TH01 and TH02, indicating the exposure of acidic groups. There a large STDEV error in TH03 was detected. This result suggests that TH03 exposed acidic groups after wet milling, however some acidic groups was hydration reaction, which respond what have been discovered in previous DSC, TGA, and PXRD studies. The chloroform probe has a less affinity for the samples, again demonstrating the exposure of acidic groups on surface.

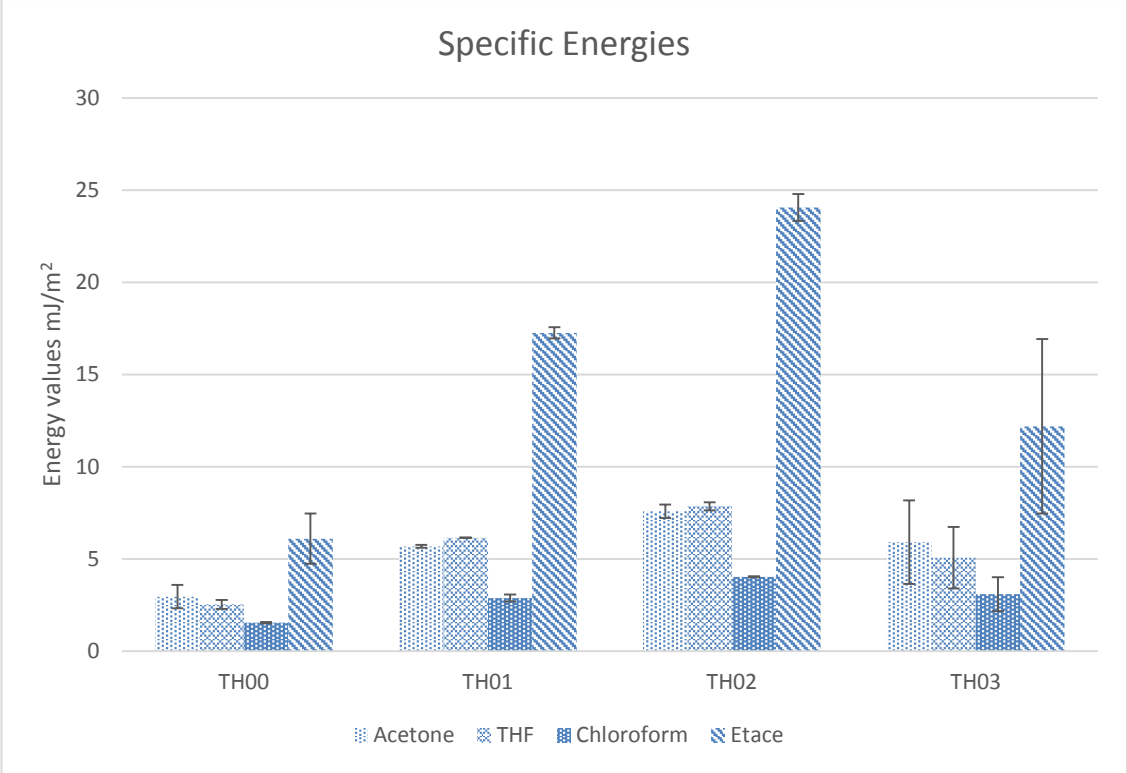

Fig. 3-4. Specific energies obtained for the TH00, TH01, TH02 and TH03. Energy values are in mJ/m^2. The numbers resented in graph are the average results for specific energies.

3.4.3.3 Scanning electron microscopy (SEM)

All materials were analysed by SEM under a range of magnifications. The obtained results are illustrated in Fig. 3-5. It can be seen that the size of particle (Fig. 3-5-B, C, D) is reduced dramatically compared with the raw materials (Fig. 3-5-A). The shape of particles is irregular; and the small particles aggregate together.

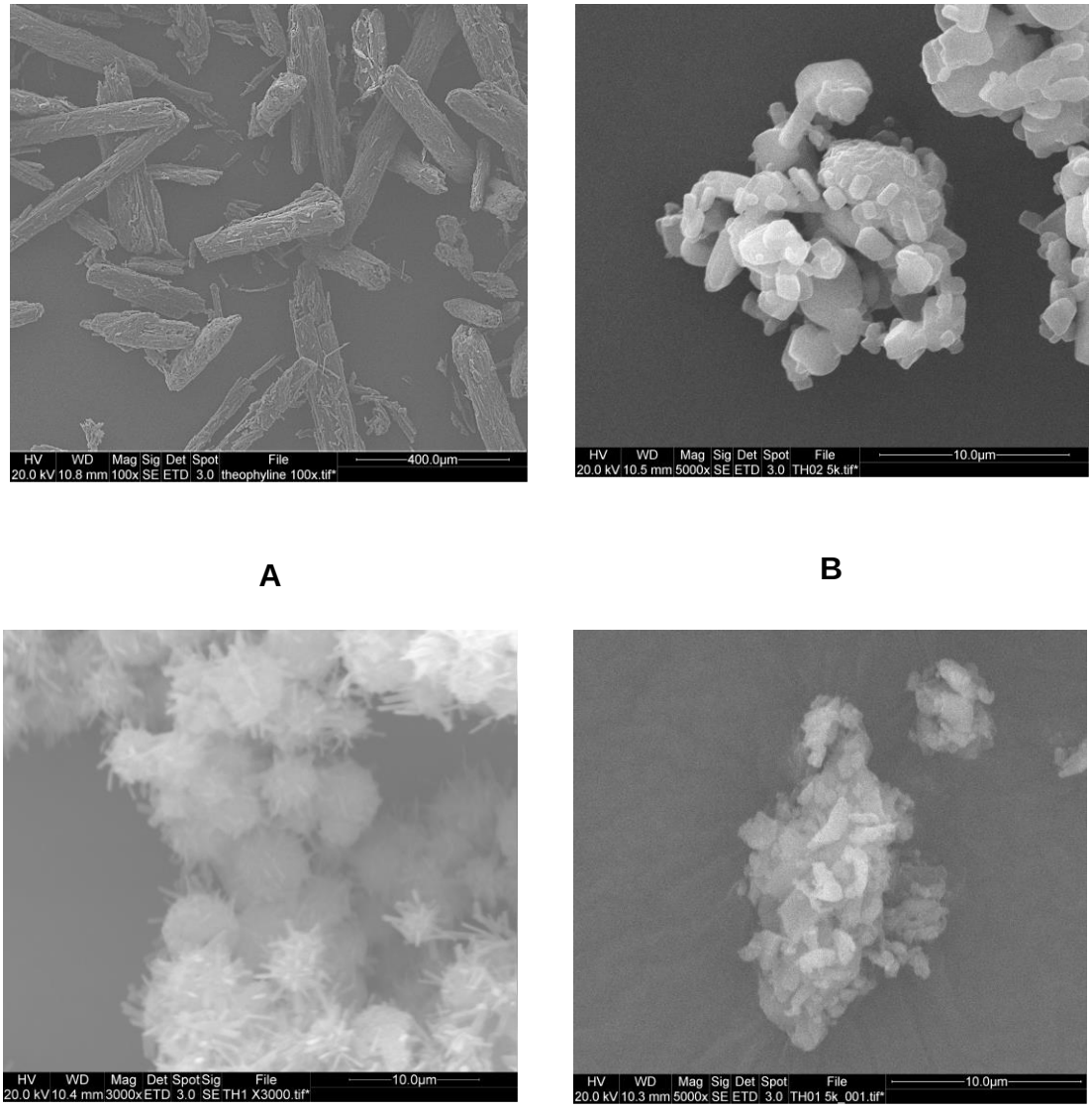

Fig. 3-5. SEM of all materials. **A**=raw theophylline x100, **B**=TH01 x5000, **C**=TH02 x3000, **D**=TH03 x5000

The laser diffraction data is described in Table 3-1, which demonstrates that the micronized batch TH01 has a narrower particle size distribution than the TH02 and TH03. SEM data confirms this result, which shows that smaller particles existed with a higher level of particle agglomerations for TH02 (Fig. 3-5-C), but SEM found the TH02 particles form a pollen-like particles. Fig. 3-5-D is the SEM

result of wet milling batch TH03. It can be observed that TH03 is smaller than TH02 and TH00, however the fine particles of TH03 are tight together and become larger, which confirms the observation of laser diffraction for TH03.

3.4.3.4 Aerodynamic behaviour

The assessment of the aerodynamic behaviour was test using the NGI. According to the morphology and thermal analysis, TH03 has been proved that it is the monohydrate theophylline. Thereby, TH01 and TH02 were used to characterize the aerodynamic properties. In the aerodynamics analysis, TH01 and TH02 were delivered by mixed/absented with lactose. The assessment results and sample batches, i.e. TH01, TH02, blend I, blend II, blend III, and blend IV, are presented in Table 3-2. All the results are the average of each analysis that was repeated three times.

Table 3-2 The aerodynamic properties of different preparations of resultant samples and lactose using Aeroliser® at 60 L/min; TH01: jet milling sample, delivery drug only; TH02: spray drying sample, delivery drug only; Blend I: physical mixture of TH01 and lactose ML001; Blend II: physical mixture of TH02 and ML001; Blend III: physical mixture of TH01, micronized budesonide(BU) and lacto ML001; Blend IV: physical mixture of TH02, BU and ML001 FPF: fine particle fraction; MMDA: mass median aerodynamic diameter

Dispersed samples	**FPF_{loaded} (%)**	**$FPF_{emitted}$ (%)**	**Impaction recovery (%)**		**MMDA**
			Theophylline	**Budesonide**	
TH01	9.6±5.3	22.4±3.0	33.3±8.9	-	4.5±0.8
TH02	11.9±2.7	21.0±2.9	33.0±8.9	-	5.1±0.02
Blend I (ML001+TH01)	19.7±1.1	20.9±1.1	9.1±2.6	-	3.6±0.1
Blend II (ML001+TH02)	16.4±1.0	17.5±1.0	15.1±3.6	-	3.6±0.1
Blend III (ML001+BU+TH01)	26.8±23.1	34.9±9.3	11.7±0.08	2.5±0.01	6.4±0.9
Blend IV (ML001+BU+TH02)	25.3±3.4	27.7±1.6	17.9±0.39	2.2±0.01	7.1±0.2

As shown as in Table 3-2, TH01 performances better aerodynamic behaviour, resulting in higher $FPF_{emitted}$ of 22.4%, rather than the spray dried sample with approximate 21% of $FPF_{emitted}$. Moreover, difference powder shapes and sizes would impact on airway deposition(Pilcer and Amighi, 2010). According to the above discussion and the SEM pictures (Fig. 3-5), TH01 and TH02 show different particle sizes and different shape. TH01 has a narrower size distribution of 0.74-1.76μm, compared to TH02 that is from 0.74 to 74.78μm. Both of them are crystalline form, however, spray dried made TH02 forms spherical shape of particle, which is easier to aggregation, rather than the irregular shape of TH01 (Fig 3-5), as irregular surface has lower cohesiveness. Furthermore, the MMDA of TH01 is less than 5μm (4.5μm), while TH02 is 5.1μm, but TH02 still is a potential formulation for inhalation, because it is spherical particle formed by needlike crystal, which contributes to a smaller aerodynamic diameter and enhances the flowability and the aerosol performance of powders emitted from the capsule (Chew et al., 2005). Thereby, according to the Fig. 3-6, the amount of API in throat is higher that the milled batches, however the deposition of the particles is significantly higher in the deeper stages such as stage 6.

Additionally, it has been found absence of lactose result in a relatively lower FPF_{load} and $FPF_{emitted}$ as expected due to the poor flowability of powder. There were more APIs retained in capsule in TH01 and TH02. This phenomenon has been reported in some articles (Yeh et al., 1976, Pilcer and Amighi, 2010, Dickhoff et al., 2003), which describe the importance of lactose being carrier. Lactose helps particles to deposit in deeper stages (Fig. 3-6), and reduces the interparticle forces which make the powder cohesive.

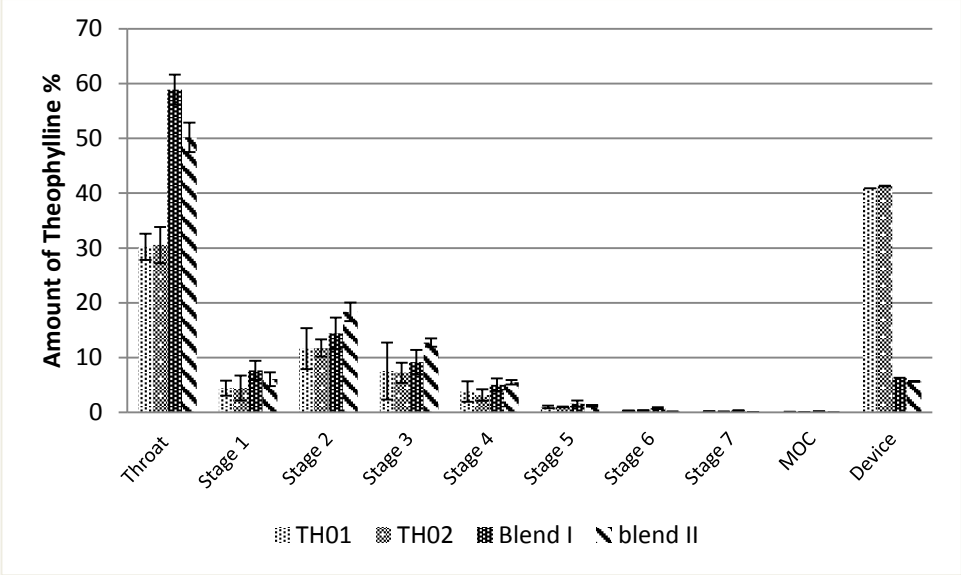

A. Overall Stages

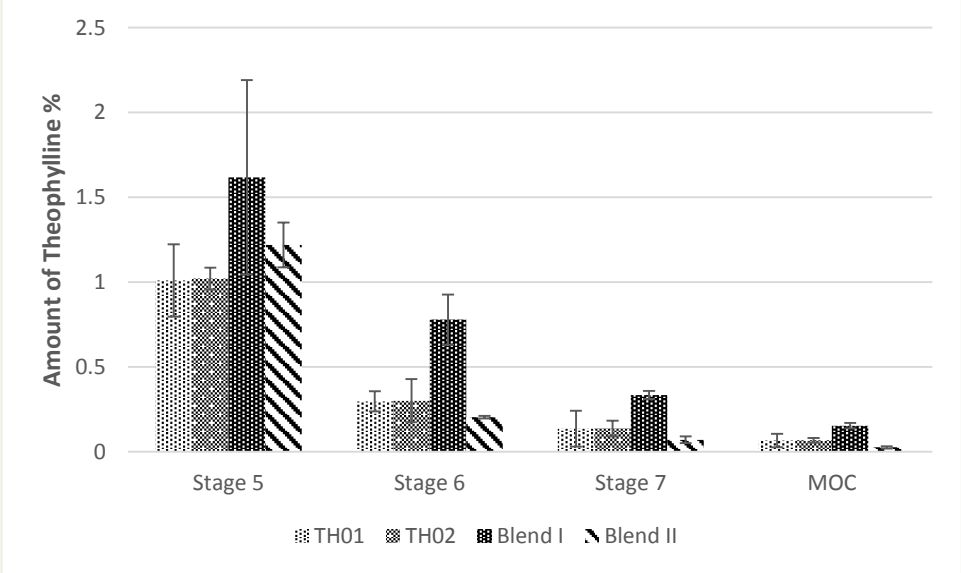

B. Magnified Stage 5, 6, 7 and MOC

Fig. 3-6. Deposition of TH01, TH02, Blend I, and Blend II on the NGI stages.

As expected, analysis of the simultaneous deposition of theophylline and budesonide from the physical mixture formulation should indicate a consistent ratio. Table 3-3 is the NGI analysis to verify the simultaneous deposition of

physical mixtures. In the mixture, theophylline is 20 (±2%) times more than budesonide. According to Table 3-3, there is no significant difference between these two blends (P>1). This stage by stage analysis find inconsistent ratio of theophylline to budesonide, indicating severe particles segregation occurred during dispersion. The adhesion of APIs is broken by shear force from the air and/or collision between the particles or between the particles and the inhaler device during dispersion. Moreover, it can be found more theophylline landed in upper stage (Throat to stage 2) than that of budesonide (Table 3-3). This is the evidence that there is high level of agglomeration in micronized theophylline. Nevertheless, theophylline has better aerosolization performance in Blend IV, as sphere shape of TH02 which spherical nature resulting in less contact with budesonide surface and better de-agglomeration (Chew et al., 2005, Muhammad et al., 2013). This also enhance more budesonide depositing in lower stages (stage 5 to MOC). Due to the high dose of theophylline, the large size theophylline become to aerosol carrier. Compare to milled theophylline, the spray drying sample (TH02) has a wider size distribution and a lower interparticle force, which help balance of cohesive and adhesive force and reduce the agglomeration of micro-budesonide, leading to a lower deposition of budesonide.

Table 3-3 The ratio of theophylline:budesonide in each stage of NGI

	Ratio of theophylline/budeosnide in each stage of NGI	
	Blend III	Blend IV
Throat	644.7±874.3	150.6±19.9
Pressep	198.2±258.9	51.8±17.8
Stage 1	81.7±22.5	87.2±9.6
Stage 2	70.3±11.4	63.9±5.1
Stage 3	36.6±7.1	32.8±5.1
Stage 4	17.9±4.7	15.6±0.6
Stage 5	8.0±2.1	7.9±0.8
Stage 6	5.7±1.9	8.0±2.0
Stage 7	3.0±0.8	9.5±3.1
MOC	20.3±9.6	204.2±149.1

3.5 Conclusion

In conclusion, the milling process and spray drying technique have been successfully employed in engineering micro particles of theophylline. These processes produce theophylline particles, are crystalline and these particles exhibit no polymorphic variations upon processing, although wet milling generate theophylline monohydrate. The micronized theophylline particles possess desired physical properties with appropriate particle size for lung delivery. Moreover, *in vitro* performance analysis, the finding suggests that the better morphological characteristics of TH01, has a greater delivery than the TH02. Although the particle size of the TH02 was not optimal for delivery to the lungs, particles are unique as the urchin-like particle resulted in a smaller aerodynamic

diameter. Compared with raw theophylline, the result shows that the micronized theophylline exposes more acidic groups and has higher surface energy and hygroscopicity than raw materials. These effects can potentially lead to relate changes in solid-state properties and interfacial properties of particles, which will impact aerosol and lung particle deposition.

These results show that the theophylline can be processed with the desired property function and produced for inhaled dosage forms via milling and spray drying.

Chapter 4 : Combination Particles Containing Theophylline and Budesonide: Formulation and Aerodynamic Assessment.

4.1 Introduction

In this chapter, a formulation was processed using a spray dry production of dual particles containing theophylline and budesonide for pulmonary delivery of drug. In contrast to the commercial physical mixture DPI products on the market, all APIs were processed simultaneously to obtain particles which contain both APIs. The objective of this study is to characterise the physicochemical properties of the combination particles. Also, the potential suitability of the spray dried powders for use in DPIs is of interest. For the used mixtures, the weight ratio of 100:5 (theophylline to budesonide, TH:BU) is chosen based on the therapeutic range of the clinical dosage of inhaled budesonide (Lim et al., 2000), and published dosage of inhaled theophylline (Barnes et al., 2010). To satisfy this required ratio, 6mg of theophylline and 0.3mg of budesonide are in a capsule to be used in this experiment.

4.2 Materials and Methodologies

4.2.1 Materials

The materials used in this study have been mentioned in Chapter 2.2.

4.2.2 Preparation of the systems

The spray drying process is same to what has been used in Chapter 2.3.2. For all experiments, both drugs were dissolved in the solvent under ultrasonication. The drugs were used in a weight ratio of 100:5 between theophylline and budesonide dissolving in solution of 80% (v/v) methanol and 20% (v/v) deionised

water. Different ratios of excipients were tested for their effects on properties of combination particles. Those were Polyvinylpyrrolidone PVP (Kollidon 25, BASF, Ludwigshafen, Germany) and hydroxypropylmethyl cellulose (HPMC, Metolose 60 SH 50, Shin-EtsuChemical,Tokyo, Japan). They were used in a range from 0.05% to 0.5%. Table 4-1 describes the experimental design for this study.

Table 4-1 Experiment was a full factorial design (HPMC: -1=0% w/v, 0=0.25% w/v, 1=0.5% w/v; PVP: -1=0%w/v, 0=0.05% w/v, 1=0.1% w/v)

	HPMC %w/v	PVP %w/v
TB-1	-1	-1
TB-2	-1	0
TB-3	-1	1
TB-4	0	-1
TB-5	0	0
TB-6	0	1
TB-7	1	-1
TB-8	1	0
TB-9	1	-1

4.2.3 Particle characterisation methods

The particle characterisation methods have been fully explained in Chapter 2.4. These methods are thermal analysis, XRD, SEM, particle sizing and aerodynamic analysis and they can be found in Chapter 2.4.3, Chapter 2.4.2, Chapter 2.4.4, Chapter 2.4.1 and Chapter 2.4.7 respectively.

4.2.4 Assessment of theophylline solubility

For solubility studies, the theophylline was dissolved with the respective excipients mixture, and an excess of drug remains at the bottom of the glass vial. The vials were closed tightly and shaken for 48 h at room temperature (20 ˚C). During shaking process, it was controlled and checked regularly to see whether a residuum remains present in each vial. If not, further drug was added to the vial. After 48 hrs, the supernatant was filtrated and drug quantification was performed as described below.

4.2.5 Drug quantification

This assessment has been illustrated in Chapter 2.4.6.

4.2.6 Statistical analysis

Fig. 4-1 shows the detailed process of the statistical analysis used in the presented work.

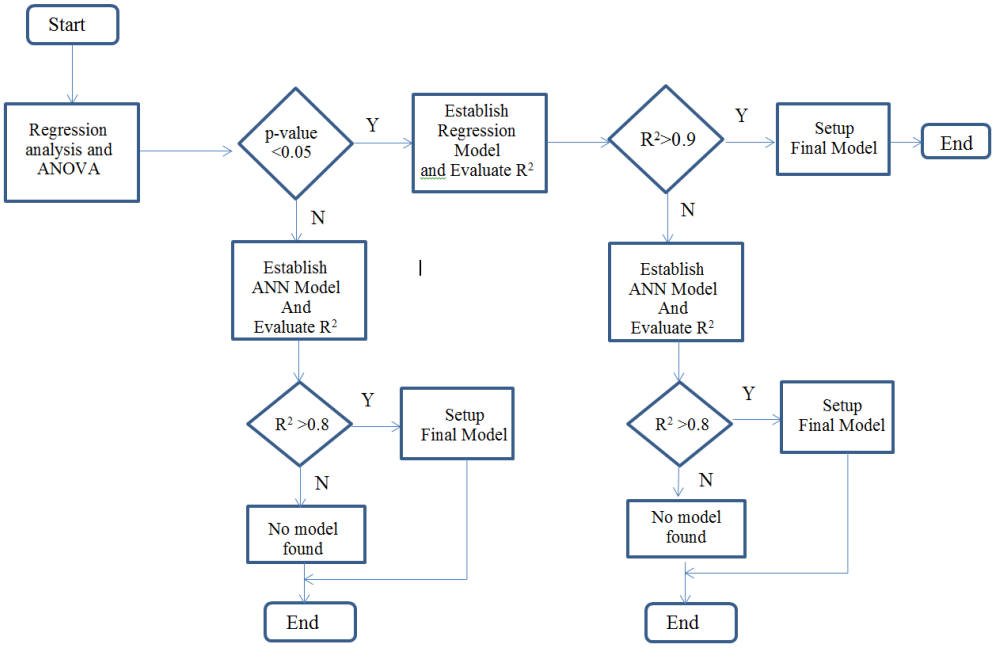

Fig. 4-1. Flowchart of statistical analysis

4.2.6.1 Regression analysis and ANOVA analysis

As can be found in Fig. 4-1, regression and ANOVA analysis are used to determine the important independent factors at the initial stage of the statistical analysis. Regression and ANOVA analysis and model generation which have been described in the Chapter 2.5.2 will be implemented in this section.

In this study, firstly it is to optimise the processing parameters of spray drying. The regression model of response variables were observed values of the solubility, the ratio between budesonides and theophylline of combination particles; and the D_{50} particle size, and explanatory variables, i.e. HPMC, PVP, inlet temperature, atomization, air flow rate, and feed rate. And then, the ANOVA analysis was applied for further studies. The primary purpose of ANOVA is to understand if there is any interaction between the independent variables on the dependent variable and detect the important factors. In this study, ANOVA methodology was to select the important factors which cause significant influences on particle size and particle composition. The significance of variables were judged by *p*-value. A low *p*-value (< 0.05) indicates that predictor is likely to be a meaningful addition to model because changes in the predictor's value are related to changes in the response variable. The predictors that have a low *p*-value were selected to establish regression model. The fit of a regression model can be judged with calculation of the correlation coefficient, R^2, defined as the correlation between the observed values of the response variable and the values predicted by the model (Paul R. Kinnear and Gray., 2008). This model was generated using SPSS software (IBM SPdSS statistics 19, USA).

4.2.6.2 ANN modelling

The regression model had a small R^2, which has been found in the above regression analysis. This result suggested the regression model is not suitable for this study. Therefore, as illustrated in Fig. 4-1, the ANN analysis was employed to discover the linkages between the excipients and physical properties of particles. In this analysis, pooled data from the experiment were analysed using commercially available ANN software (INForm v3.4, Intelligensys, UK). A description of this software and its utility for modelling pharmaceutical formulation and processing data has previously been given in (de Matas et al., 2008).

In neural network training process, HPMC and PVP were treated as independent variables (inputs), where the solubility, the ratio between budesonides and theophylline of combination particles (TH:BU), and the D_{50} particle size as the response variable (output). Due to the available amount of data set, the ANN model was established by leave-one-out methodology. The database is divided into a training set which has 7 data records, a test set with 1 data records and a validation set with 1 data records. Training and test data sets are used by the ANN to learn the cause effect relationships and inherent characteristics in the data set, while the validation data sets which are excluded from training, are used to assess the predictability of generated models.

4.3 Results and discussion

4.3.1 Optimization of spray drying process

The particles used for pulmonary drug delivery have the ability to manipulate and control a variety of parameters of spray drying such as solvent composition, solute concentration, solution and gas feed rate, temperature and relative humidity, droplet size, etc (Pilcer and Amighi, 2010). In this study, the spraying

nozzle and solution composition were fixed. The two levels of spray drying processes parameters were applied to investigate influences on particle size and composition. The data was analysed by ANOVA to select the significant factors that cause important effects on particles. The independent variables were excipients, i.e. HPMC and PVP, and spray drying parameters, i.e. inlet temperature, atomization, air flow rate, and feed rate. Table A1 in Appendix presents the observed results. This result was analysed by factorial ANOVA and regression to see the important factors and detect the reactions between the variables.

According to the ANOVA and regression results which were shown in Appendix's Table A2 to A5, it suggests that HPMC and PVP are significant factors which influence ratio of theophylline and budesonide in particle with *p*-value<0.000. It is also found that the particle size is associated with concentration of HPMC. In contrast to HPMC, particle size of PVP does not have effects. Interestingly, it is noticeable that the spray drying process parameters do not have significant influences in this study. Due to these findings, excipients were used to develop models to predict and control the particle size and composition.

4.3.2 Generation of models: solubility of theophylline, and particle size and composition

As found in previous section 4.3.1, the fixed process parameters were manipulated in this experiment. The expansion of level of excipients was selected. In this study, the 3 level of concentrations of excipients were operated to obtain quality models which can be used to explain the association between excipients and particles. Table 4-2 is the observed results of this study, which is used to be analysed by regression and ANN.

Table 4-2 Summary of result, where TH is theophylline; BU is the budesonide; TH:BU is the ratio between theophylline and budesonide.

	HPMC	PVP	TH:BU	Solubility (mg/ml)	Size (VMD) (μm)
TB-1	-1	-1	14.90±3.33	0.281±0.034	8.19±2.80
TB-2	-1	0	16.79±2.21	0.306±0.012	35.68±10.85
TB-3	-1	1	16.94±2.32	0.310±0.003	15.62±2.36
TB-4	0	-1	19.66±1.87	0.323±0.021	13.72±2.40
TB-5	0	0	20.03±2.13	0.330±0.001	9.16±1.23
TB-6	0	1	20.62±0.43	0.326±0.002	7.66±1.02
TB-7	1	-1	19.4±1.61	0.336±0.020	8.99±0.33
TB-8	1	0	17.96±3.13	0.335±0.006	8.81±0.6
TB-9	1	1	20.10±2.16	0.340±0.003	5.76±0.63

4.3.2.1 Regression model generation

The regression model was established by implementing SPSS software. The result is displayed in Table 4-3 and 4-4. According to Table 4-3 and 4-4, HPMC and PVP do not cause any effects on the ratio between theophylline and budesonide (TH:BU), due to the *p*-value of them are greater than 0.05.

Table 4-3 Regression model of TH:BU

Regression Statistics	
Multiple R	0.71164892
R Square	0.506444185
Adjusted R Square	0.34192558
Standard Error	1.574181774
Observations	9

	Coefficients	Standard Error	*p*-value
Intercept	18.48941938	0.524727	3.48E-08
HPMC	1.470870924	0.642657	0.062052
PVP	0.615870924	0.642657	0.374908

Table 4-4 Summary of ANOVA data: regression model of TH:BU

ANOVA

	df	SS	MS	F	Significance F
Regression	2	15.25655	7.628275	3.07834	0.120229
Residual	6	14.86829	2.478048		
Total	8	30.12484			

To further verify the finding, the factorial ANOVA model was applied to optimize regression models, where TH:BU was dependent variables; and excipients were set as independent variables. The summary of ANOVA model is shown in Table 4-5 and the mathematical model can be expression as below:

$$Y = \beta_0 + \beta_1 x_1 + \beta_2 x_2 + \beta_{11} x_{11} + \beta_{22} x_{22} + \beta_{12} x_{12} + \beta_{112} x_{112} + \beta_{122} x_{122} + \beta_{1122} x_{1122} + \epsilon \quad \text{(Equation 4-1)}$$

Where the indicator variable, x_1=HPMC, x_2=PVP; the β is the effects coefficient for the main effects of factors (HPMC, PVP), β_{12} , β_{13} … β_{1234} are the effect coefficients for the interactions of variables.

As can be observed in Table 4-5, it suggests that the change of TH:BU is related to HPMC concentration with a *p*-value of 0.006. However, its regression model which is shown in Table 4-6 has lower R^2 of 0.43, therefore, this result indicates that regression analysis is not suitable in this study.

Table 4-5 ANOVA model of the ratio between theophylline and budesonide (TH:BU)

Tests of Between-Subjects Effects

Dependent Variable: TH:BU

Source	Type III Sum of Squares	df	Mean Square	F	Sig.
HPMC	5.384	2	2.692	13.666	.006
PVP	.469	2	1.256	.273	.770
HPMC * PVP	3.518	2	1.759	.397	.689
HPMC²*PVP	4.943	2	2.471	.589	.584
PVP² * HPMC	17.723	2	8.861	4.287	.070
HPMC²	11.721	1	11.721	4.458	.073
PVP²	.237	1	.237	.055	.821
HPMC² * PVP²	3.072	1	3.072	.795	.402
Error	.000	0	.		
Total	3106.853	9			

a. R Squared = 1.000 (Adjusted R Squared = .)

Table 4-6 Summary of regression model of TH:BU, which was generated using HPMC

Regression Statistics	
Multiple R	0.656429
R Square	0.430899
Adjusted R Square	0.349599
Standard Error	1.564977
Observations	9

	Coefficients	Standard Error	*p*-value
Intercept	18.48942	0.521659	3.69412E-09
HPMC	1.470871	0.638899	0.054813468

Moreover, the results for the regression analysis of particle sizes are shown in Table 4-7 and 4-8 and its corresponding ANOVA study is given in Table 4-9. These results have confirmed that excipients did not influence on the particle size, because that the *p*-value of all independent variables are greater than 0.05.

Table 4-7 Regression model of particle size

Regression Statistics	
Multiple R	0.681661
R Square	0.464661
Adjusted R Square	0.286215
Standard Error	2.531861
Observations	9

	Coefficients	Standard Error	*p*-value
Intercept	8.652222	0.843954	5.0248E-05
HPMC	-2.28167	1.033628	0.06938794
PVP	-0.59833	1.033628	0.58373982

Table 4-8 Summary of ANOVA data: regression model of particle size

ANOVA

	df	SS	MS	F	Significance F
Regression	2	33.3840	16.6920	2.6039286	0.153421
Residual	6	38.4619	6.41032		
Total	8	71.84596			

Table 4-9 ANOVA model of particle size of dry powder

Tests of Between-Subjects Effects

Dependent Variable: Particle size

Source	Type III Sum of Squares	df	Mean Square	F	Sig.
HPMC	33.307	2	16.106	2.438	.168
PVP	19.471	2	1.811	.159	.856
HPMC * PVP	14.408	2	7.204	.753	.511
$HPMC^2$ * PVP	.380	2	.190	.016	.984
PVP^2 * HPMC	10.606	2	5.303	.520	.619
$HPMC^2$	.975	1	.975	.096	.765
PVP^2	1.473	1	1.473	.147	.713
$HPMC^2$ * PVP^2	.044	1	.044	.004	.950
Error	.000	0	.		
Total	745.595	9			

a. R Squared = 1.000 (Adjusted R Squared = .)

Furthermore, the relationship between solubility and excipients is discovered. According to the regression analysis of Table 4-10, the model has small value of *p* ($p<0.05$). This gives a good indication of HPMC has significant effects on solubility of theophylline (ST) at room temperature. Meanwhile, it is also noticed in Table 4-11, the model of ST has higher R^2 of 0.84 as well as its Significance F< F in its ANOVA data. This demonstrates that the model is reliable for predicting ST. To further optimize the result of regression analysis, a factorial ANOVA method is carried out in the following study.

Table 4-10 Regression model of solubility of theophylline

Regression Statistics	
Multiple R	0.917792
R Square	0.842342
Adjusted R Square	0.789789
Standard Error	0.008672
Observations	9

	Coefficients	Standard Error	P-value
Intercept	0.320752	0.002891	3.6114E-11
HPMC	0.019093	0.00354	0.00167456
PVP	0.006101	0.00354	0.13559148

Table 4-11 Summary of ANOVA data: regression model of solubility of theophylline

ANOVA

	df	SS	MS	F	Significance F
Regression	2	0.00241	0.00120	16.028486	0.003919
Residual	6	0.00045	7.52E-05		
Total	8	0.00286			

Table 4-12 summarises output of ANOVA study. According to this table, HPMC, PVP, and PVP^2 * HPMC are important variables to theophylline solubility. These factors are used to generate the regression model, which has been shown in Table 4-13. Compared Table 4-10 with Table 4-13, it was found that R^2 of the model was improved from 0.84 to 0.86; and also in Table 4-14, F > F-sig. demonstrates that this model is reliable for predicting ST. Therefore, according to the pervious finding, regression model can be performed by adopting the following equation. Mathematical model of theophylline solubility can be described as:

$$Y = \beta_0 + \beta_1 x_1 + \beta_2 x_2 + \beta_{122} x_{122} + \epsilon \qquad \text{(Equation 4-2)}$$

$$Y = 0.321 + 0.015 x_1 + 0.006 x_2 + 0.007 x_{122} + \epsilon$$

R^2=0.86

Table 4-12 ANOVA model of the solubility of theophylline that were used for spray drying

Tests of Between-Subjects Effects

Dependent Variable: Solubility

Source	Type III Sum of Squares	df	Mean Square	F	Sig.
HPMC	.000	2	.001	12.826	.007
PVP	.000	2	.000	.306	.047
HPMC * PVP	.000	2	.000	.315	.741
$HPMC^2$*PVP	.000	2	.000	.480	.640
PVP^2 * HPMC	.002	2	.001	6.229	.034
$HPMC^2$	.000	1	.000	.339	.579
PVP^2	.000	1	.000	.103	.758
$HPMC^2$ * PVP^2	.000	1	.000	.295	.604
Error	.000	0	.		
Total	.929	9			

a. R Squared = 1.000 (Adjusted R Squared = .)

Table 4-13 Summary output of regression model, which was built between (HPMC, PVP, and PVP^2 * HPMC) and theophylline solubility that was at room temperature

Regression Statistics	
Multiple R	0.92891178
R Square	0.862877095
Adjusted R Square	0.780603353
Standard Error	0.008859284
Observations	9

	Coefficients	Standard Error	P-value
Intercept	0.32075156	0.002953	1.25E-09
HPMC	0.01466739	0.006264	0.066268
PVP	0.00610119	0.003617	0.152428
HPMC*PVP2	0.006639135	0.007672	0.426418

Table 4-14 Summary of ANOVA data: regression model of solubility of theophylline (independent variables are HPMC, PVP, and PVP^2 * HPMC)

ANOVA

	df	SS	MS	F	Significance F
Regression	3	0.002469	0.000823	10.48788	0.01347
Residual	5	0.000392	7.85E-05		
Total	8	0.002862			

4.3.2.2 Generation of ANN model

As discussed in section 4.3.2.1, regression technique has limited capabilities to excavate the potential connections between excipients and particles. In order to establish a more reliable and accurate mathematical model that defines the relationship between excipients and physical properties of particles, the more sophisticated statistical learning model – ANN was applied in this study. This ANN models were programmed and setup using INForm v3.4. The training time is different slightly for networks with different numbers of hidden layers, nodes and transfer function. For this type of model, it was established by one hidden layer and two nodes to prevent over-fitting.

The R^2 of regression model and ANN model on each output are indicated in Table 4-15. As shown in Table 4-15, it is clear that regression analysis only capable to conduct precise predictions of theophylline solubility with R^2 value of 0.86, whereas neural network analysis could be used for generation of models of both theophylline solubility and TH:BU with R^2 value of 0.90 and 0.78 respectively.

Table 4-15 Correlation coefficient R^2 of regression model and ANN model on solubility of theophylline in solutions, TH:BU, D50 particles size. [Solution: saturated solution (about 3%, w/v); solvent: 80% Methanol+20% Deionised Water].

	R^2 of observed versus predicted value	
	Regression	ANN
Solubility of theophylline	0.86	0.90
TH:BU	0.51	0.78
D50 particle size	0.46	0.24

The ANN model of theophylline solubility is formed by using transfer function of Symmetric Sigmoid and output transfer function of Asymmetric Sigmoid. Compared with regression model in Fig. 4-2, both of the models have same tendency, where ANN and regression models have high R^2 of 0.9 and 0.84, respectively. This leads to evident that existence of a strong connection between the excipients and solubility of theophylline.

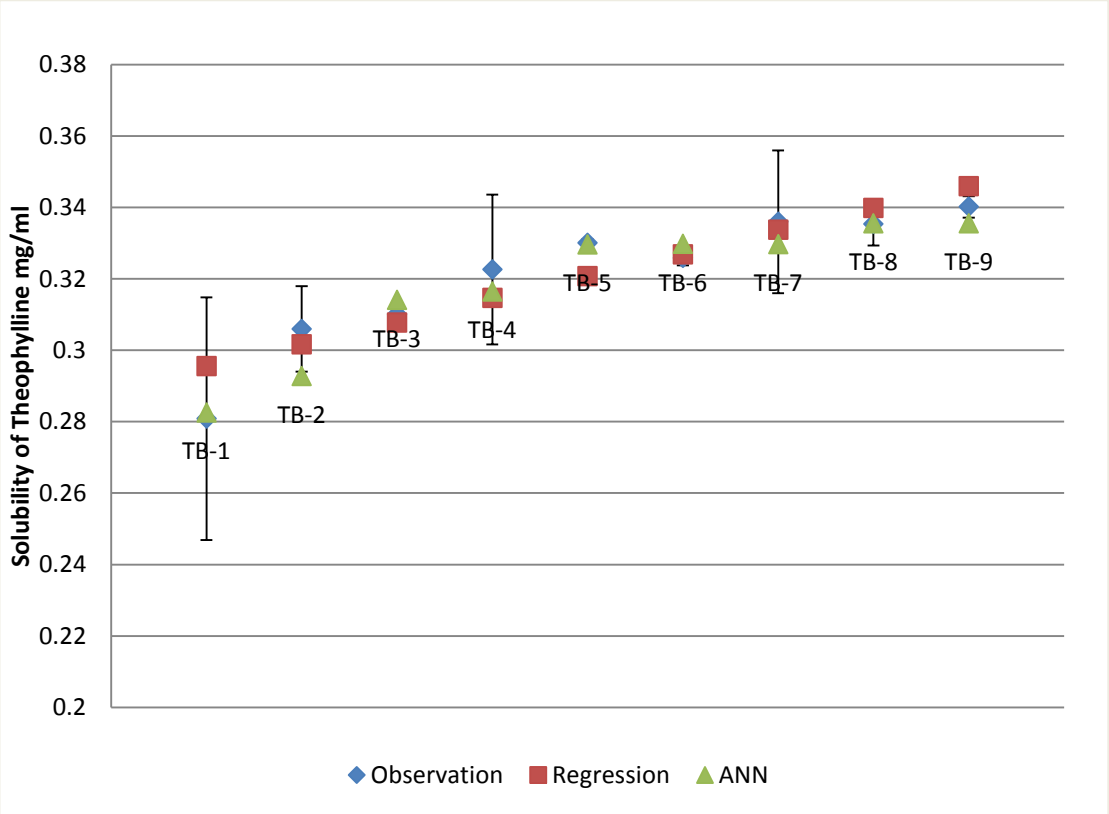

Fig. 4-2. Solubility of theophylline observation data and its regression and ANN model.

Moreover, Fig. 4-2 shows the predictions are closed to the observation data where the mean squared error (MSE) of ANN model is 3.43×10^{-5} and regression model is 5.01×10^{-5}. Owing to availability of small data set, the ANN model was further validated using cross validation method. This has resulted in a low cross

validation error of 1.40 x 10^{-5}. This result proves that the ANN model of theophylline solubility is not overfitting or underfitting and leads to further confirm that ANN model is reliable and accurate enough for prediction and estimation of ST.

On the other hand, the ANN model of TH:BU was generated from Asymmetric Sigmoid of transfer function and Tanh of output transfer function. From the presented results from Table 4-15, it is clear seen that ANN model leads to better R^2 of 0.7776, compared to R^2 of 0.506 of regression model. This result reveals that ANN model could be able to predict a better value for TH:BU ratio. To check whether occurrence of overfitting in the predicted ANN model, it is to compare the regression model and ANN model to investigate whether they have similar tendency, and again cross validation method is applied in ANN model. As can be observed in Fig.4-3, ANN model has similar tendency to regression model, but the there is a big difference between ANN result and regression result at sample of TB-1 to TB-3, in contrast ANN model has a small cross validation error of 1.15, so that this model does not be over trained. Therefore, TH:BU model can be produced by ANN.

According to the above discussion, it leads to conclusion that ANN is better than regression analysis in term of producing better models for theophylline solubility and TH:BU ratio.

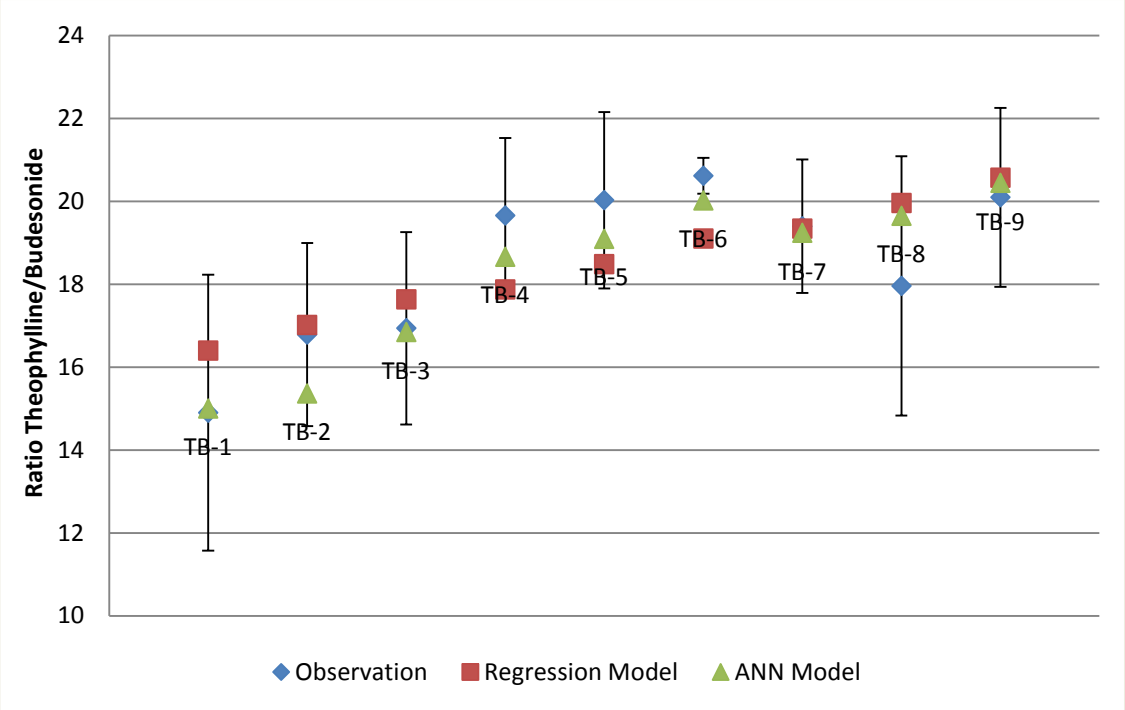

Fig. 4-3. The predicated and observed result for the ratio between theophylline and budesonide in combination particles (TH:BU), including regression model and ANN model.

4.3.3 Influence of excipient

It has been well known that surface active substances can affect particle size by rapidly covering new surfaces, which could inhibit crystal growth (Westmeier and Steckel, 2008). It also has been proved that a hydrophilic agent with surface activity help the powder absorbs the water and thus increases the dissolution in the lung fluid (Raghavan et al., 2001).Therefore, different ratios of excipients were tested for their influence on solubility of theophylline, particle size and aerodynamic behaviour of the combined particles. The experiment group was designed as shown in Table 4-1.

In this study, it can be found that solubility of theophylline is related to concentration of excipients. As can be seen in Fig.4-4, excipients enhance its

solubility. By further examining Fig. 4-4, it was also found that there is a slightly raise in average solubility by increasingly concentration of PVP from 0.0% to 0.05% or 0.1%, and small changes when introducing solubility of high concentration of HPMC.

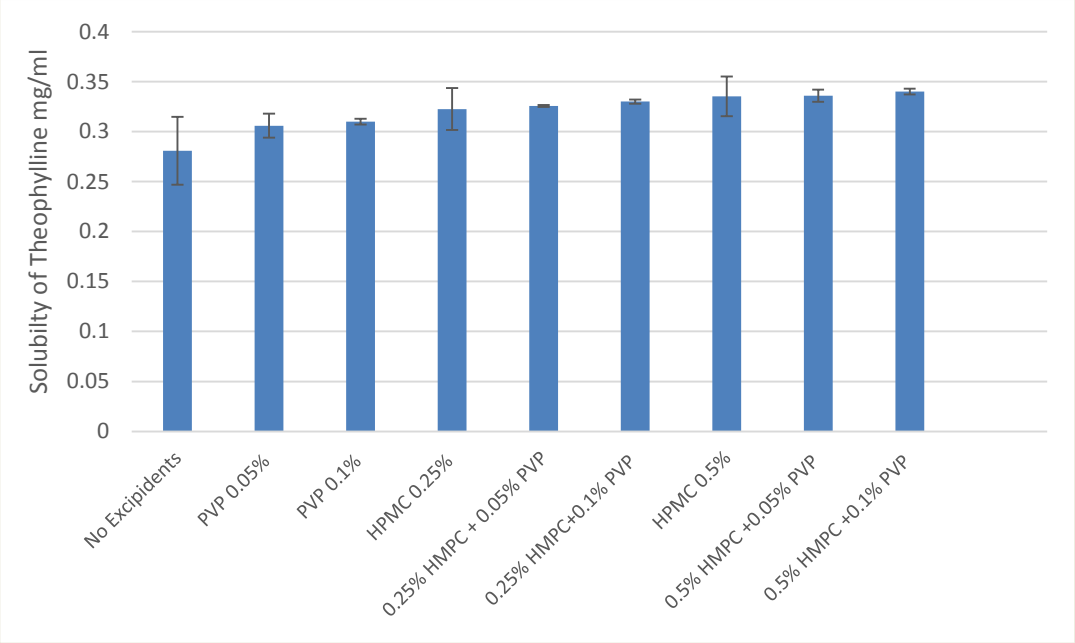

Fig. 4-4. Excipients effect on solubility of theophylline (solvent: 80% Methanol+20% Deionised Water)

As discussed in chapter 4.3.2, those data was used to establish a neural network model via ANN software, where the R^2 =0.901 of model demonstrates a good quality prediction. This model is performed by Matlab surface fitting tool and it is plotted in Fig. 4-5.

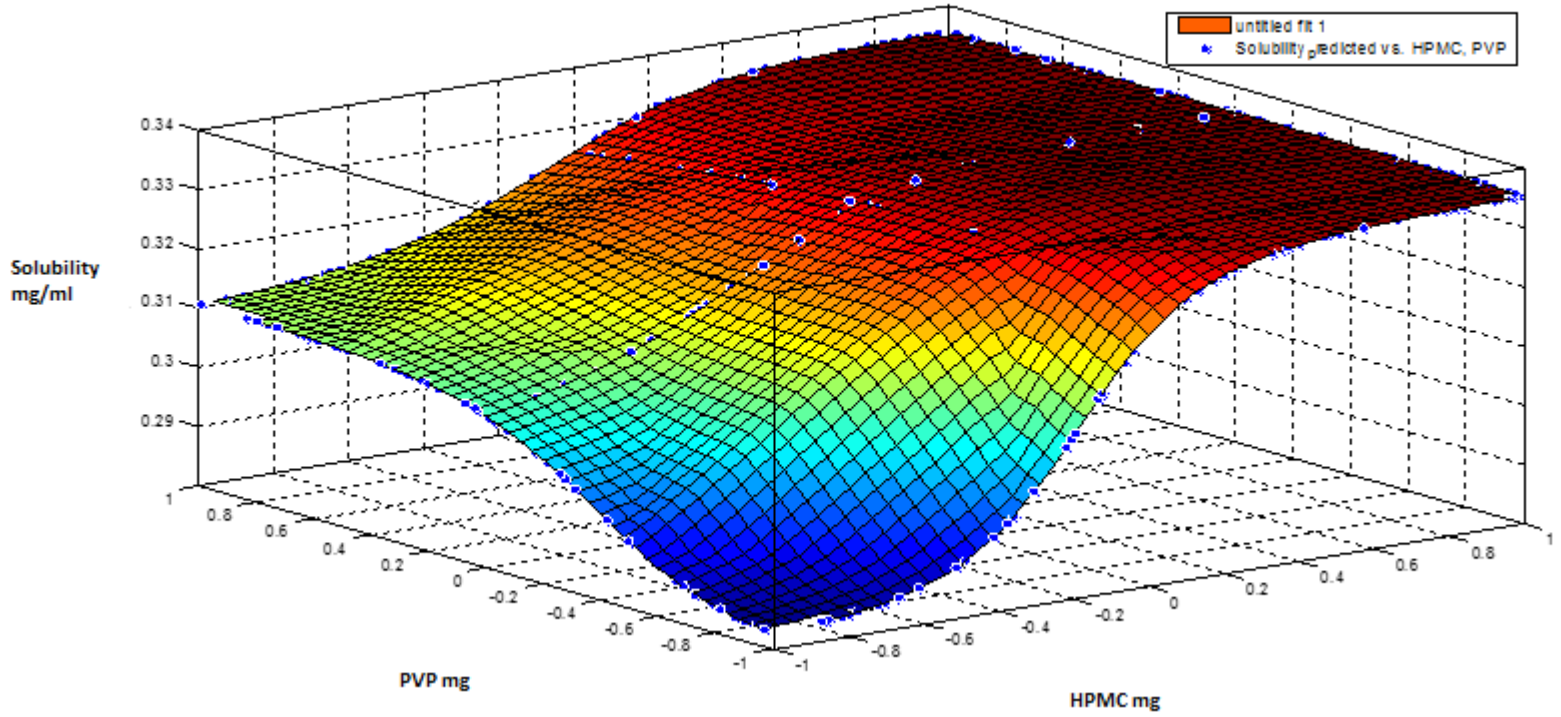

Fig. 4-5. Response surface model of Matlab in accordance with the neural network model: predicted solubility at the different concentrations of excipients, where R^2 is 0.9.

As illustrated in Fig. 4-5, individual excipient can be able to cause increase in solubility of theophylline, but the solubility become steady when HPMC and PVP use together, however, the model reveals that HPMC causes significant effects in accordance with Fig. 4-5. The solubility rises up remarkably by increasing concentration of HPMC. Additionally, the ratio of theophylline to budesonide in combination particles also has been modelled by ANN. The R^2 of the model is 0.75, which is described as Fig. 4-6. As can be seen in Fig. 4-6, theophylline is about 20 (±3) times more than budesonide in the combination particles. It indicates that neither HPMC nor PVP produce any remarkable impacts on the ratio of theophylline:budesonide, nevertheless, higher concentration of them make it more stable.

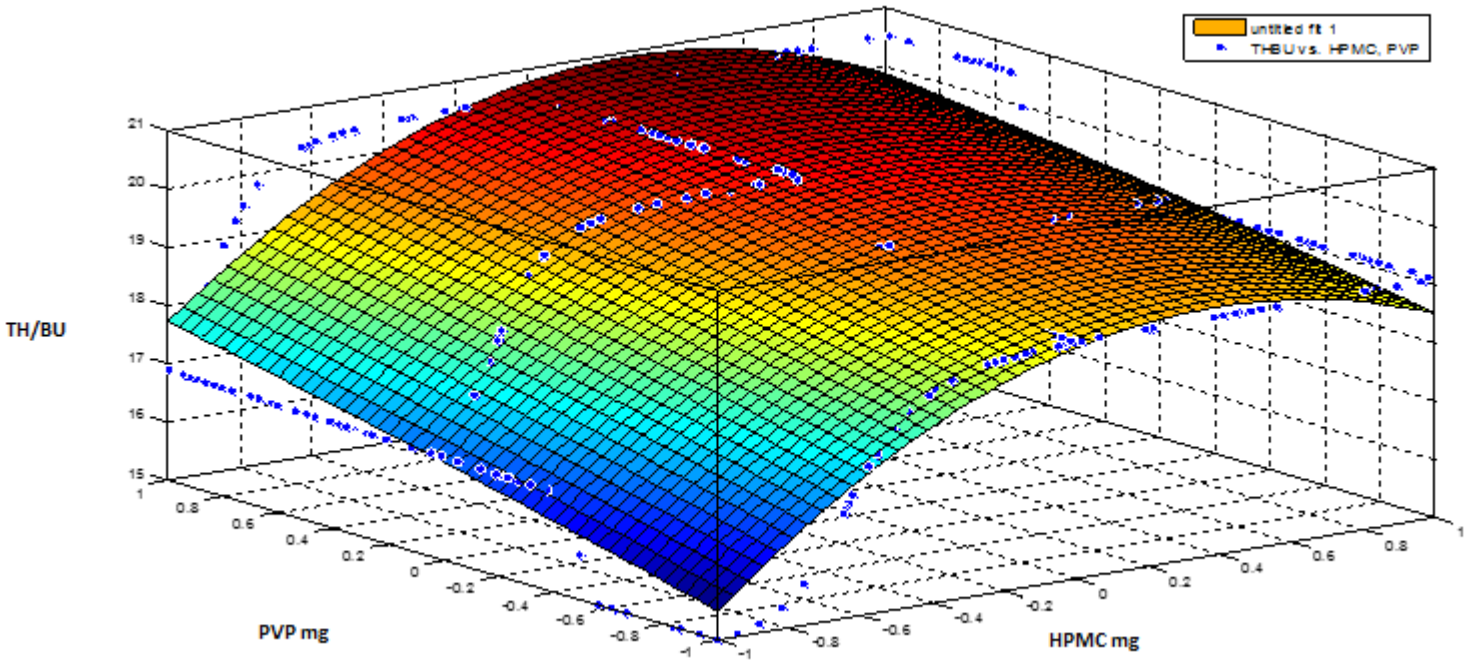

Fig. 4-6. Response surface model of neural network model: predicted value of ratio between theophylline and budesonide in combination particles. R^2=0.9

Fig. 4-7 summarizes the particle size distribution of each sample. As can be found in Fig. 4-7, excipients have effects on particle size, which result in slightly bigger particles compared to a precipitation without excipients.

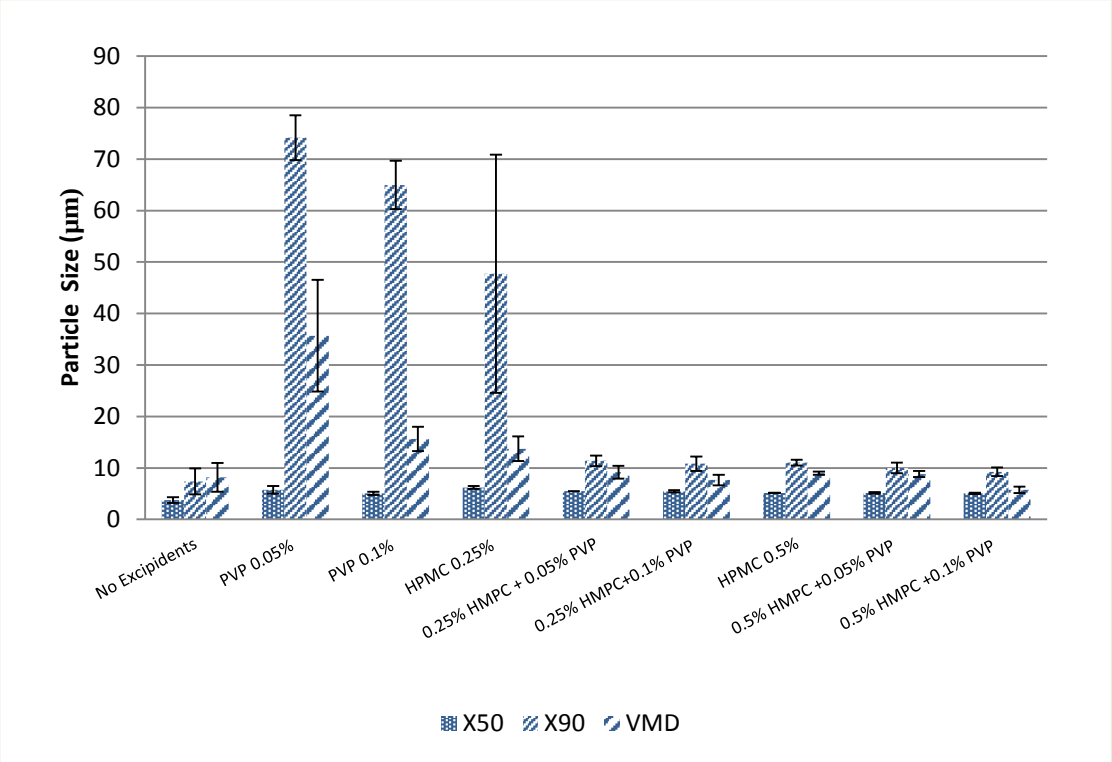

Fig. 4-7. Average particle size after spray-drying with or without excipients. [Solution: saturated solution (about 3%, w/v); solvent: 80% Methanol+20% Deionised Water]

According to Fig. 4-7, varying concentrations of surfactants from 0.05%to 0.1%, leads to a significant increase in average particle size of x^{90} indicating a particle agglomeration after spray drying. This phenomenon is caused by limited flow properties of powder, due to typical mechanical stresses increase particle surface energy and hence make the powder adheres. In addition, the other cause is that the obtained particle shape could affect interparticle forces, for instance, the flat surfaces of needle-like particles have a large contact surface areas. Due to this

characteristic, the particles would experience high interparticle forces and form aggregates (Fukunaka et al., 2005). This speculation is further proved by SEM. According to the SEM graph of Fig. 4-11, it can be seen that the spherical particles have needle-like crystals on the surface, which increase the contact area and result in high level of cohesion.

Furthermore, as can be found in Fig. 4-7, the samples with absence or low amount of HPMC have larger particles. This is because excipients have different capability to inhibit crystallization, where HPMC has a better inhibiting effect than PVP. Owing to this reason, sample with PVP could lead to bigger particle size when compared with HPMC. Hence, when the water soluble excipient HPMC was added in, the particle becomes a smaller and a better flowability. The mechanism of this effect is that the HPMC creates a steric barrier, which prevent close contact and subsequently inhibit particle growth (Raghavan et al., 2001).

4.3.4 Crystallinity

In this study, DSC and X-ray diffraction were applied to characterise the physicochemical properties of the samples in order to determine the crystal or cocrystal formation.

Preliminary studies address a potential cocrystal formation of theophylline and budesonide using a computation of energies by STFC Chemical Database Service (Sci-Tech Daresbury, UK). This study reveals that some binding between the two molecules might occur, but a cocrystal formation would be rather unlikely.

Fig. 4-8 is the result of DSC analysis. As shown in Fig. 4-8-A, it notices that DSC measurements cannot detect budesonide and theophylline melting peak in their

physical mixtures. This situation is caused by two main actions. Firstly, the small amount of budesonide, which is 20 times less than theophylline, creates no interpretable DSC signal. Secondly, the thermal decomposition of theophylline presents with melting of budesonide during the DSC study, which is consistent with some degree of interaction and/or miscibility between the two components, and resulting endotherm peak of theophylline is shifted, broadened and asymmetric. Furthermore, in Fig. 4-8-B-C, the shifted melting peck of theophylline and flatten the curve whichever in physical mixtures or after spray drying are detected. This phenomenon can be suggested that it is caused by HPMC and PVP were immiscible (Nyamweya and Hoag, 2000), resulting in a lower temperature shifts and deeper glass transition, subsequently affecting the peak of APIs melting.

However, this change of peak cannot eliminate assumption of cocrysal. Therefore, polarized light microscopy was operated to detect cocrystal of theophylline and budesonide. Fig. 4-9 is the graph obtained from polarized light microscopy. In the image, two types of crystal were discovered. Due to the higher concentration of theophylline, theophylline performed (produces) a larger needle-like crystal than budesonide that is small flat crystal at the fringe. Overall DSC data and microscopy image provide an evidence which confirms that theophylline and budesonide cannot form cocrystal. The DSC graphs of single sample are shwon in Appendix Fig. A3.

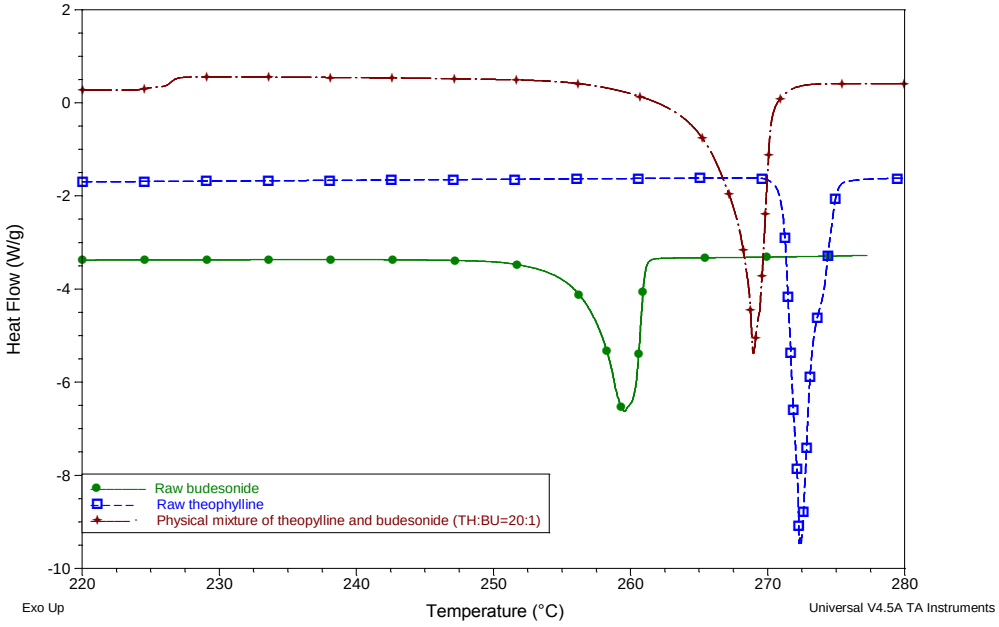

A: theophylline and budesonide physical mixture; TH= theophylline; BU= budesonide

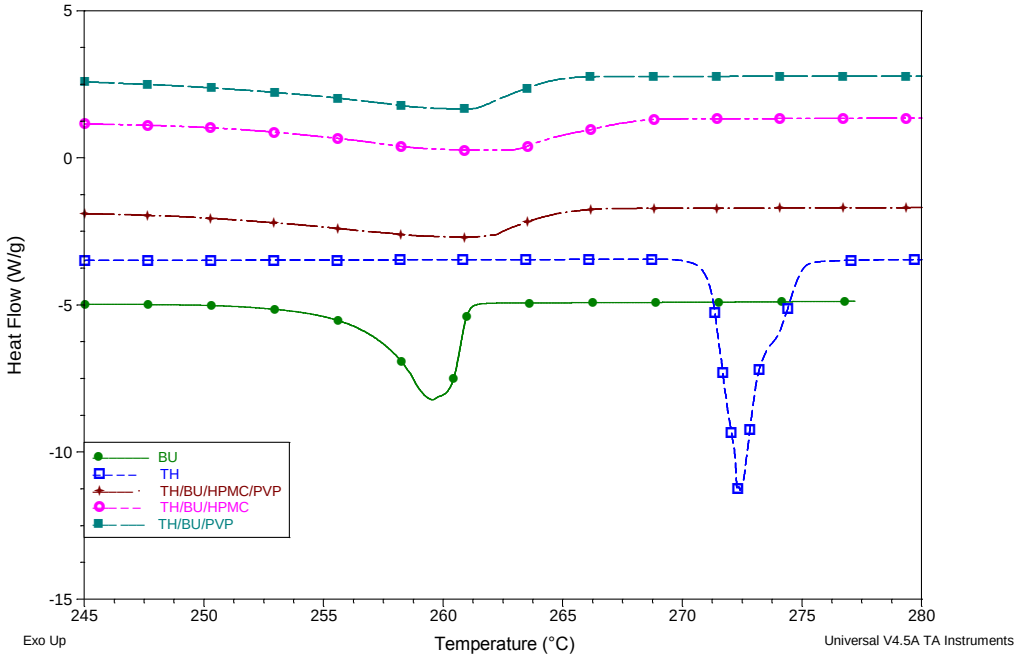

B: Physical mixture of APIs and exipidents

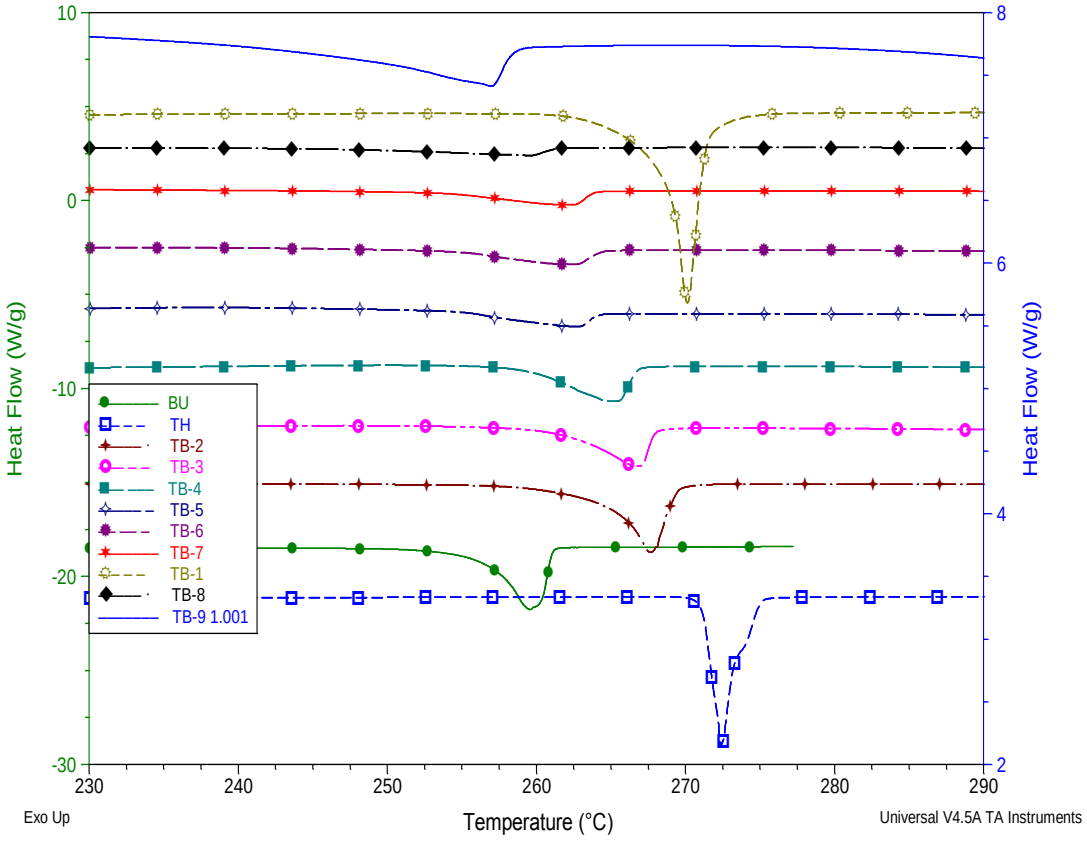

C: Spray drying sample from TB-1 to TB-9

Fig. 4-8. DSC curves from single APIs, physical mixtures and combined precipitates [Solution: saturated solution (about 3%, w/v); solvent: 80% Methanol+20% Deionised Water].

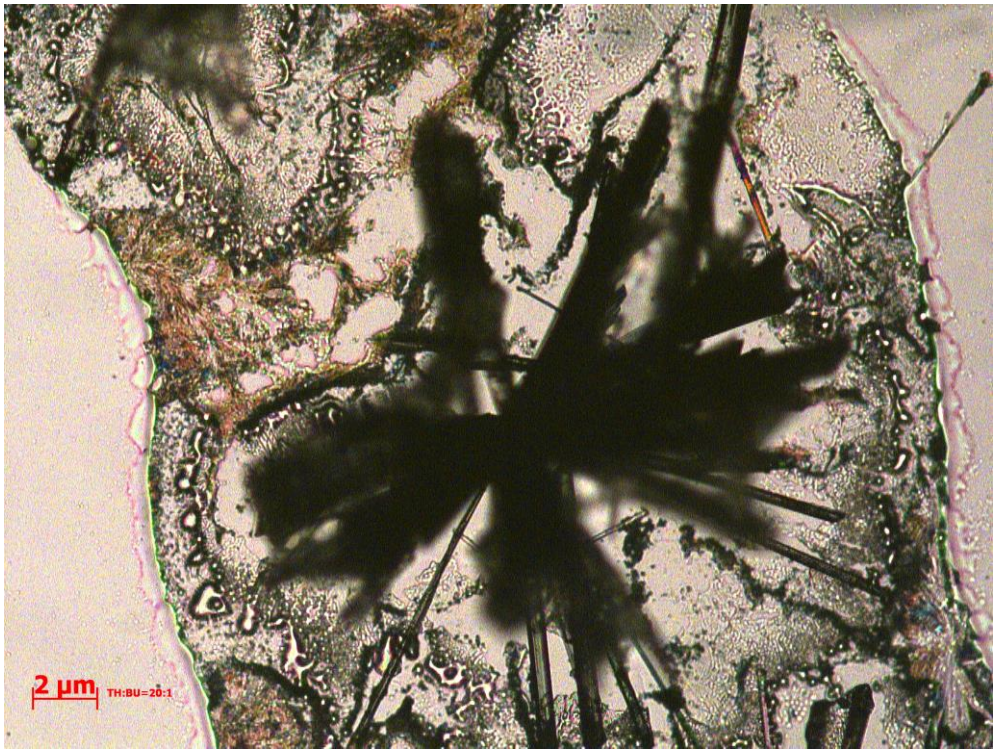

Fig. 4-9. Polarized light microscopy image of particles which were recrystallized by evaporated solvent that was used for spray drying

Fig. 4-10 describes the X-ray pattern of both APIs and combination particles with/without excipient, which was produced from X-ray diffraction measurements. As illustrated in Fig. 4-10, the particle shows a partly crystalline pattern with excipient, as excipient masking crystal peaks. Correlation of the pattern peaks to peaks of single substances can be done, but it does not show a consistent pattern for every peak. These data indicate that there might be a slight change, but it cannot prove neither cocrystallisation nor theophylline monohydrate in the sample. Therefore it is assumed that spray drying results in a coprecipitate, but not generation of cocrystal. The XRD patterns of single sample are exhibited in Appendix Fig. 4A.

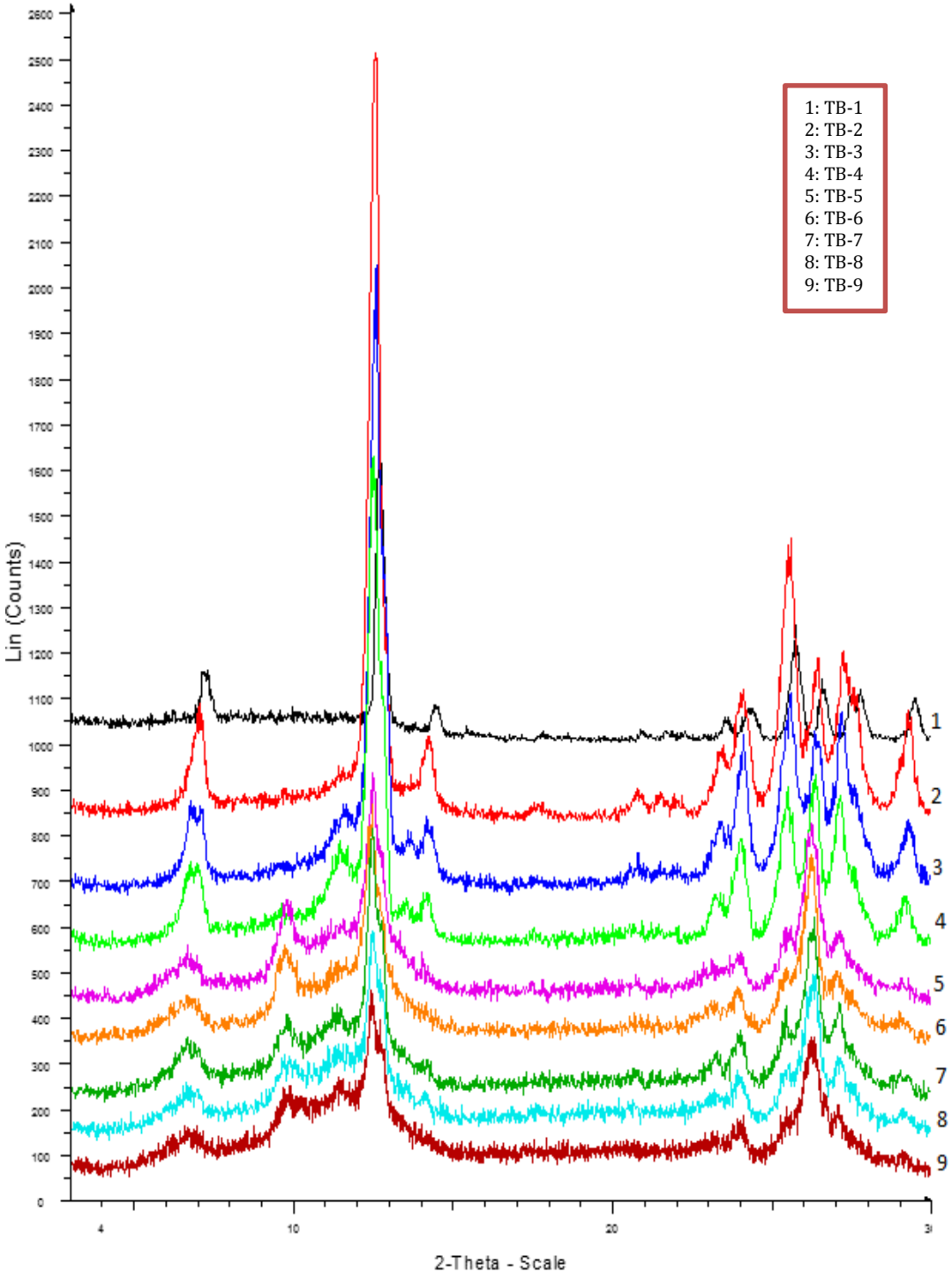

Fig. 4-10. X-ray pattern of both APIs and combination particles with/without excipient [Solution: saturated solution (about 3%, w/v); solvent: 80% Methanol+20% Deionised Water], the blue and black patterns are raw materials of theophylline (TH00) and budesonide (BU00), respectively.

4.3.5 Morphology

Fig. 4-11 is the SEM graph of particles containing theophylline and budesonide, which were produced from solutions of these APIs. The raw material of theophylline exhibits a needle-like shape, and budesonide is used as micronized material. After spray drying, the APIs form a sphere shape particles, which can be depicted in Fig. 4-11. When APIs precipitate together from spray drying, the needle-like particles become sphere-like without excipients, which is noticeable in Fig. 4-11-A, and the particles produced with excipients is a part of needle-like adhesive to the sphere particle, which are found in Fig. 4-11 (B to I). Among them, Fig.4-11(B) and Fig.4-11(C) have longer needles, while Fig.4-11 (D-I) illustrates the number of sphere particles have increased gradually.

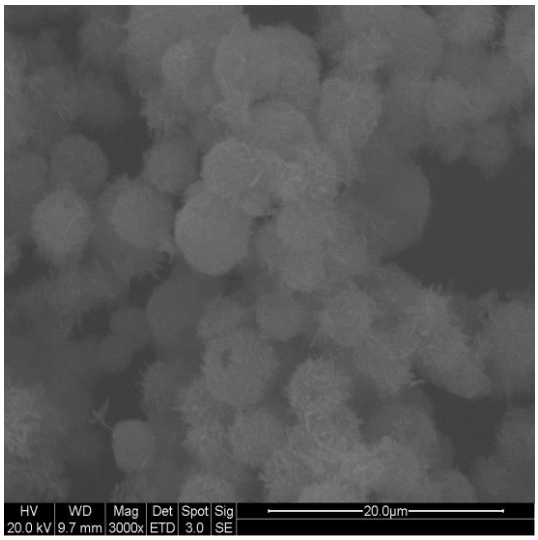

A: No Excipients TB-1

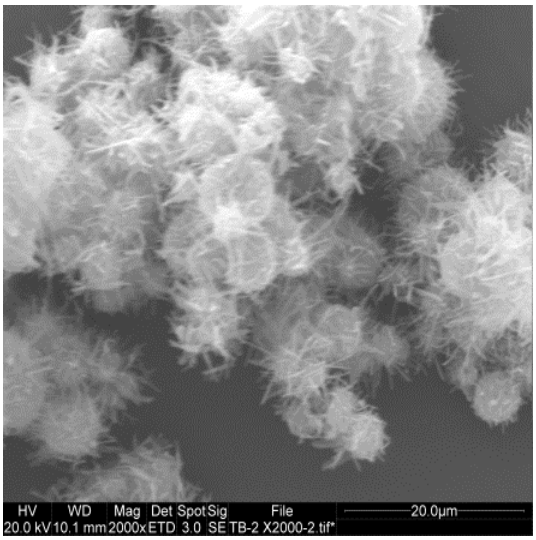

B: 0.05% PVP TB-2

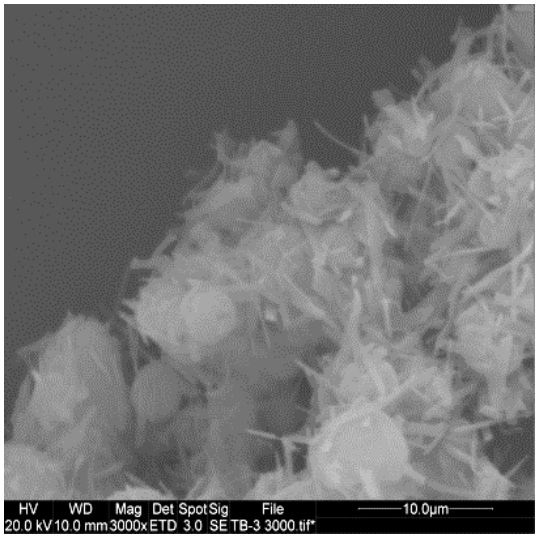

C: 0.1% PVP TB-3

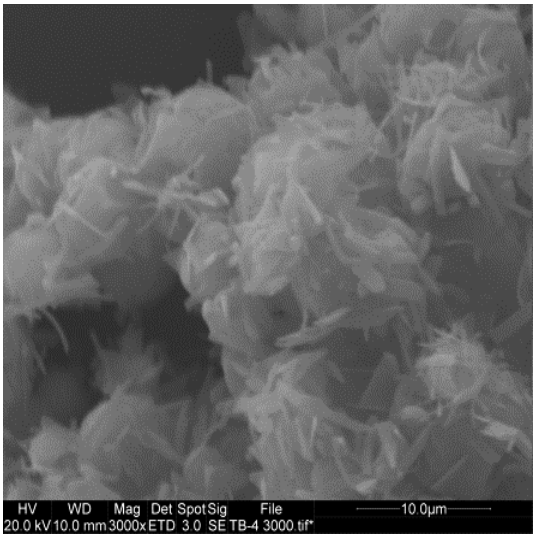

D: 0.25% HPMC TB-4

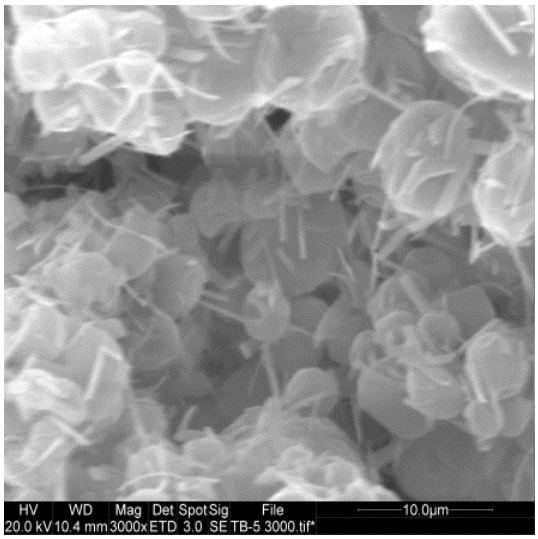

E: 0.25% HPMC+0.05% PVP TB-5

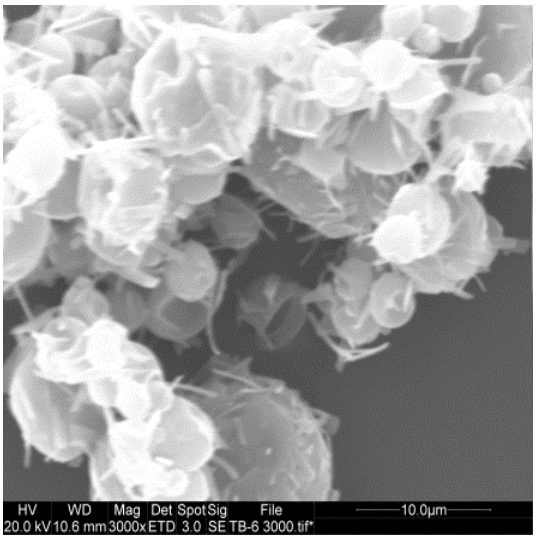

F: 0.25% HPMC+ 0.1% PVP TB-6

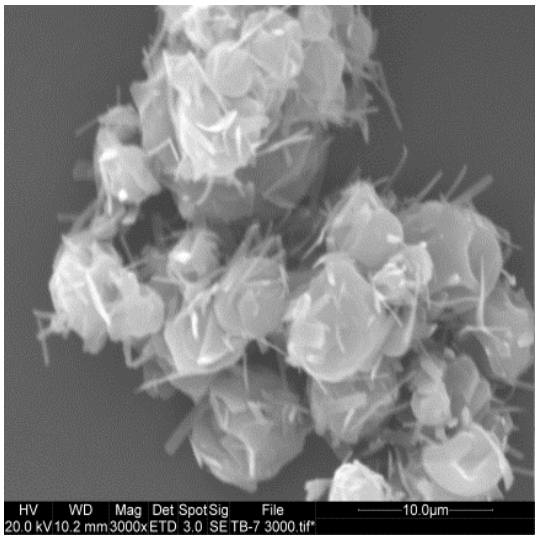

G: 0.5% HPMC TB-7

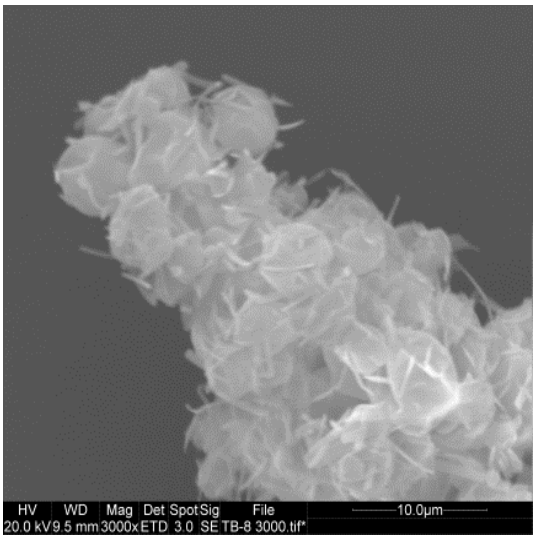

H: 0.5% HPMC + 0.05% PVP TB-8

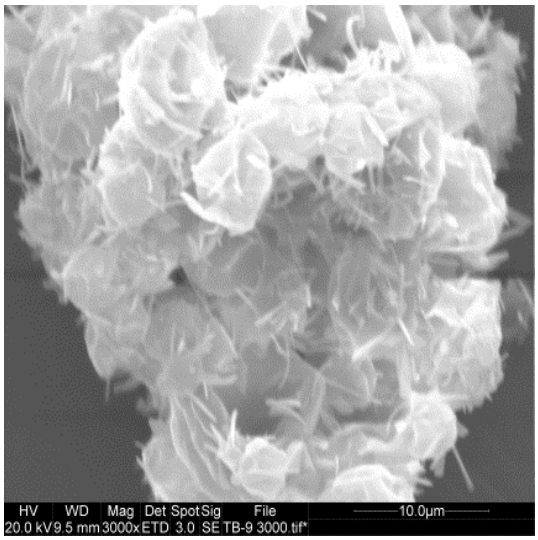

I: 0.5% HPMC + 0.1% PVP TB-9

Fig. 4-11. Spray-dried dual particles [Spray drying conditions: Solution: saturated solution (about 3%, w/v); solvent: 80% Methanol+20% Deionised Water].

According to these observations, most particles which were obtained from the solvent with no or lower concentration of HPMC, are needle-like with a length of about 10 µm. By increasing the amount of HPMC, it makes the needles become shorter and flat. Particles produced from PVP solution results in a longer shape than the particles generated from HPMC. Conversely, the addition of PVP forms more regular shape of spheres, since smaller molecule PVP can rapidly touch the particle surfaces and act as lubricant between the particles to form a relatively smooth surface on particles during the spray drying. Furthermore, PVP could work with HPMC to enhance HPMC binding with APIs and reduce the APIs lost during the spray dry to generate a stable combination particle as shown in Fig. 4-6. This result indicates that the polymers help to produce sphere shape particles.

4.3.6 Aerodynamic behaviour

According to the results of laser sizer and HPLC, the TB-5, TB-6, TB-8 and TB-9 were chosen to be carried out the aerodynamic assessment, due to their smaller size distribution and constant ratio of TH:BU. The assessment of the aerodynamic

behaviour is tested using the NGI. These assessments includes: (1). disposition of combination particle only; (2). 80% lactose mixture; (3). 96% lactose mixture.

The overall result of assessment is displayed in Fig. 4-12, which describes the FPF of each blend. According to Fig. 4-12, it can be found absence or low concentration of lactose result in a low FPF from 4-18% as expected due to the poor flowability.

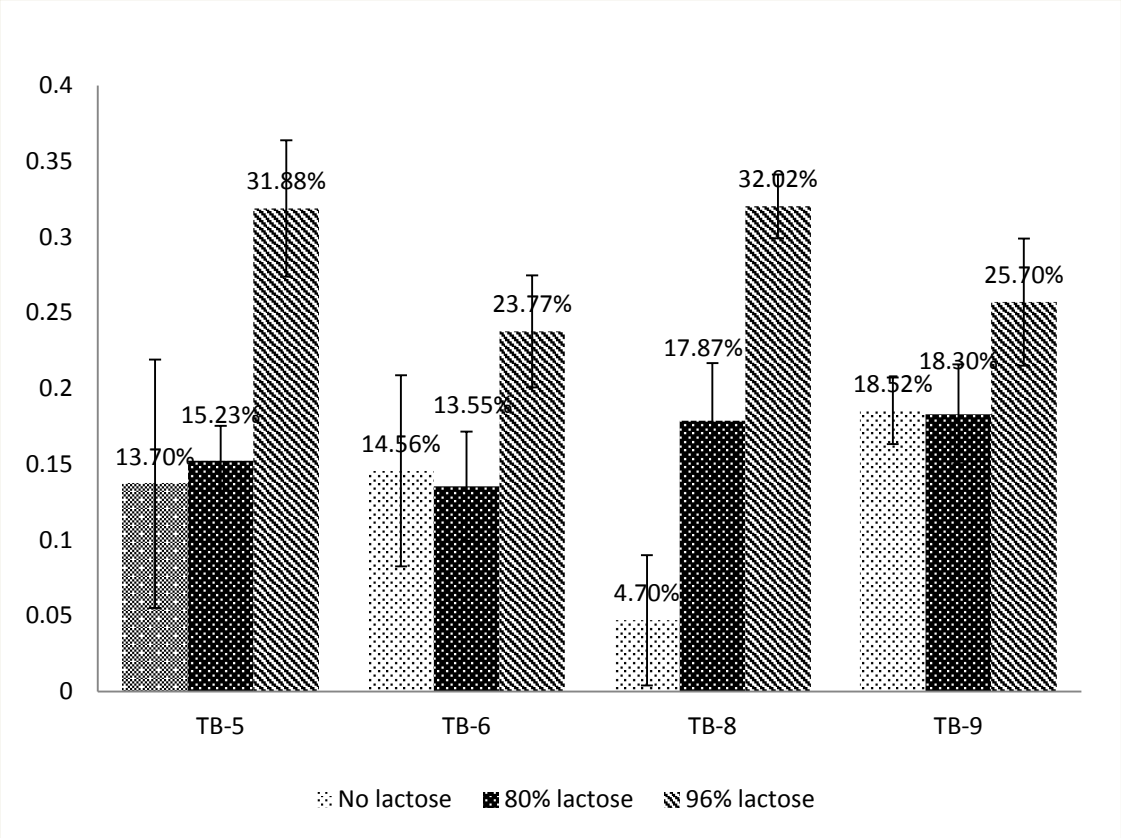

Fig. 4-12. Average Fine Particle Fractions (FPF) of combined particles in presence/absence of lactose in a physical mixture [precipitation conditions: Spray drying conditions: Solution: saturated solution (about 3%, w/v); solvent: 80% Methanol+20% Deionised Water].

As most DPI formulations deal with lactose blends where coarse lactose of several 100 µm acts as carrier for the micronized API (Chapter 2.2.2), hence a mixture of combined particles with lactose was prepared and tested for its aerodynamic behaviour in the NGI. This study demonstrates that the capsule is not as completely emptied without lactose, as lactose particles in the blend might press the combined particles to the inner surface. Nevertheless, the performance of this blend is even better with respect to an FPF of 32.02% as expected in Fig. 4-12, due to the lower interparticle adhesion forces in a lactose blend. It is also found that bigger amount of lactose enhances the FPF significantly and depends on the concentration used. This can be attributed to lactose reduces the interparticle forces which make the powder cohesive. This is also related to balance of cohesive and adhesive forces, as stronger cohesive force may enhance agglomerate formation and excessive adhesive forces may prevent elutriation of the respirable particles from the carrier surfaces, which are leading to upper airway deposition.

Furthermore, it also worth to determine whether there are any effect on the FPF when the powder is precipitated from different solutions. By linking the discussion above with the SEM results as in Fig.4-11, it was interestingly found that there should be a difference between the powder precipitated with PVP and HPMC, as they show different particle sizes and slightly different shapes. This could also be verified that particles with lower concentration of PVP in a mixture show a significant 6% higher of FPF as plotted in Fig.4-12. As can be seen in Fig. 4-13, the deposition of the single drugs theophylline and budesonide on the stages of the NGI shows a very uniform distribution, indicating that both drugs are codeposited and has a FPF of 32.02%. Compared with the commercial product

Seretide® 500, which is a tertiary mix of the APIs with lactose and is distributed with Aeroliser®, its resulting FPF of about 27% was found (Taki et al.).

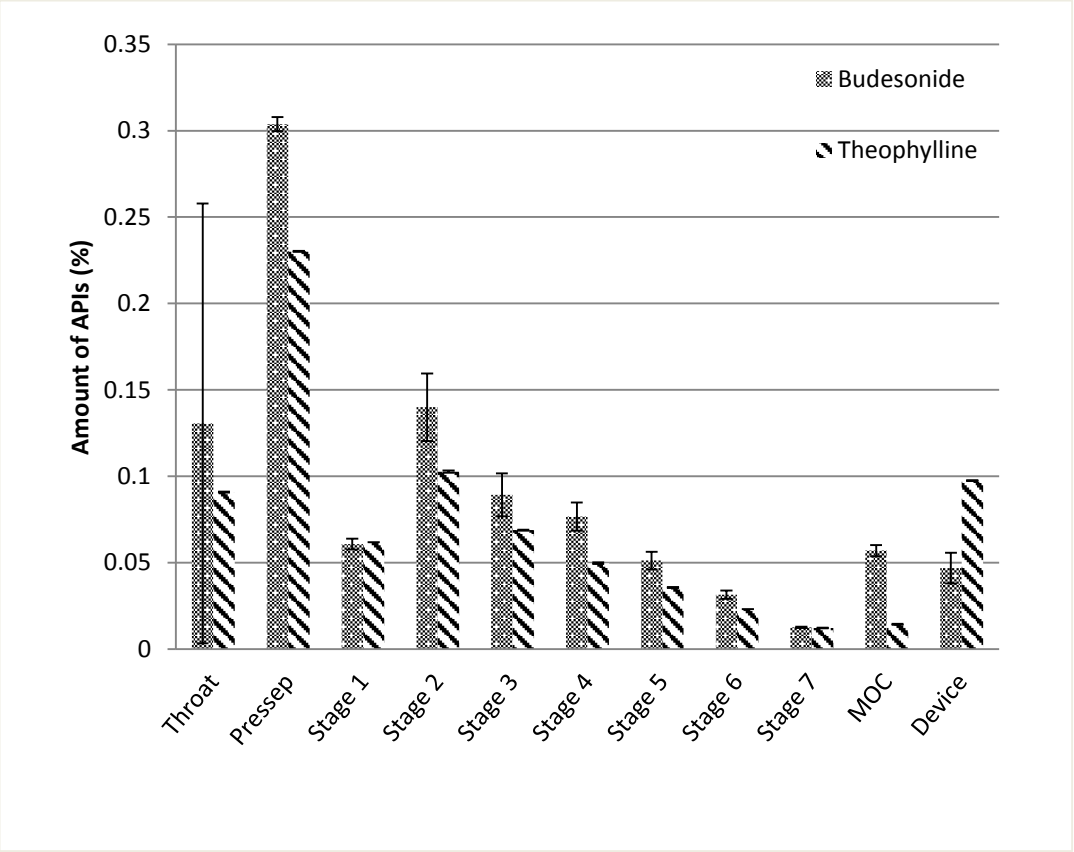

Fig. 4-13. Deposition of the APIs from combined particles (TB08) mixed with 96% lactose on the NGI stages with regard to distribution of the single substances [theophylline and budesonide], [precipitation conditions: Solution: saturated solution (about 3%, w/v); solvent: 80% Methanol+20% Deionised Water (0.5% HPMC, 0.05% PVP)].

4.4 Conclusion

Addition of excipients during the precipitation process is essential for stabilisation and for achievement of dual particles in the low micro scale. The experiment

results showed that the excipients influence the flowability of the particles. A combination of PVP and HPMC in equal shares resulted in combined particles of theophylline and budesonide with an average particle size in the respirable range. The product is partly crystalline after spray drying and meets the requirement of pulmonary delivery. The excipients also influences the habit of the precipitate as well as aerodynamic behaviour of particles.

Without further processing, the dual particles have a moderate FPF of about 14%, however, because of high dosage of APIs, the FPF is only 4% from the mixture with lower amount of lactose; nevertheless the higher amount of carrier can be able to remarkably increase the FPF to 32%. This is a significant improvement compared to the commercial product(Taki et al.). Furthermore this study shows that both APIs are evenly distributed throughout the stages of the NGI thus indicating a codeposition of both substances. The co-particles have a benefit in both FPF and codelivery can be achieved. Additionally, ANN models provide good estimation of the quantity of theophylline in solution and in the combination particle with small amount of data. It is an ideal tool to help the future study to control and optimise the formulation procedures. In summary, the technique of combined spray drying is an interesting approach for the production of dual particles, nevertheless formation of coprecipitate is not completely resolved yet. These experiments indicate that some optimisation studies could be carried out to improve dispersibility of AIPs with high dosage.

Chapter 5 : Ultrasound Assisted to Formulate Combination Particles Containing Theophylline and Budesonide

5.1 Introduction

In chapter 4, the spray drying was operated to generate combination particles, which were sphere-like particles with constant composition. However the desired aerodynamic performance of these particles, which were deliveried from high dosage formulation, was not achieved. In order to meet this requirement, this chapter is devoted to analyse low density particles, i.e. porous or hollow structure particles. Fig. 5-1 shows the procedures on how to construct the porous particles. As can be seen, Fig.5-1(a) decribes the general spray drying procedures. To better understand the detailed process, Fig. 5-1(b) illustrates the experimental steps to achieve macroporous or nanostructured hollow particles using spray drying. It is noticable that the precursor should be nano-suspension containing APIs and templating particles of a defined diameter. During spray drying, suspension is atomized to form spherical droplets with fix concentration of particles. Meanwhile, the solvent of droplets is evaporated to form submicrometer-sized nanostructured particles. This is in constrast to the process to obtain practicle as shown in Fig.5-1(c) which was used in previous chapter.

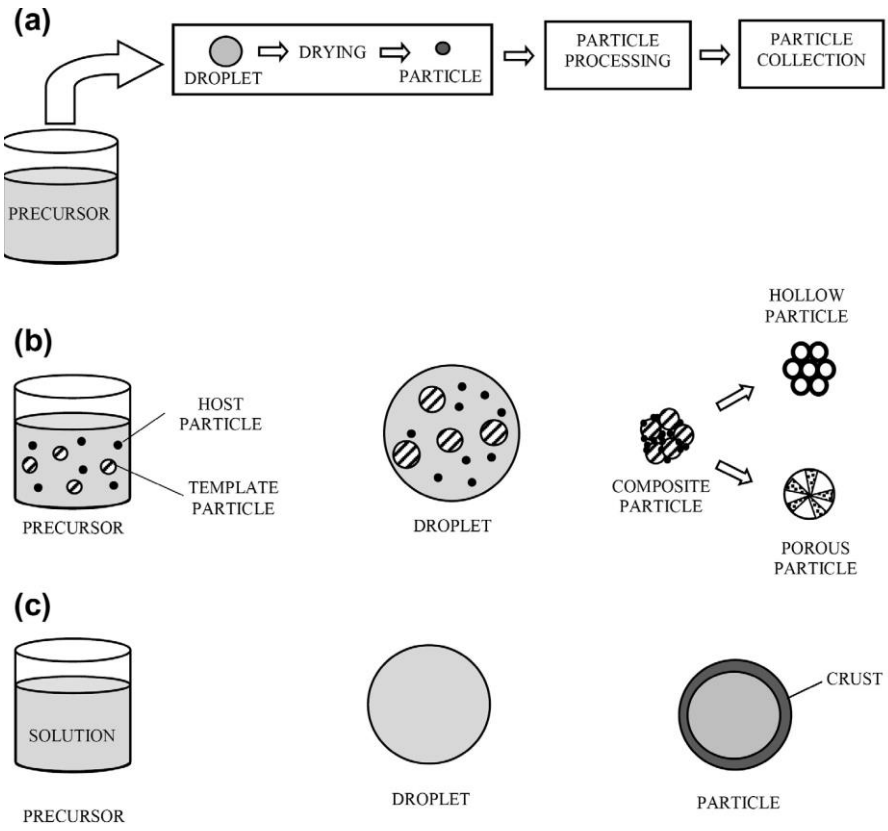

Fig. 5-1. Particle engineering by spray-drying: (a) a general idea of the process, (b) and (c) tuning of the particle morphology through precursor composition and process conditions(Gradon and Sosnowski, 2014)

Application of ultrasound during crystallization is known to maintain uniform conditions reasonably throughout the crystallization vessel (Louhi-Kultanen et al., 2006). Application of power ultrasound to control crystallization from solution is known as sonocrystallization (Louhi-Kultanen et al., 2006, Dhumal et al., 2009, Kaerger and Price, 2004). This technique has been widely reported to produce nanosuspensions.

The aim of this study is to investigate the feasibility of producing micron-sized combination particles of theophylline and budesonide by an ultrasonic technique. Our hypothesis is to conduct the process which could enhance the homogeneous

nucleation of APIs (theophylline and budesonide) and allows reducing the consumption of organic solvent and power for the production of a desirable particle size. This approach is based on the fact that a gradual addition of a solution to an antisolvent (water) in a liquid–liquid antisolvent process increases the degree of supersaturation. The effects of operating parameters, i.e. feed rate, concentration of excipients and sonication power, on the particle size of combination particles were examined. To obtain the best of these parameters, an experimental design was adopted to produce suspensions which are suitable for generation of combination particles via spray drying. After this process, the physical-chemical properties of the processed powder and its aerosol performance were measured.

5.2 Materials and methodologies

5.2.1 Materials

The materials used in this study are same in the chapter 2.2.

5.2.2 Preparation of the systems

5.2.2.1 Submicron-suspension production

The submicron suspension was obtained by ultrasound equipment. This methodology has been mentioned in Chapter 2.3.4.

In each experiment, a peristaltic pump was used to feed 25 ml APIs solution with flow rate of 5 ml/min, and 10 ml/min to the crystalliser. Then, ultrasound was applied to the clear solution with the same volume of water. Table 5-1 shows the setting for the ultrasound at various amplitudes and pulse of 10 s with relaxation time of 2 s. Typically the micronization process was only run for 3min due to injection of small volume of solution to the anti-solvent. The temperature of the solution was maintained constant during this short period.

The sonifier was connected to a computer. This can enable the pre-adjustment of important control parameters such as amplitude, pulse length and sonication time. The precipitation reaction was kept at 5 ◦C. The particles were produced at different conditions as depicted in Table 5-1. The amplitudes were set at 27%, and 45%. APIs solution was injected into the anti-solvent at each run. In the solution, solvent was formed by water and ethanol at the ratio of 20:80. The APIs were dissolved with various amounts of excipients to form the solutions at temperature of 50 ◦C (Table 5-1). The weight ratio of theophylline and budesonide was at 100:5 that is chosen to cover the therapeutic range of the clinical dosage of inhaled budesonide (Barnes et al., 2010, Evans et al., 1997), where the concentration of solution was about 3.5% w/v.

5.2.2.2 Spray drying

The processing procedures have been described in chapter 2.3.2. The suspension of theophylline and budesonide were dried using spray drying. The mixtures were kept in a sealed container and stored in a desiccator at room temperature for further characterisation.

5.2.2.3 Particle characterisation methods and drug quantification

The particle characterisation methods have been fully described in Chapter 2.4, such as thermal analysis (Chapter 2.4.3), XRD (Chapter 2.4.2), SEM (Chapter 2.4.4), particle sizing (Chapter 2.4.1), and aerodynamic analysis (Chapter 2.4.7). Drug quantification was also illustrated in chapter 2.4.6.

5.3 Results and discussion

5.3.1 Experimental design

The effects of independent process variables namely HPMC, PVP, amplitudes, and feed rate on the particle size distribution of particles are presented in Table 5-1.

Table 5-1 Design matrix in the full factorial design with factors, and factors' levels. (HPMC: -1=0% w/v, 1=0.5% w/v; PVP: -1=0% w/v, 1=0.1% w/v; Amplitudes: -1=27%, 1=45%; Feed rate: -1=5ml/min, 1=10ml/min).

Sample	Factors			
	HPMC	PVP	Amplitudes	Feed rate
TB1	1	1	1	1
TB2	1	-1	1	1
TB3	1	1	-1	1
TB4	1	1	1	-1
TB5	1	-1	-1	1
TB6	1	1	-1	-1
TB7	1	-1	1	-1
TB8	1	-1	-1	-1
TB9	-1	1	1	1
TB10	-1	-1	1	1
TB11	-1	1	-1	1
TB12	-1	1	1	-1
TB13	-1	-1	-1	1
TB14	-1	1	-1	-1
TB15	-1	-1	1	-1
TB16	-1	-1	-1	-1

In response to screening modelling technique, a regression model was fitted to establish the relationship between the particle size and the variables, which is shown in Table 5-2, where the coefficient of the regression model and the p-value displays the significance of each factors.

Table 5-2 Summary of output

Regression Statistics	
Multiple R	0.983108018
R Square	0.966501376
Adjusted R Square	0.954320058
Standard Error	425.6136278
Observations	16

Calculated coefficient values.

	Coefficients	Standard Error	P-value
Intercept	2060.04375	106.403407	7.57066E-10
HPMC	-1860.45625	106.403407	2.24797E-09
PVP	-362.98125	106.403407	0.005811171
Amplitudes	-11.36875	106.403407	0.916835119
Feed rate	0.51875	106.403407	0.996197372

According to Table 5-2, HPMC and PVP were found as main effects on particles size. However, it is unknown that how co-effects were produced by HPMC, PVP, amplitudes and feed rates, thereby, the ANOVA analysis was applied for further studies. The primary purpose of ANOVA is to understand if there is an interaction between the independent variables on the dependent variable. In this study, ANOVA is applied to understand whether there is an interaction between

excipients (HPMC/PVP) and processing parameters (amplitude/feed rate) on the observed particle size of suspension, where HPMC, PVP, amplitudes and feed rates are independent variables, and particle size is dependent variable. This model is shown in the following equation, which is a full factorial analysis model.

$$Y = \beta_0 + \beta_1 x_1 + \beta_2 x_2 + \beta_3 x_3 + \beta_4 x_4 + \beta_{12} x_{12} + \beta_{13} x_{13} + \beta_{14} x_{14} + \beta_{23} x_{23} + \beta_{24} x_{24} + \beta_{34} x_{34} + \beta_{123} x_{123} + \beta_{134} x_{134} + \beta_{234} x_{234} + \beta_{1234} x_{1234} + \epsilon$$

(Equation 5-1)

Where the indicator variable, x_1=HPMC, x_2=PVP, x_3= Amplitudes, x_4= Feed rate; the β is the regression coefficient for the main effects of factors (HPMC, PVP, amplitude, and feed rate), $\beta_0 =$ 2060.04375, $\beta_1 =$ -1860.45625, $\beta_2 =$ -362.98125, $\beta_3 =$-11.36875, $\beta_4 =$0.51875. β_{12} , β_{13} … β_{1234} are the regression coefficients for the interactions of variables.

Table 5-3 is the summary of ANOVA output. As presented in Table 5-3, the *p*-value (sig.) of HPMC, PVP and HPMC*PVP was less than 0.05, thus these variables act as the most significant factors.

Table 5-3 Summary of ANOVA output

Dependent Variable:Observed

Source	Type III Sum of Squares	df	Mean Square	F	Sig.
HPMC	55380759.331	1	55380759.331	3419.352	.000
PVP	2108086.206	1	2108086.206	130.159	.006
Amplitudes	2067.976	1	2067.976	.128	.917
Feed	4.306	1	4.306	.000	.996
HPMC * PVP	1838939.406	1	1838939.406	113.541	.000
HPMC * Amplitudes	993.826	1	993.826	.061	.811
HPMC * Feed	4.306	1	4.306	.000	.983
PVP * Amplitudes	11220.106	1	11220.106	.693	.429
PVP * Feed	41056.891	1	41056.891	.000	.983
Amplitudes * Feed	120.451	1	120.451	.000	.996
HPMC * PVP * Amplitudes	11897.356	1	11897.356	.735	.416
HPMC * PVP * Feed	39750.391	1	39750.391	4.244	.073
HPMC * Amplitudes * Feed	256.801	1	256.801	.001	.983
PVP * Amplitudes * Feed	25082.641	1	25082.641	.004	.954
HPMC * PVP * Amplitudes * Feed	23294.391	1	23294.391	.000	.993
Error	1992616.562	11	181146.960		
Total	1.274E8	16			
Corrected Total	59483534.379	15			

a. R Squared = .931 (Adjusted R Squared = .871)

According to regression and ANOVA analysis, it was found that excipients and HPMC*PVP were potential elements causing considerable effects on the particle

size. Therefore, it can be able to generate a mathematical model to predict particle size by using the following expression:

$$Y = \beta_0 + \beta_1 x_1 + \beta_2 x_2 + \beta_{12} x_{12} + \epsilon \qquad \text{(Equation 5-2)}$$

$$\mathrm{Y} = 2060.04 - 1860.46\mathrm{x}_1 - 362.98\mathrm{x}_2 + 339.02\mathrm{x}_{12} + \epsilon$$

$$R^2 = 0.997$$

The predicted results are descried in Table 5-4. This result was plot as 3D-scatter figure as can be found in Fig. 5-2, where the predicted result closes to the observation and has similar tendency. Moreover, the R^2 of model is 0.997. Therefore, this finding suggests that this model has capability to estimate the particle size in this experiment.

Table 5-4 The responds of model

Sample	Results/Responds	
	Observed particle size, nm	Predicted particle size, nm
TB1	171.4	175.625
TB2	225.4	223.55
TB3	180.3	175.625
TB4	171.3	175.625
TB5	225.4	223.55
TB6	179.5	175.625
TB7	216.3	223.55
TB8	227.1	223.55
TB9	3068	3218.5
TB10	4721	4622.5
TB11	3168	3218.5
TB12	3438	3218.5
TB13	4725	4622.5
TB14	3200	3218.5
TB15	4378	4622.5
TB16	4666	4622.5

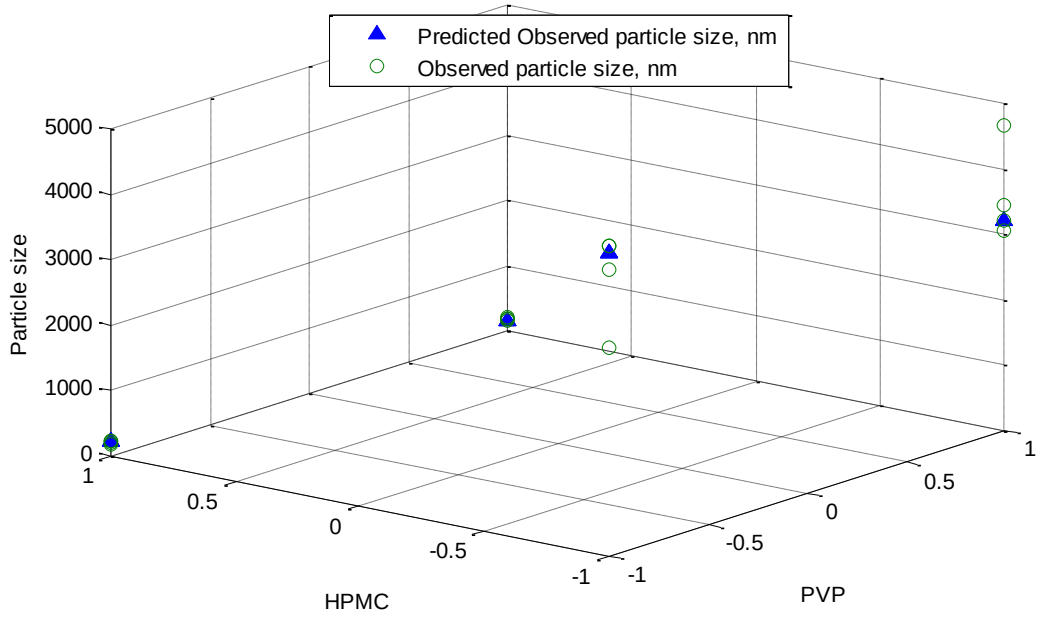

Fig. 5-2. Predicted and observed particle size at different levels of excipients

Following the above study, excipients was indicated as main causes on particle size, therefore, the diversity concentrations of excipients were used in the second run of experimental design that has be displayed in Table 5-5. Table 5-5 describes the experiments were operated at a fixed amplitude of 27% and feed rate of 10 ml/min.

Table 5-5 Design matrix in the full factorial design with factors, factors' levels and response values. (HPMC: -1=0% w/v,0=0.25%, 1=0.5% w/v; PVP: -1=0% w/v, 0=0.05%, 1=0.1%)

Sample	Factors	
	HPMC	PVP
TB01	-1	-1
TB02	-1	0
TB03	-1	1
TB04	0	-1
TB05	0	0
TB06	0	1
TB07	1	-1
TB08	1	0
TB09	1	1

Table 5-6 is the observed result for this study. As can be found in Table 5-6, there is no significant influence on the ratio of theophylline:budesonide, so the model was established using excipients and particle size.

Table 5-6 Result of experiments

Sample	Results/Responds	Ratio between theophylline and budesonide in suspension
	Observed particle size, nm	
TB01	4725	21:1
TB02	3668	20:1
TB03	3168	19:1
TB04	579.1	20:1
TB05	226	21:1
TB06	214.1	21:1
TB07	225.4	20:1
TB08	173.2	20:1
TB09	171.4	21:1

In order to obtain the model, firstly, the ANOVA study was used to understand the interaction between excipients (HPMC/PVP) on the observed particle size of suspension. This model is a full factorial analysis model can be formulated as below:

$$Y = \beta_0 + \beta_1 x_1 + \beta_2 x_2 + \beta_{11} x_{11} + \beta_{22} x_{22} + \beta_{12} x_{12} + \beta_{112} x_{112} + \beta_{122} x_{122} + \beta_{1122} x_{1122} + \epsilon$$

(Equation 5-3)

Where the indicator variable, x_1 =HPMC, x_2 =PVP; the β is the regression coefficient for the main effects of factors (HPMC, PVP), β_{12} , β_{13} … β_{1234} are the regression coefficients for the interactions of variables.

Table 5-7 shows the results from the ANOVA analysis. According to Table 5-7, HPMC and PVP2*HPMC^2 have a significant influence on particle size, where the sig. was less than 0.05.

Table 5-7 The result of ANOVA analysis

Tests of Between-Subjects Effects

Dependent Variable:Size

Source	Type III Sum of Squares	df	Mean Square	F	Sig.
HPMC	25792600.987	2	12896300.493	57.244	.000
PVP	700753.887	2	350376.943	.079	.925
HPMC^2	5658920.820	1	5658920.820	1.844	.217
PVP^2	49991.220	1	49991.220	.013	.913
HPMC*PVP	3255450.332	2	1627725.166	.409	.682
HPMC^2*PVP	3339528.332	2	1669764.166	.421	.674
PVP^2*HPMC	16738951.692	2	8369475.846	4.826	.500
HPMC^2*PVP^2	2690698.082	1	2690698.082	.770	.049
Error	1299597.907	4	324899.477		
Total	46358525.980	9			

a. R Squared = .972 (Adjusted R Squared = .937)

Table 5-8 presents the result of regression analysis. From Table 5-8, 0.4631 of sig. is found and this demonstrates that PVP was not an important factor in this study. Thereby, HPMC and PVP^2*HPMC^2 were employed to build model, which is can be found in the following equation

$$Y = \beta_0 + \beta_1 x_1 + \beta_{1122} x_{1122} + \epsilon \qquad \text{(Equation 5-4)}$$

$$Y = 972.8 - 1831.83 x_1 + 1100.37 x_{1122} + \epsilon$$

R^2=0.897

Table 5-8 Regression analysis output

Regression Statistics	
Multiple R	8.750E-01
R Square	7.657E-01
Adjusted R Square	6.876E-01
Standard Error	1.030E+03
Observations	9.000E+00

Calculated coefficient values.

	Coefficients	Standard Error	P-value
Intercept	1.461E+03	3.432E+02	5.335E-03
HMPC	-1.832E+03	4.203E+02	4.780E-03
PVP	-3.293E+02	4.203E+02	4.631E-01

A plot of observed and predicted of particle size versus excipients is shown in Fig. 5-2. It depicts that the deviation between experimental values and predicted values is less than 10%. Table 5-9 illustrates that F-statistic >F-critical. All these characteristics demonstrate that the model is suitable for predicting particle size within the range examined.

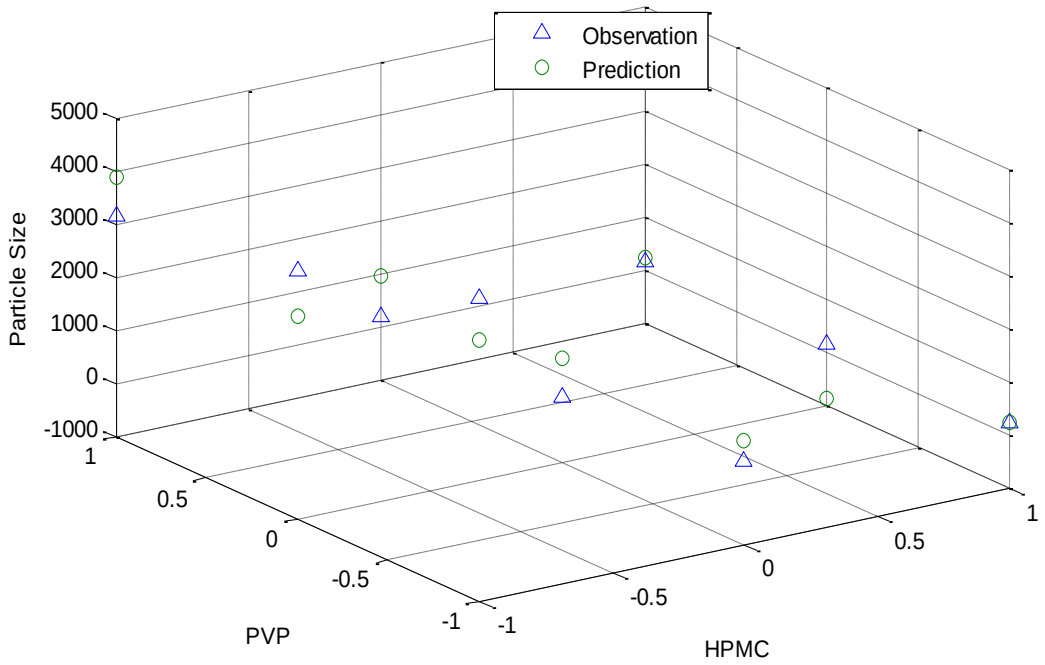

Fig. 5-3. Predicted and observed particle size at different levels of excipients

Table 5-9 Summary of ANOVA data.

	df	SS	MS	F	Significance F
Regression	2	22824378.25	11412189	15.85043816	0.004030876
Residual	6	4319952.171	719992		
Total	8	27144330.42			

DF: degree of freedom, SS: sum of square, MS: mean sum of square, SD: standard deviation, F: F-statistic, Significance F: F-critical

The data in Fig. 5-4 displays the predicted particle size with their lower and upper limits versus each of excipients. The lower and upper limits of particles size represent the minimum and maximum limits which are achieved within the range of operating conditions examined. These plots demonstrate that all variables are negatively correlated to the particle size, however, the particle size relatively

grows up at higher concentration of PVP. As can be observed in Fig. 5-3 and 5-4, the best condition is to adopt processed solution containing highest concentration of excipients, where HPMC is 0.5% and PVP is 0.1%. However, the inhalable formulation requires less excipients, although the observed size of particles is 171.4 nm produced from highest concentration of excipients (TB09), the particle size of TB05 (generated from medium concentration of excipients) is 226nm that meets the requirement of spray drying and aerodynamic measurement. This area also is the best range as found in Fig. 5-4.

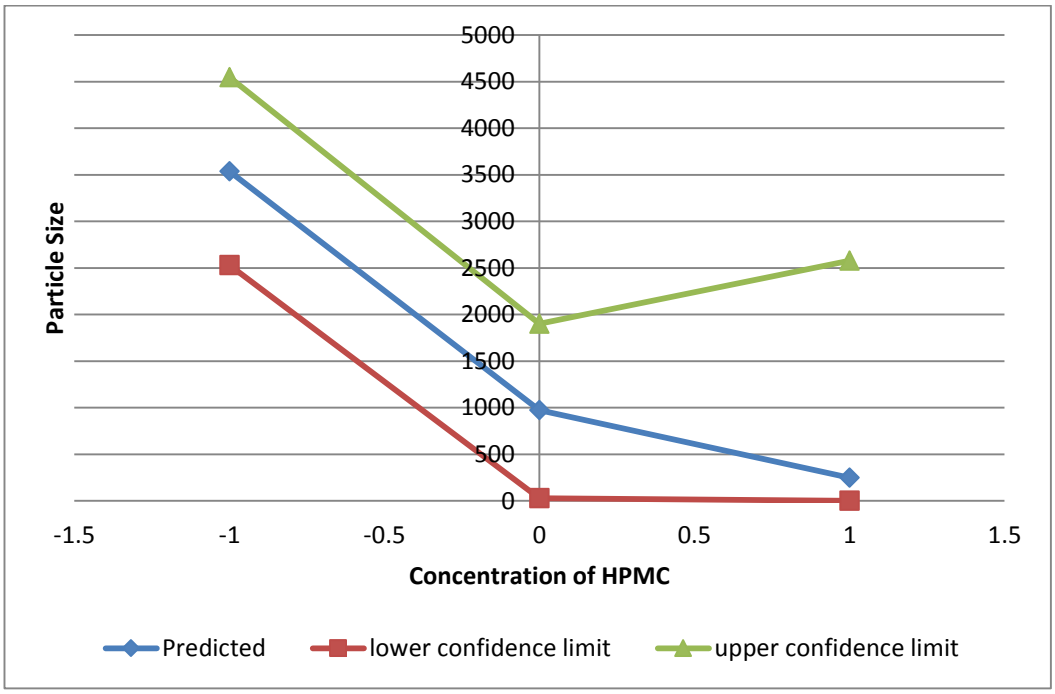

a.

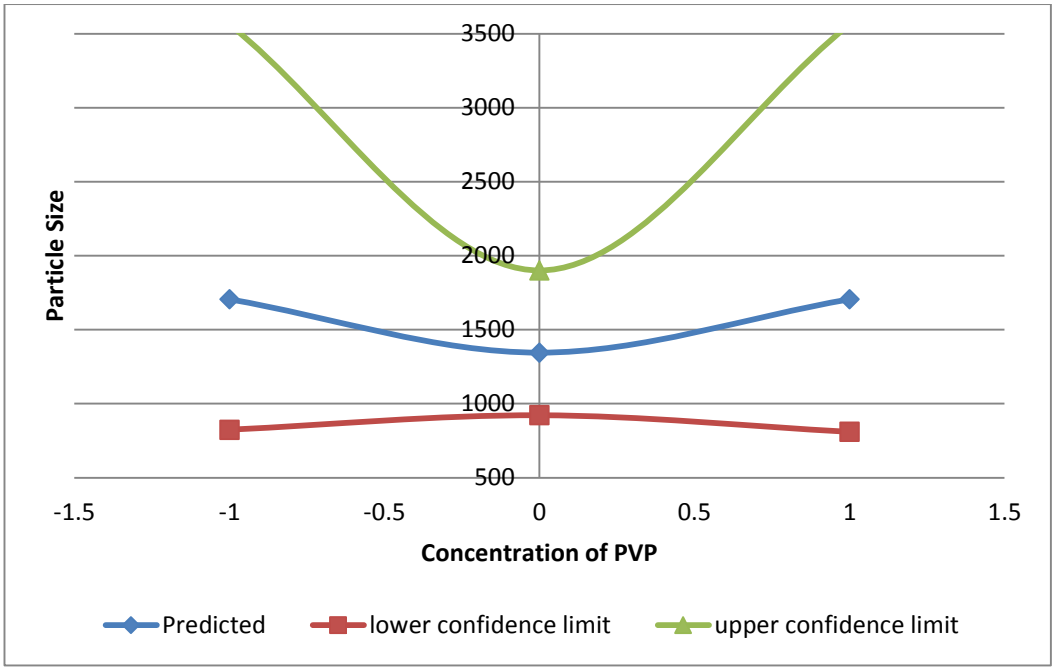

b.

Fig. 5-4. Predicted particle size (blue) with upper confidence limit (green) and lower confidence limit (red) versus (a) concentration of HPMC and (b) concentration of PVP

5.3.2 Crystallinity

According to the study of experimental design in chapter 5.3.1, TB05 was selected to be spray dried, where the dry powder was namely TB002. In order to compare the ultrasonic process with spray drying, the solution which was used to generate TB05 was adopted for spray drying to form dry powder (TB003). Sample TB001 was spray dried using APIs solution without excipients. In this study, DSC and X-ray diffraction were applied to characterise the physicochemical properties of the samples and to determine the crystal formation.

Fig. 5-5 plots the DSC results. As can be found in Fig. 5-5, DSC measurements suggested that it cannot detect budesonide melting peak in spray dried sample TB001, as small amount of it, therefore, it creates no interpretable DSC signal.

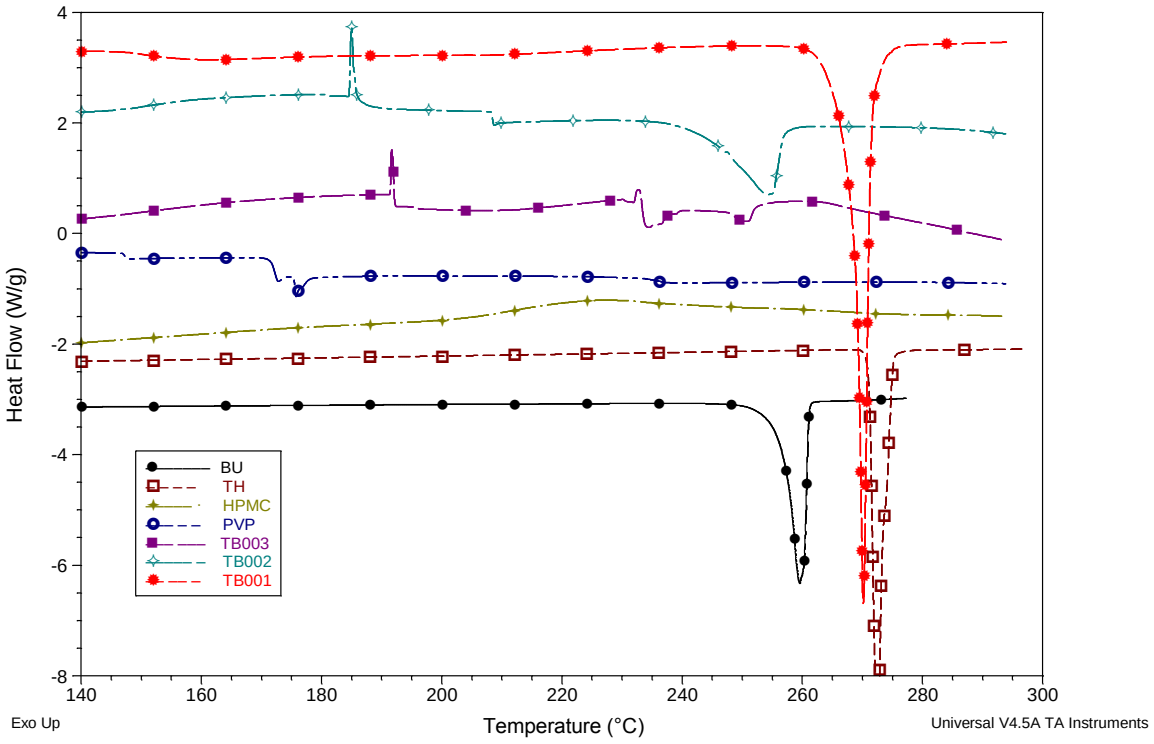

Fig. 5-5. DSC curves from single APIs, physical mixtures and processed samples, TH=theophylline, BU=budesonide, TB001=spray dried particle without excipients; TB002= spray dried nanosuspension TB05; TB003=spray dried solution of TB05

However, the endotherm signal of budesonide is explored in TB002 as depicted in Fig. 5-6. The results of XRD pattern reveal a strong signal belongs to budesonide in TB002. This also well agrees in the finding in SEM as shown in Fig.5-7 E, in which it can be seen that some crystal locate on the surface of sphere particle of TB002. According to these detections, it can be assumed that

higher concentration of theophylline and its xanthine group would occupy the hydrogen bond of polymer, thus some budesonide are miss loaded. Therefore, after spray drying, the budesonide crystals are formed and stay on the surface of particles.

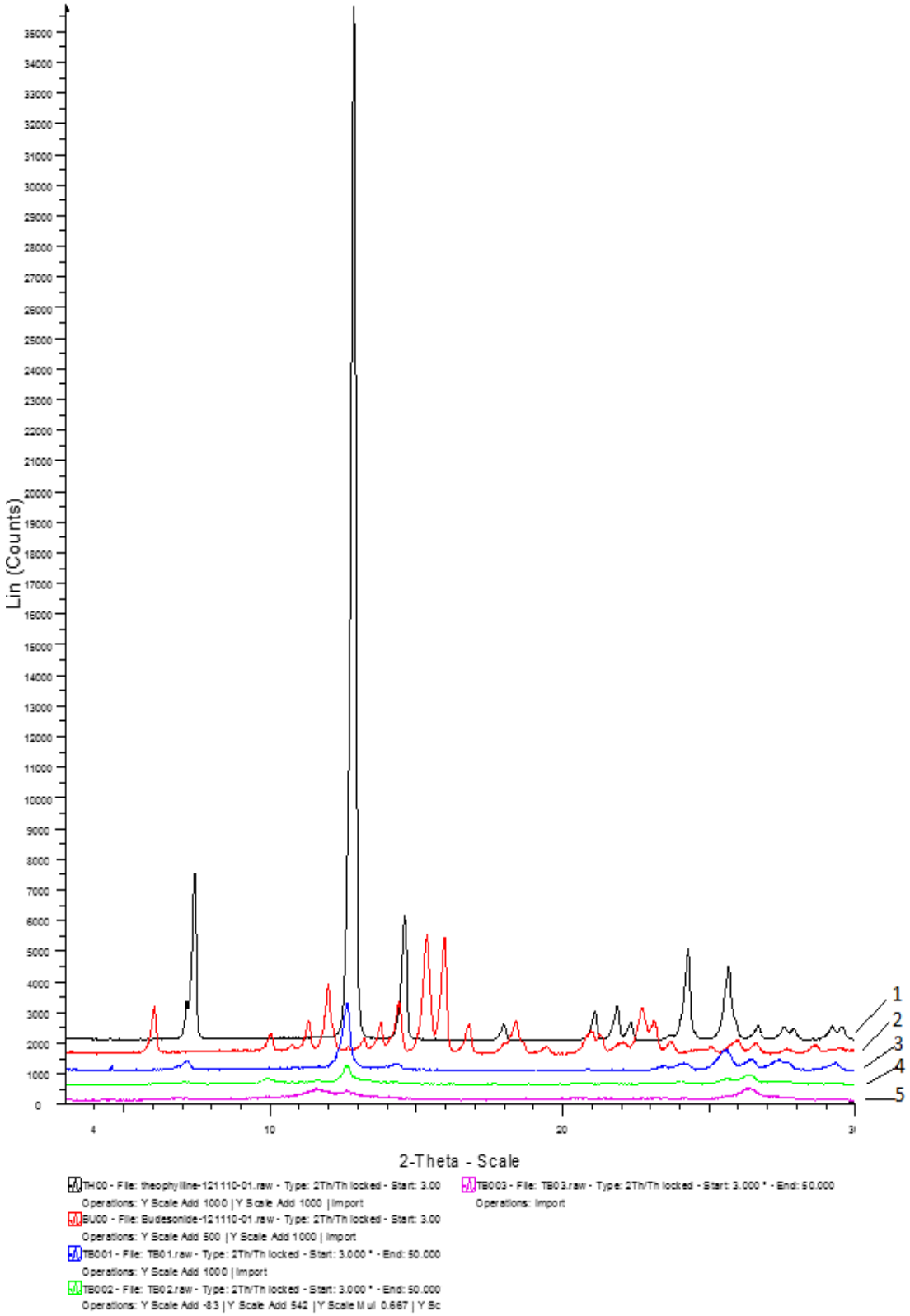

Fig. 5-6. X-ray pattern of processed sample TB001, TB002, and TB003. 1: raw theophylline (TH00); 2: raw budesonide (BU00); 3: TB001; 4: TB002; 5: TB003

In X-ray diffraction measurements as illustrate in Fig. 5-6, the particle shows a partly crystalline pattern with excipient when excipient is masking with crystal peaks. Correlation of the pattern peaks to peaks of single substances can be done, but it is not consistent for every peak. These data indicate that there might be a slight change, but it cannot prove neither cocrystallisation nor theophylline monohydrate in the sample. Therefore it is assumed that spray dry results in a coprecipitate, but not generation of cocrystal.

5.3.3 Morphology

The SEM images for untreated material, spray dried samples, and TB002 (Ultrasound treated) are shown in Fig. 5-7. The raw material of theophylline exhibits a needle-like shape while budesonide is used as micronized material. When they precipitate together, the particle is needle-like forming to sphere without excipients, which is similar to spray dried theophylline in Fig.5-7-C-D. As shown in Fig. 5-7-E, the ultrasound sample exhibits a porous shape, which is a part of crystal adhesive to the sphere particle. Fig. 5-7-F is the graph of the particles spray dried directly from solution. As can be clearly seen, these particles are sphere-like with smooth surface.

Table 5-10 describes the laser diffraction result of particle size distribution. This result shows that the resultant samples are formed with approximate size of 0.91-8.53µm. As a result of slight aggregation between these particles and their shape, ultrasound treated sample has narrower size distribution than the spray dried sample, and average particle sizes which are measured by laser technique, is around 5µm, as can been found in Table 5-10. The results confirm that it is suitable for inhalation drug delivery.

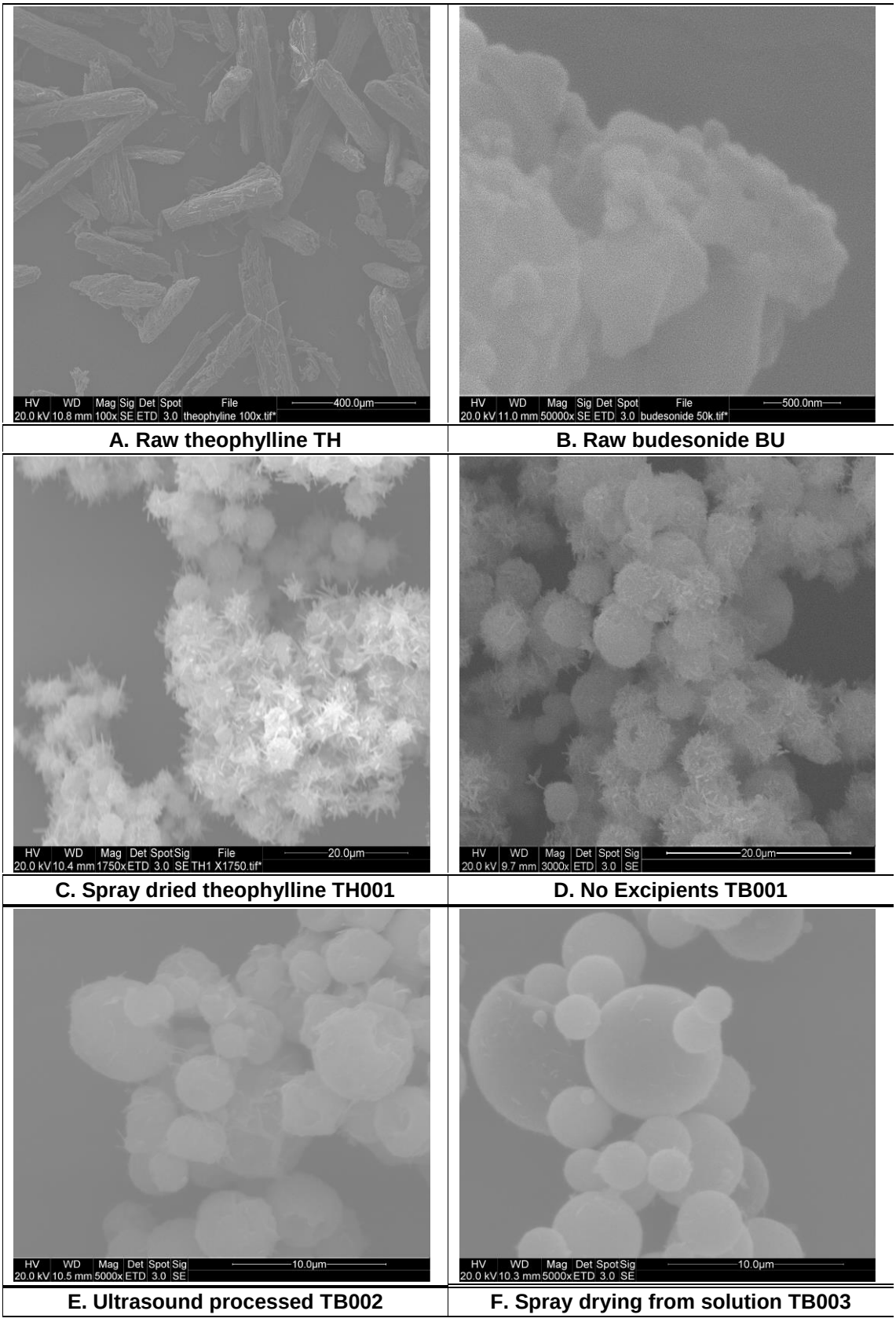

A. Raw theophylline TH | **B. Raw budesonide BU**

C. Spray dried theophylline TH001 | **D. No Excipients TB001**

E. Ultrasound processed TB002 | **F. Spray drying from solution TB003**

Fig. 5-7. Spray-dried dual particles

Table 5-10 Particle sizes of TB001, TB002 and TB003 which are measured by using laser sizer.

Sample	Particle Size µm		
	X_{10}	X_{50}	X_{90}
TB001	0.91±0.41	4.04±0.32	8.53±1.23
TB002	2.68±0.62	5.35±0.33	8.42±0.94
TB003	1.88±1.22	4.27±0.52	8.52±1.01

5.3.4 Aerodynamic behaviour

The aerosol performances of TB001, TB002, TB003, blend I, blend II, and blend III are presented in Table 5-11. This experiment was repeated three time for each analysis to ensure that the results are reliable and reproducible.

Table 5-11 The aerodynamic properties of different preparations of resultant samples and lactose using Aeroliser® at 60 L/min

Dispersed samples	FPF_{loaded} (%)	$FPF_{emitted}$ (%)	Capsule and device retention (%)	Impaction recovery (%)		MMDA
				Theophylline	Budesndie	
TB001	7.2±1.6	23.0±0.7	14.8±2.4	93.1±0.40	58.5±0.04	5.4±0.15
TB002	9.9±0.9	28.2 ±1.4	9.5±0.1	88.9±0.1	60.6±0.14	5.4±0.01
TB003	14.8±1.7	32.6±2.2	6.1±0.1	75.5±0.07	69.8±0.02	4.9±0.06
BlendI (ML001+TB001)	3.1±1.6	24.9±1.7	18.8±0.01	20.1±0.51	14.5±0.01	4.3±0.03
BlendII(ML001+TB002)	7.8±0.8	27.0±0.5	11.8±0.004	21.7±0.08	20.5±0.01	4.3±0.10
BlendIII(ML001+TB003)	25.8±12.3	50.0±9.8	26.5±0.02	22.9±0.39	18.2±0.01	4.4±0.38

Blend I, II and III consist of formulations that comprise of TB001, TB002 and TB003, respectively, where all powders are blended with coarse lactose (ML001) particle size between 4μm and 170μm. The powders of TB003 and TB002 have slightly higher $FPF_{emitted}$ of 32.6% and 28.2%, while the TB001 has the $FPF_{emitted}$ of 23%. It has been proved that spherical nature of particles can be able to improve aerosol performance profile of particles due to their uniform size distribution and pitted particle surface (Kaerger and Price, 2004, Pilcer and Amighi, 2010).

However, as shown in Table 5-11, the capsule and device retention for the dry powder become higher after mixing with lactose. Simultaneously, a higher loss is found in blended batches. It is due to the low density particle caused by polymers, resulting in a sample loss during the NGI measurement (Musante et al., 2002). Nevertheless, the higher $FPF_{emitted}$ of blend batches is discovered, where absence of lactose results in about 30% lower of FPF as expected due to the poor flowability. The reason is that lactose reduces the interparticle forces which make the powder cohesive. Blend I has a lower $FPF_{emitted}$ of 24.9% compared to blend II and blend III, which have $FPF_{emitted}$ of 27.0% and 50.4% respectively, as shown in Table 5-11.

In the Fig. 5-8, although TB002 has a slightly higher $FPF_{emitted}$ of 28.2% than its blended batch Blend II which has 27% of $FPF_{emitted}$, there are more deposition of Blend II in lower stages, compared to TB002. This result suggests excipients help to improve aerodynamic performance of particle by change the morphology of particles.

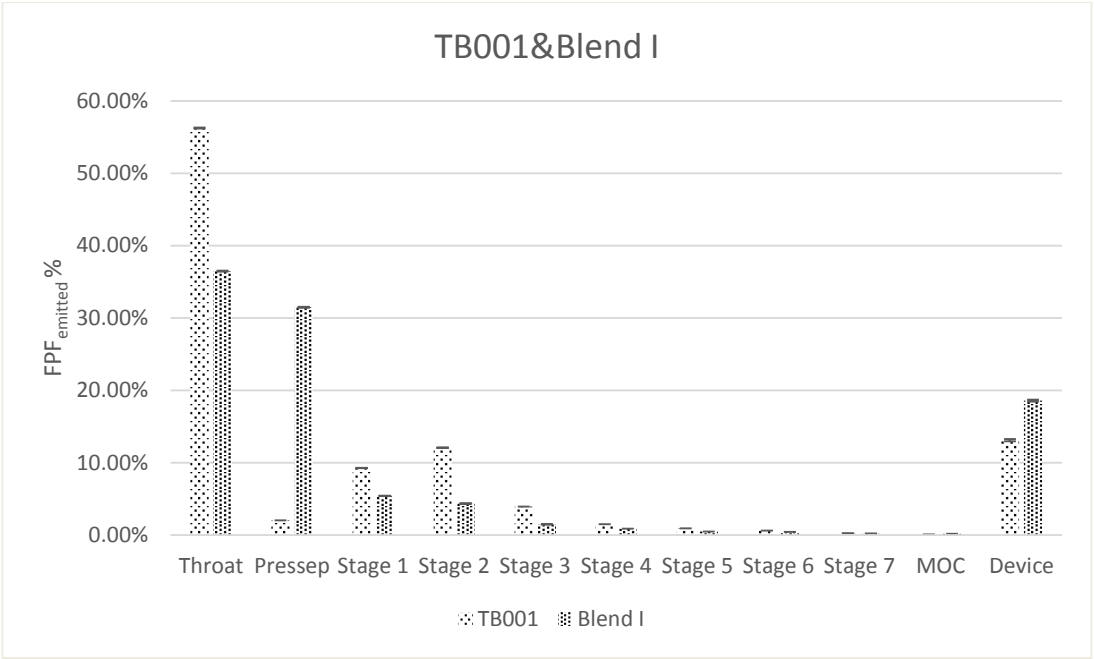
TB001&Blend I
60.00%
50.00%
40.00%
30.00%
20.00%
10.00%
0.00%
FPF emitted %
Throat
Pressep
Stage 1
Stage 2
Stage 3
Stage 4
Stage 5
Stage 6
Stage 7
MOC
Device
TB001
Blend I

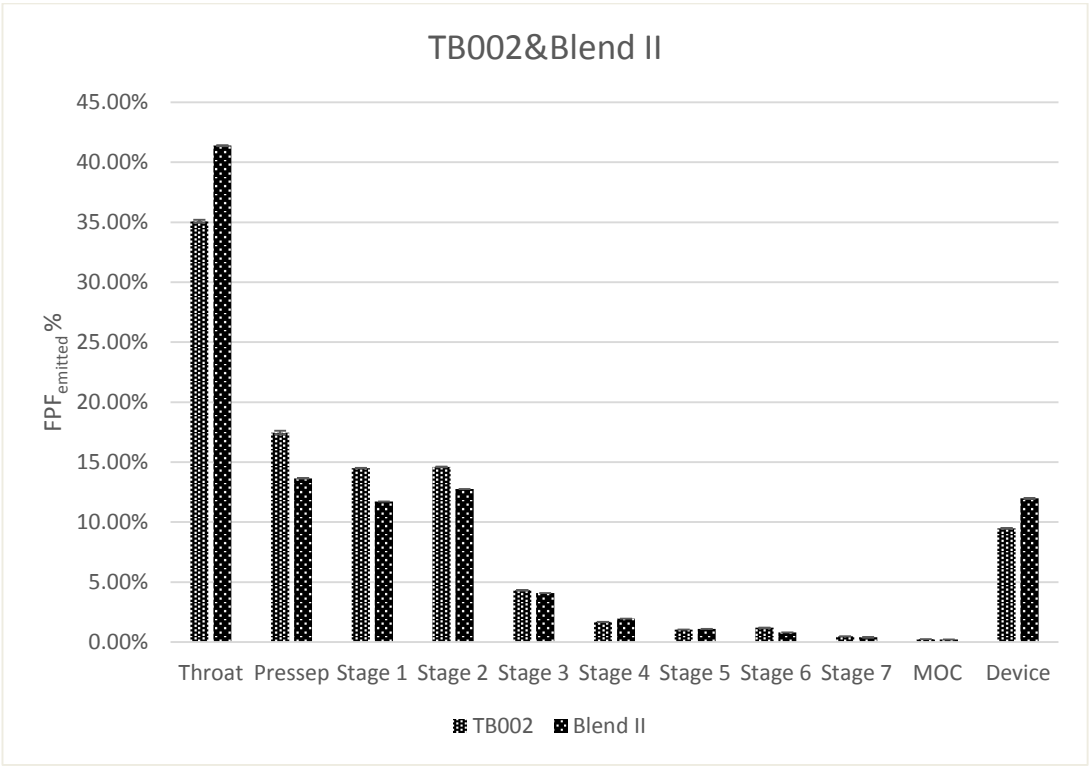
TB002&Blend II
45.00%
40.00%
35.00%
30.00%
25.00%
20.00%
15.00%
10.00%
5.00%
0.00%
FPF emitted %
Throat
Pressep
Stage 1
Stage 2
Stage 3
Stage 4
Stage 5
Stage 6
Stage 7
MOC
Device
TB002
Blend II

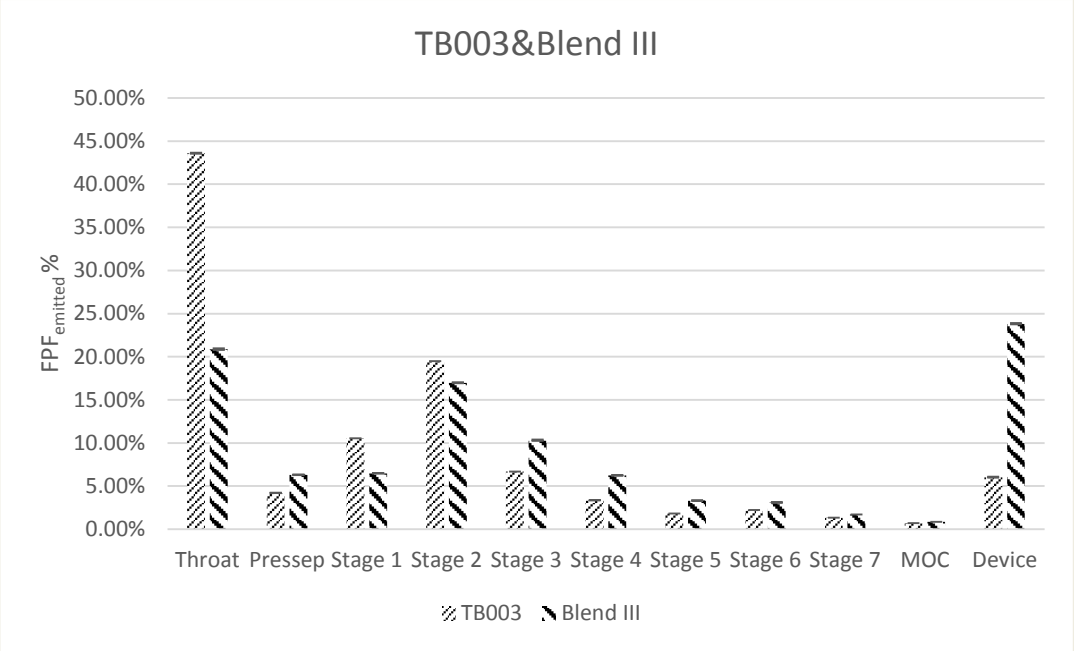

Fig. 5-8. Deposition of the APIs from combined particles

Table 5-12 depicts the finding from the analysis of the simultaneous deposition of theophylline and budesonide from the combination particles formulation. It indicates consistent ratio all over and this is in good agreement with the expectation.

Table 5-12 The ratio of theophylline:budesonide in each stage of NGI

	Ratio of theophylline:budesonide in each stage of NGI					
	TB001	**TB002**	**TB003**	**Blend I**	**Blend II**	**Blend II**
Powder	18.22±3.05	19.31±1.22	20.70±1.33	21.22±1.12	20.90±0.96	19.84±1.83
Throat	22.50±0.68	29.70±1.33	20.54±1.75	22.72±1.42	18.40±0.29	25.07±0.52
Pressep	31.00±3.73	79.32±1.27	25.94±1.08	17.60±1.41	20.63±0.40	22.92±1.29
Stage 1	20.50±1.87	18.05±2.34	21.85±0.90	23.12±1.16	19.17±0.59	24.76±1.98
Stage 2	31.90±14.98	18.24±1.93	20.56±0.13	24.43±1.22	18.98±0.63	23.94±0.93
Stage 3	20.60±1.33	20.79±0.03	21.43±0.25	22.64±1.46	19.51±0.59	20.65±0.55
Stage 4	23.66±3.40	25.54±1.54	24.21±0.09	21.68±1.36	19.22±2.85	23.52±2.91
Stage 5	34.08±11.59	30.26±0.66	26.41±0.90	25.38±1.56	21.43±0.49	21.77±3.82
Stage 6	35.66±11.46	28.26±0.84	24.93±0.04	21.43±1.13	20.33±1.41	23.21±3.09
Stage 7	33.36±0.27	32.13±0.41	26.71±0.95	26.60±1.22	14.98±0.47	24.21±2.82
MOC	33.59±11.40	35.08±8.59	30.74±2.28	20.00±0.00	14.84±0.00	30.83±2.53

According to Table 5-12, the efficiency of the spray drying and mixing of APIs suggests no significant influence on ratio of theophylline:budesonide, indicating no particle segregation occurs during the spray drying and mixing processes. All batches are a homogeneous mixture of both components. Furthermore, among of un-blended batches (TB001, TB002, and TB003), TB002 and TB003 are relatively more stable than TB001 in each stage, particularly, in lower stage (from stage 4), owing to the bond between polymer and APIs. This can be attributed to the explanation on why the sample TB003 more stable than TB002. This also has been suggested in previous discussion, there are some fine crystals of budesonide adhering to the surface of sphere particle in TB002 (Fig. 5-7-E). These crystals can be easily segregated during the airway deposition. However, these crystalline budesonide can get in circulatory system faster than the bonded budesonide does, which reduce the inflammatory cells, such as eosinophils, T lymphocytes, mast cells, and dendritic cells in the airway s(Barnes and Adcock, 2003) fast. The theophylline can relatively slow to be separated from polymer to inhibit resistance of steroid in COPD (Barnes, 2003). This mechanism has a potentiality to improve the therapeutic efficiency and reduce the side effects of theophylline. Additionally, the loss of budesonide are decreased in Blend II. Thereby, it appears that ultrasonic process is not only can help to improve the effects of drug, but also can reduce the cost of formulation.

Generally, APIs-lactose mixture behaves a better sedimentation, due to reduction of shear force by lactose (Coates et al., 2005, 2006). Combination particle TB002 has an $FPF_{emitted}$ of 27%. Compared with the commercial product Seretide® 500, it is a tertiary mix of the APIs with lactose and it is distributed with Aeroliser®, resulting FPF of about 27% was found (Taki et al.).

5.4 Conclusion

By introducing an anti-solvent ultrasonic process after the spray drying is an efficient technique for the production of micronized and generation of combination particles of theophylline-budesonide which is suitable for inhalation drug delivery. Conducting the ultrasound in designed experiments decreases ultrasonic power and consumption, feed rate, and excipients in the process. The analysis discover that the excipient is the significant factor that associate to particle size of sub-micro suspensions. According to the experimental design, the selected parameters of ultrasonic process are applied to generate dry powder through spray drying.

The sphere-shaped particles with size distribution of 0.91–8.53 μm are achieved after spray drying. The particle characteristic of combination produced by this process is suitable for inhalation drug delivery. The aerosol performance of ultrasound processed combination particles is 27% of FPF after blending with lactose. This is a similar to the commercial product (Taki et al.). Furthermore, this study also shows that both APIs are evenly distributed throughout the stages of the NGI. This is indicating a codeposition of both substances and the co-particles which have a benefit in both FPF and codelivery can be achieved. However, it should be noticed that the dosage of commercial product Seretide® 500 is 50 μg of salmeterol and 500 μg of fluticasone propionate, while this proposed study uses formulation contains 6mg of theophylline and 300 μg of budesonide. By comparing both dosages, this study has opened an alternative avenue to tackle the research challenge of using higher dosage and greater ratio of APLs in generating inhalation formulation.

In conclusion, ultrasound is an ideal tool to help the future study to control and optimise the formulation procedures. These experiments indicate that some optimisation studies could be carried out to improve dispensability of AIPs with high dosage. This leads to conclude that the proposed technique of combined spray dry is an interesting approach for the production of dual particles. Moreover, spray dry technology also can be recommended as a potential methodology to form combination particle.

Chapter 6: General Discussion and Future Works

6.1 Introduction

The objective of pharmaceutical engineering of inhalation dosage forms is the generation of a drug product that enable the delivery of medicines efficiently and effectively to the human airways. Currently, the processing of these dosage forms remains highly empirical, which corresponds with high failure rates of these drug products during development and manufacturing. The primary source of dry powder inhaler (DPI) formulation failure is the lack of control on key physicochemical properties of the actives ingredients, which can be related to the process of micronization that is used to generate respirable particles. To fill in this knowledge gap, the methodologies to control the specific performance and stability properties of DPI dosage forms have been proposed. To achieve this goal, the central design principle in DPI manufacturing has to focus on design of particle interfaces, leading to enable careful control of particle-particle interactions and enhance drug product performance.

This principle must be taken one-step further with respect to combined inhalation products, which are significantly more complicated than binary formulations. As asthma and COPD are two common conditions of the airways, the most effective treatment for reducing smooth muscle dysfunction and inflammation is to use combined therapy of corticosteroid (ICS) and theophylline (TH) together in order to illicit significant clinical advantages. It has been demonstrated that addition of oral theophylline to an inhaled corticosteroid (ICS) is superior to ICS alone in achieving anti-inflammation (Ito et al., 2002). Furthermore, there is evidence to

suggest that patients with COPD may also benefit from combined inhalation therapy with TH and ISC (Spears et al., 2009).

The improved clinical outcome on therapy on combined inhaled ICS and oral TH is reported. The results suggested it enhances the efficiency of corticosteroids and recovers their anti-inflammatory actions in COPD treatment (Lim et al., 2000, Spears et al., 2009, Ford et al., 2010). The opportunity for synergistic action is enhanced by co-deposition of both particles on the same cells of the airways. Moreover, inhalation of TH would be an ideal delivery methodology to avoid the side effects caused by high concentration of TH; and slower and uncontrollable metabolism yield by its oral administration, leading to better bioavailability and treatment performance (Cosio et al., 2004). Therefore, administration of the two drugs by a single inhaler would lead to an increased chance for co-deposition compared with administration via two separate inhalers. However, current combined inhalation products are subject to a greater variability in dose delivery of each active ingredient (Kumon et al., 2010, Corrigan et al., 2006, Tajber et al., 2009b). Hence, there is a requirement of processes that may enable production of combination inhaled products that will allow both drugs to be delivered more effectively and independently of dose variations.

6.2 Summary

Following physical characterisation of the materials utilised in the study, compared ultrasonic, spray drying, and physical mixture, the development of the ultrasonic and spray drying process in the lab-scale size was successfully achieved by controlling excipients. Many factors, including amplitudes, solvents, feed rates and temperatures, did not have significant effect on properties of

resultant materials. As a result, a laboratory spray drying and ultrasonic system were proposed to enable the formation of small scale batches with a significant level of control and manipulation of excipients.

In this study, the spray drying, jet milling, and wet milling process was used initially to generate single drug particles and the result found that they reduce the material down to micro size range, especially, spray drying was possible to modify morphology of theophylline with suitable properties for the inhaled drug. Moreover, theophylline spray dried particles were found to outperform micronized theophylline particles as determined by *in vitro* performance testing. Furthermore, urchin-like shape crystalline particles of theophylline with geometric diameter of 0.74-74.78 μm were produced, which were found to help more budesonide deposit in lower stage that is 2 fold higher than jet milled theophylline.

Secondly, the spray drying process was also used to produce individual particle of two active ingredients. This allows effective delivery of combination medicaments and independently of dose variation. All physicochemical characterisation results demonstrated that the spray dried combination particles of TH and BU were successfully co-processed into individual particles with crystalline properties. According to the statistics analysis, it found that the spray drying process parameter didn't have significant effects on particles size. This can be attributed to the cause of the relatively low concentration of solutions. From the findings via regression and ANN analysis, HPMC has more significant effects on solubility of theophylline at room temperature when it is compared to PVP. ANOVA analysis suggested that HPMC, PVP, and PVP^2 * HPMC are important variables to theophylline solubility. However it found null effects on

particle size and composition when implementing the regression model. Nevertheless, ANN model proves that HPMC and PVP were important factors to solubility of theophylline with better predicable model (R^2 was 0.90; regression model of R^2 is 0.86). Moreover, ANN also found that there were some associations between polymers and particle compositions. The ratio between theophylline and budesonide becomes more stable when exposed to higher concentration of excipients. Additionally, the stage by stage studies of *in vitro* performance strongly confirmed that all formulations exhibit a constant delivery and independently of dose variation.

In addition, the combined drug particles of BU and TH were produced via the ultrasonic system. The amplitude and feed rate were controlled in this study, but there was no evident shown amplitude and feed are significantly related to the particle size ($p \geq 1$) according to ANOVA analysis. For the combination drugs, it has been demonstrated that the combination particles of TH:BU formulation was significantly ($p<0.05$) greater than a micronized TH:BU formulation. The ultrasonic combination TH:BU particles were more consistent in the delivery of both active ingredients than micronized sample. After blending with lactose the performance of the TH:BU combination particles was remarkably improved, which may be related to the fact that the shear force breaking agglomerated powders into individual particles. This approach, however, presents itself as novel means to produce inhaled combination dosage forms which may lead to enhance clinical efficacy.

In conclusion, the ultrasonic and spray drying process has been successfully utilised in modifying the surface morphology of crystalline particles suitable for

pulmonary drug delivery. This proposed technique has been successfully developed by controlling all crucial factors which are identified in the system. Furthermore, the process has been successfully employed to engineer drug particles with optimum properties for delivery to the lungs. In individual particle, the particle characterisations revealed that theophylline and budesonide are co-processed into each particles. However, the micronized budesonide located on surface of combination particles that was characterized by XRD, DSC and SEM in ultrasonic sample, which was not detected in spray dried product. This feature helps to enhance the delivery of budesonide into lower stage in NGI, thus ultrasonic sample has a higher FPF of budesonide than spray dried product. Moreover, the *in vitro* performance study strongly confirmed that the combined formulations are stable and perform uniform deposition in each stage of NGI. Nevertheless, according to *in vitro* analysis, aerodynamic performance of ultrasonic produced formulation is significantly greater than spray dried formulation by 2 fold or more, due to ultrasonic particle has rougher surface than spray dried one using same concentration of excipients, which leads to a better flowability. Therefore, the ultrasound process are progressively utilised to produce combination particles of two active ingredients which would allow the delivery of combination medicaments effectively and achieve independently of dose variation. Combination dosage form for respiratory products is a novel means to achieve an advanced drug actions and effects.

6.3 Further works

According to these data presented in the thesis, the ultrasonic process shows significant promise for generating combination particles for delivery to the lungs. In Chapter 5 and 6, it can be found that the particle engineering via the ultrasonic

and spray drying processes lead to an important opportunity to generate particles containing two or more active ingredients, which will allow an effective delivery of combination medicaments and independently of dose variation. As conditions such as COPD are multi-factorial (Albert and Calverley, 2008), a further development of this approach may investigate the potential of these processes to generate particles with multiple active ingredients in one particle (Kumon et al., 2010). It would be beneficial to design the work by adding another essential drug to generate triple drug particles in order to formulate the pulmonary dosage form to help prevent COPD and asthma patients for the long-term treatment.

However, the high dosage of theophylline results in poor flowability, which requires high amount of lactose to improve the aerodynamic behaviour (Chapter 3, 4, 5). This is not suitable for DPIs delivery. Therefore, the future work could consider the non-carrier formulation. It is believe that such proposed work can be able to achieve through controlling the morphology of particles. In chapter 3, it was found that spray dried product of theophylline forms like urchin shape, it is possible to generate a large size and low density of urchin-like particles containing crystalline TH and BU via spray drying. This type of particles could contribute to a smaller aerodynamic diameter and a lower cohesiveness, thus to enhance the flowability and the aerosol performance of powders.

Finally, according to Chapter 5, a sphere-like particle is obtained. This result indicates a possibility to generate a type of porous particles. These particles have a lower density, well meet the requirement of pulmonary delivery, and specially help reduce carrier using in the process. In order to produce this type of particles, generation of high quality nano-scale suspensions is an initial step. As discussed in Chapter 5, ultrasonic technical is a type of bottom-up approach for production

of nano-suspension (Van Eerdenbrugh et al., 2008). However, this procedure is more suitable for the soluble APIs, rather than the slightly soluble or insoluble compound (theophylline and budesonide). This is shown in Chapter 5 that there was a sample lost after spray drying, due to the low concentration of suspension. Therefore, in the future, a top-down approach can be applied, such as media milling and high-pressure homogenization (Van Eerdenbrugh et al., 2008). This technique can be able to process large amount sample and obtain a uniform suspension, which would be a novel method to produce combination particles that particularly useful for the insoluble compounds.

References

AFSHIN MALEKI, HIUA DARAEI, LOGHMAN ALAEI & FARAJI, A. 2014. Comparison of QSAR models based on combinations of genetic algorithm, stepwise multiple linear regression, and artificial neural network methods to predict K d of some derivatives of aromatic sulfonamides as carbonic anhydrase II inhibitors. *Russian Journal of Bioorganic Chemistry* 40**,** 61-75.

AGENCY, B. P. C. S. O. T. M. A. H. P. R. 2014. The British Pharmacopoeia 2014. TOS.

ALBERT, P. & CALVERLEY, P. M. A. 2008. Drugs (including oxygen) in severe COPD. *European Respiratory Journal,* 31**,** 1114-1124.

ALI, H. S. M., YORK, P. & BLAGDEN, N. 2009. Preparation of hydrocortisone nanosuspension through a bottom-up nanoprecipitation technique using microfluidic reactors. *International Journal of Pharmaceutics,* 375**,** 107-113.

ALI, M. E. & LAMPRECHT, A. 2014. Spray freeze drying for dry powder inhalation of nanoparticles. *European Journal of Pharmaceutics and Biopharmaceutics,* 87**,** 510-517.

AULTON, M. E. 2009. *Aulton's pharmaceutics : the design and manufacture of medicines,* 3rd. Edinburgh, Churchill Livingstone Elsevier.

BARNES, N., SNAPE, S., FOX, J. C., FITZGERALD, M., SNELL, N., PAVORD, I. D., JEFFERY, P., QIU, Y., SINGH, D., ANTCZAK, A. & NIZANKOWSKA-MOGILNICKA, E. 2010. Effects of low dose inhaled theophylline (ADC4022) co-administered with budesonide on inflammatory markers and lung function in patients with COPD. *American Thoracic Society Annual Conference 2010.* American

BARNES, P. J. 2003. Theophylline - New perspectives for an old drug. *American Journal of Respiratory and Critical Care Medicine,* 167**,** 813-818.

BARNES, P. J. 2006. Theophylline for COPD. *Thorax,* 61**,** 742-744.

BARNES, P. J. & ADCOCK, I. M. 2003. How do corticosteroids work in asthma? *Annals of Internal Medicine,* 139**,** 359-370.

BARRENTINE, L. B. 1999. *An Introduction to Design of Experiments: A Simplified Approach*. ASQ Quality Press.

BATEMAN, E. D., HURD, S. S., BARNES, P. J., BOUSQUET, J., DRAZEN, J. M., FITZGERALD, M., GIBSON, P., OHTA, K., O'BYRNE, P., PEDERSEN, S. E., PIZZICHINI, E., SULLIVAN, S. D., WENZEL, S. E. & ZAR, H. J. 2008. Global strategy for asthma management and prevention: GINA executive summary. *European Respiratory Journal,* 31**,** 143-178.

BENTHAM, A. C., KWAN, C. C., BOEREFIJN, R. & GHADIRI, A. 2004. Fluidised-bed jet milling of pharmaceutical powders. *Powder Technology,* 141**,** 233-238.

BTS, B. T. S. S. 2011. British Guideline on the Management of Asthma.

BUCAR, D. K. & MACGILLIVRAY, L. R. 2007. Preparation and reactivity of nanocrystalline cocrystals formed via sonocrystallization. *Journal of the American Chemical Society,* 129**,** 32-33.

BUCKTON, G. & GILL, H. 2007. The importance of surface energetics of powders for drug delivery and the establishment of inverse gas chromatography. *Advanced Drug Delivery Reviews,* 59**,** 1474-1479.

BYRON, P. R. 1986. Some future perspectives for unit dose inhalation aerosols. *Drug Development and Industrial Pharmacy,* 12**,** 993-1015.

C. SURYANARAYANA & NORTON, M. G. 1998. *X-Ray Diffraction: A Practical Approach*. Plenum Press.

CALVERLEY, P., PAUWELS, R. & VESTBO, J. 2003. Combined salmeterol and fluticasone in the treatment of chronic obstructive pulmonary disease: a randomised controlled trial. (vol 361, pg 449, 2003). *Lancet,* 361**,** 1660-1660.

CAZZOLA, M. & HANANIA, N. A. 2006. The role of combination therapy with corticosteroids and long-acting beta2-agonists in the prevention of exacerbations in COPD. *International journal of chronic obstructive pulmonary disease,* 1**,** 345-54.

CAZZOLA, M., SEGRETI, A. & MATERA, M. G. 2010. Novel bronchodilators in asthma. *Current Opinion in Pulmonary Medicine,* 16**,** 6-12.

CHAUDHURI, R., LIVINGSTON, E., MCMAHON, A. D., THOMSON, L., BORLAND, W. & THOMSON, N. C. 2003. Cigarette smoking impairs the therapeutic response to oral corticosteroids in chronic asthma. *American Journal of Respiratory and Critical Care Medicine,* 168**,** 1308-1311.

CHEW, N. Y., TANG, P., CHAN, H. K. & RAPER, J. A. 2005. How much particle surface corrugation is sufficient to improve aerosol performance of powders? *Pharm Res,* 22**,** 148-52.

CHIKHALIA, V., FORBES, R. T., STOREY, R. A. & TICEHURST, M. 2006. The effect of crystal morphology and mill type on milling induced crystal disorder. *European Journal of Pharmaceutical Sciences,* 27**,** 19-26.

COATES, M. S., CHAN, H. K., FLETCHER, D. F. & RAPER, J. A. 2005. Influence of air flow on the performance of a dry powder inhaler using computational and experimental analyses. *Pharm Res,* 22**,** 1445-53.

COLBOURN, E. A. & ROWE, R. C. Novel approaches to neural and evolutionary computing in pharmaceutical formulation: challenges and new possibilities.

CORRIGAN, D. O., CORRIGAN, O. I. & HEALY, A. M. 2006. Physicochemical and in vitro deposition properties of salbutamol sulphate/ipratropium bromide and salbutamol sulphate/excipient spray dried mixtures for use in dry powder inhalers. *International Journal of Pharmaceutics,* 322**,** 22-30.

COSIO, B. G., TSAPROUNI, L., ITO, K., JAZRAWI, E., ADCOCK, I. M. & BARNES, P. J. 2004. Theophylline restores histone deacetylase activity and steroid responses in COPD macrophages. *Journal of Experimental Medicine,* 200**,** 689-695.

CROMPTON, G. K. 1982. PROBLEMS PATIENTS HAVE USING PRESSURIZED AEROSOL INHALERS. *European Journal of Respiratory Diseases,* 63**,** 101-104.

DAHL, R., GREEFHORST, L., NOWAK, D., NONIKOV, V., BYRNE, A. M., THOMSON, M. H., TILL, D., DELLA CIOPPA, G. & FORMOTEROL CHRONIC OBSTRUCTIVE, P. 2001. Inhaled formoterol dry powder versus ipratropium bromide in chronic obstructive

pulmonary disease. *American Journal of Respiratory and Critical Care Medicine,* 164**,** 778-784.

DE BOER, A. H., GJALTEMA, D., HAGEDOORN, P. & FRIJLINK, H. W. 2002. Characterization of inhalation aerosols: a critical evaluation of cascade impactor analysis and laser diffraction technique. *International Journal of Pharmaceutics,* 249**,** 219-231.

DE MATAS, M., SHAO, Q., RICHARDSON, C. H. & CHRYSTYN, H. 2008. Evaluation of in vitro in vivo correlations for dry powder inhaler delivery using artificial neural networks. *European Journal of Pharmaceutical Sciences,* 33**,** 80-90.

DHILLON A, PITCHAYAJITTIPONG C, SHUR J & PRICE R Combination Particles Containing Fluticasone Propionate and Theophylline for Lung Delivery. Bath: University of Bath.

DHILLON A. Year. Triple formulation for COPD. *In:* APS inhlalation 2009, 2009 University of Nottingham.

DHUMAL, R. S., BIRADAR, S. V., PARADKAR, A. R. & YORK, P. 2009. Particle engineering using sonocrystallization: Salbutamol sulphate for pulmonary delivery. *International Journal of Pharmaceutics,* 368**,** 129-137.

DICKHOFF, B. H., DE BOER, A. H., LAMBREGTS, D. & FRIJLINK, H. W. 2003. The effect of carrier surface and bulk properties on drug particle detachment from crystalline lactose carrier particles during inhalation, as function of carrier payload and mixing time. *Eur J Pharm Biopharm,* 56**,** 291-302.

DRUGBANK Theophylline. drug bank.

DUMITRIU, S. & POPA, V. 2013. *Polymeric Biomaterials: Medicinal and Pharmaceutical Applications*. CRC Press.

EVANS, D. J., TAYLOR, D. A., ZETTERSTROM, O., CHUNG, F., OCONNOR, B. J. & BARNES, P. J. 1997. A comparison of low-dose inhaled budesonide plus theophylline and high-dose inhaled budesonide for moderate asthma. *New England Journal of Medicine,* 337**,** 1412-1418.

FORD, P. A., DURHAM, A. L., RUSSELL, R. E. K., GORDON, F., ADCOCK, I. M. & BARNES, P. J. 2010. Treatment Effects of Low-Dose Theophylline Combined With an Inhaled Corticosteroid in COPD. *Chest,* 137**,** 1338-1344.

FUKUNAKA, T., SAWAGUCHI, K., GOLMAN, B. & SHINOHARA, K. 2005. Effect of particle shape of active pharmaceutical ingredients prepared by fluidized-red jet-milling on cohesiveness. *Journal of Pharmaceutical Sciences,* 94**,** 1004-1012.

GAMBLE, J., F. , LEANE, M., OLUSANMI, D., TOBYN, M., SUPUK, E., KHOO, J. & NADERI, M. 2011. Surface energy analysis as a tool to probe the surface energy characteristics of micronized materials-A comparison with inverse gas chromatography. *Int J Pharm*.

GEVREY, M., DIMOPOULOS, I. & LEK, S. 2003. Review and comparison of methods to study the contribution of variables in artificial neural network models. *Ecological Modelling,* 160**,** 249-264.

GRADON, L. & SOSNOWSKI, T. R. 2014. Formation of particles for dry powder inhalers. *Advanced Powder Technology,* 25**,** 43-55.

GREENING, A. P., IND, P. W., NORTHFIELD, M. & SHAW, G. 1994. Added salmeterol versus higher-dose corticosteroid in asthma patients with symptoms on existing inhaled corticosteroid

Lancet, 344**,** 219-224.

HER, J.-Y., SONG, C.-S., LEE, S. J. & LEE, K.-G. 2010. Preparation of kanamycin powder by an optimized spray freeze-drying method. *Powder Technology,* 199**,** 159-164.

HINDS, W. C. 1982. Aerosol teAerosol technology - properties, behavior, and measurement of airborne particles. New York: Wiley.

HUSSAIN, A., ARNOLD, J. J., KHAN, M. A. & AHSAN, F. 2004. Absorption enhancers in pulmonary protein delivery. *Journal of Controlled Release,* 94**,** 15-24.

ITO, K., LIM, S., CARAMORI, G., CHUNG, K. F., BARNES, P. J. & ADCOCK, I. M. 2001. Cigarette smoking reduces histone deacetylase 2 expression, enhances cytokine expression,

and inhibits glucocorticoid actions in alveolar macrophages. *FASEB Journal,* 15**,** 1110-1112.

ITO, K., LIM, S., CARAMORI, G., COSIO, B., CHUNG, K. F., ADCOCK, I. M. & BARNES, P. J. 2002. A molecular mechanism of action of theophylline: Induction of histone deacetylase activity to decrease inflammatory gene expression. *Proceedings of the National Academy of Sciences of the United States of America,* 99**,** 8921-8926.

JMP. *FULL FACTORIAL DESIGNS* [Online]. Available: http://www.jmp.com/support/help/Full_Factorial_Designs.shtml [Accessed].

JMP. *SCREENING DESIGNS* [Online]. Available: http://www.jmp.com/support/help/Screening_Designs.shtml [Accessed].

JONES, M. D. & PRICE, R. 2006. The influence of fine excipient particles on the performance of carrier-based dry powder inhalation formulations. *Pharm Res,* 23**,** 1665-74.

JULIE, P. 2013. *SPSS survival manual : a step by step guide to data analysis using IBM SPSS,* 5th edition. Maidenhead, Berkshire : McGraw Hill.

KAERGER, J. S. & PRICE, R. 2004. Processing of spherical crystalline particles via a novel solution atomization and crystallization by sonication (SAXS) technique. *Pharmaceutical Research,* 21**,** 372-381.

KARAVAS, E., GEORGARAKIS, E. & BIKIARIS, D. 2006. Application of PVP/HPMC miscible blends with enhanced mucoadhesive properties for adjusting drug release in predictable pulsatile chronotherapeutics. *European Journal of Pharmaceutics and Biopharmaceutics,* 64**,** 115-126.

KELLER, J. B. & MIKSIS, M. 1980. Bubble oscillations of large-amplitude

Journal of the Acoustical Society of America, 68**,** 628-633.

KORDYLLA, A., KRAWCZYK, T., TUMAKAKA, F. & SCHEMBECKER, G. 2009. Modeling ultrasound-induced nucleation during cooling crystallization. *Chemical Engineering Science,* 64**,** 1635-1642.

KUMAR, S. & BURGESS, D. J. 2014. Wet milling induced physical and chemical instabilities of naproxen nano-crystalline suspensions. *International Journal of Pharmaceutics,* 466**,** 223-232.

KUMON, M., KWOK, P. C. L., ADI, H., HENG, D. & CHAN, H. K. 2010. Can low-dose combination products for inhalation be formulated in single crystalline particles? *European Journal of Pharmaceutical Sciences,* 40**,** 16-24.

LASSETER, K. C., AUBETS, J., CHUECOS, F. & GIL, E. G. 2011. Aclidinium Bromide, a Long-Acting Antimuscarinic, Does Not Affect QT Interval in Healthy Subjects. *Journal of Clinical Pharmacology,* 51**,** 923-932.

LIM, S., JATAKANON, A., GORDON, D., MACDONALD, C., CHUNG, K. F. & BARNES, P. J. 2000. Comparison of high dose inhaled steroids, low dose inhaled steroids plus low dose theophylline, and low dose inhaled steroids alone in chronic asthma in general practice. *Thorax,* 55**,** 837-841.

LOUHI-KULTANEN, M., KARJALAINEN, M., RANTANEN, J., HUHTANEN, M. & KALLAS, J. 2006. Crystallization of glycine with ultrasound. *International Journal of Pharmaceutics,* 320**,** 23-29.

MILLER-LARSSON, A. & SELROOS, O. 2006. Advances in asthma and COPD treatment: Combination therapy with inhaled corticosteroids and long-acting beta(2)-agonists. *Current Pharmaceutical Design,* 12**,** 3261-3279.

MIRZAIE, M., DARVISHZADEH, R., SHAKIBA, A., MATKAN, A. A., ATZBERGER, C. & SKIDMORE, A. 2014. Comparative analysis of different uni- and multi-variate methods for estimation of vegetation water content using hyper-spectral measurements. *International Journal of Applied Earth Observation and Geoinformation,* 26**,** 1-11.

MOREN, F. 1987. Dosage forms and formulations for drug administration to the respiratory-tract. *Drug Development and Industrial Pharmacy,* 13**,** 695-728.

MOULTON, B. C. & FRYER, A. D. 2011. Muscarinic receptor antagonists, from folklore to pharmacology; finding drugs that actually work in asthma and COPD. *British Journal of Pharmacology,* 163**,** 44-52.

MUHAMMAD, S. A. F. A. S., OUBANI, H., ABBAS, A., CHAN, H.-K., KWOK, P. C. L. & DEHGHANI, F. 2013. The production of dry powder by the sonocrystallisation for inhalation drug delivery. *Powder Technology,* 246**,** 337-344.

MULLIN & WILLIAM J. 2001. *Crystallization,* 4th. Oxford, Butterworths.

MUSANTE, C. J., SCHROETER, J. D., ROSATI, J. A., CROWDER, T. M., HICKEY, A. J. & MARTONEN, T. B. 2002. Factors affecting the deposition of inhaled porous drug particles. *Journal of Pharmaceutical Sciences,* 91**,** 1590-1600.

NARDUCCI, O., JONES, A. G. & KOUGOULOS, E. 2011. Continuous crystallization of adipic acid with ultrasound. *Chemical Engineering Science,* 66**,** 1069-1076.

NHS 2004. Management of chronic obstructive pulmonary disease in adults in primary and secondary care. *clinical guideline,* 12.

NHS 2010. Management of chronic obstructive pulmonary disease in adults in primary and secondary care. *NICE clinical guideline,* 12.

NOLAN, L. M., TAJBER, L., MCDONALD, B. F., BARHAM, A. S., CORRIGAN, O. I. & HEALY, A. M. 2009. Excipient-free nanoporous microparticles of budesonide for pulmonary delivery. *European Journal of Pharmaceutical Sciences,* 37**,** 593-602.

NYAMWEYA, N. & HOAG, S. W. 2000. Assessment of polymer-polymer interactions in blends of HPMC and film forming polymers by modulated temperature differential scanning calorimetry. *Pharmaceutical Research,* 17**,** 625-631.

OTSUKA, M. & KINOSHITA, H. 2010. Quantitative Determination of Hydrate Content of Theophylline Powder by Chemometric X-ray Powder Diffraction Analysis. *Aaps Pharmscitech,* 11**,** 204-211.

PACHUAU, L., SARKAR, S. & MAZUMDER, B. 2008. Formulation and evaluation of matrix microspheres for simultaneous delivery of salbutamol sulphate and theophylline. *Tropical Journal of Pharmaceutical Research,* 7**,** 995-1002.

PAUL R. KINNEAR & GRAY., C. D. 2008. *SPSS 15 made simple* Hove : Psychology.

PELTONEN, L. & HIRVONEN, J. 2010. Pharmaceutical nanocrystals by nanomilling: critical process parameters, particle fracturing and stabilization methods. *Journal of Pharmacy and Pharmacology,* 62**,** 1569-1579.

PILCER, G. & AMIGHI, K. 2010. Formulation strategy and use of excipients in pulmonary drug delivery. *International Journal of Pharmaceutics,* 392**,** 1-19.

PITCHAYAJITTIPONG C, SHUR J & R, P. *De Novo* Engineering of Crystalline Low Dose Combination Inhalation Particles of a Long-acting β2-agonist and Corticosteroid. Bath: University of Bath.

PITCHAYAJITTIPONG, C., SHUR, J. & PRICE, R. 2009. Engineering of crystalline combination inhalation particles of a long-acting beta2-agonist and a corticosteroid. *Pharm Res,* 26**,** 2657-66.

RAGHAVAN, S. L., TRIVIDIC, A., DAVIS, A. F. & HADGRAFT, J. 2001. Crystallization of hydrocortisone acetate: influence of polymers. *International Journal of Pharmaceutics,* 212**,** 213-221.

RENNARD, S. I. 2004. Treatment of stable chronic obstructive pulmonary disease. *Lancet,* 364**,** 791-802.

RUECROFT, G., HIPKISS, D., LY, T., MAXTED, N. & CAINS, P. W. 2005. Sonocrystallization: The use of ultrasound for improved industrial crystallization. *Organic Process Research & Development,* 9**,** 923-932.

SADRZADEH, N., GLEMBOURTT, M. J. & STEVENSON, C. L. 2007. Peptide drug delivery strategies for the treatment of diabetes. *Journal of Pharmaceutical Sciences,* 96**,** 1925-1954.

SARTOR, M. *Dynamic light scattering to determine the radius of small beads in Brownian motion in a solution* University of California San Diego.

SEPASSI, S., GOODWIN, D. J., DRAKE, A. F., HOLLAND, S., LEONARD, G., MARTINI, L. & LAWRENCE, M. J. 2007. Effect of polymer molecular weight on the production of drug nanoparticles. *Journal of Pharmaceutical Sciences,* 96**,** 2655-2666.

SEVILLE, P. C., LEAROYD, T. P., LI, H. Y., WILLIAMSON, I. J. & BIRCHALL, J. C. 2007. Amino acid-modified spray-dried powders with enhanced aerosolisation properties for pulmonary drug delivery. *Powder Technology,* 178**,** 40-50.

SHAO, Q., ROWE, R. C. & YORK, P. 2006. Comparison of neurofuzzy logic and neural networks in modelling experimental data of an immediate release tablet formulation. *European Journal of Pharmaceutical Sciences,* 28**,** 394-404.

SHEKUNOV, B. Y., FEELEY, J. C., CHOW, A. H. L., TONG, H. H. Y. & YORK, P. 2003. Aerosolisation behaviour of micronised and supercritically-processed powders. *Journal of Aerosol Science,* 34**,** 553-568.

SHOYELE, S. A. 2008. Engineering protein particles for pulmonary drug delivery. *Methods in Molecular Biology***,** 149-160.

SHOYELE, S. A. & CAWTHOME, S. 2006. Particle engineering techniques for inhaled biopharmaceuticals. *Advanced Drug Delivery Reviews,* 58**,** 1009-1029.

SHOYELE, S. A., SIVADAS, N. & CRYAN, S.-A. 2011. The Effects of Excipients and Particle Engineering on the Biophysical Stability and Aerosol Performance of Parathyroid Hormone (1-34) Prepared as a Dry Powder for Inhalation. *Aaps Pharmscitech,* 12**,** 304-311.

SINGH, M. N., HEMANT, K. S. Y., RAM, M. & SHIVAKUMAR, H. G. 2010. Microencapsulation: A promising technique for controlled drug delivery. *Research in pharmaceutical sciences,* 5**,** 65-77.

SMYTH, H. D. C. & HICKEY, A. J. 2011. *Controlled Pulmonary Drug Delivery*. Springer New York.

SOFIA SILVA, A., TAVARES, M. T. & AGUIAR-RICARDO, A. 2014. Sustainable strategies for nano-in-micro particle engineering for pulmonary delivery. *Journal of Nanoparticle Research,* 16.

SPEARS, M., DONNELLY, I., JOLLY, L., BRANNIGAN, M., ITO, K., MCSHARRY, C., LAFFERTY, J., CHAUDHURI, R., BRAGANZA, G., ADCOCK, I. M., BARNES, P. J., WOOD, S. & THOMSON, N. C. 2009. Effect of low-dose theophylline plus beclometasone on lung function in smokers with asthma: a pilot study. *European Respiratory Journal,* 33**,** 1010-1017.

STANFORDPHD. *cross-validation* [Online]. Available: http://stanfordphd.com/Cross-validation.html [Accessed].

STECKEL, H. & BRANDES, H. G. 2004. A novel spray-drying technique to produce low density particles for pulmonary delivery. *International Journal of Pharmaceutics,* 278**,** 187-195.

STOREY, B. D. & SZERI, A. J. 2001. A reduced model of cavitation physics for use in sonochemistry. *Proceedings of the Royal Society of London Series a-Mathematical Physical and Engineering Sciences,* 457**,** 1685-1700.

SUIHKO, E., KETOLAINEN, J., POSO, A., AHLGREN, M., GYNTHER, J. & PARONEN, P. 1997. Dehydration of theophylline monohydrate - a two step process. *International Journal of Pharmaceutics,* 158**,** 47-55.

SUPPORT, M. *What is a design resolution in a factorial design?* [Online]. Available: http://support.minitab.com/en-us/minitab/17/topic-library/modeling-statistics/doe/factorial-designs/what-is-a-design-resolution/ [Accessed].

SUTHERLAND, E. R., ALLMERS, H., T AYAS, N., VENN, A. J. & MARTIN, R. J. 2003. Inhaled corticosteroids reduce the progression of airflow limitation in chronic obstructive pulmonary disease: a meta-analysis. *Thorax,* 58**,** 937-941.

SUTHERLAND, E. R. & CHERNIACK, R. M. 2004. Management of chronic obstructive pulmonary disease - The authors reply. *New England Journal of Medicine,* 351**,** 1463-1463.

SZAFRANSKI, W., CUKIER, A., RAMIREZ, A., MENGA, G., SANSORES, R., NAHABEDIAN, S., PETERSON, S. & OLSSON, H. 2003. Efficacy and safety of budesonide/formoterol in the management of chronic obstructive pulmonary disease. *European Respiratory Journal,* 21**,** 74-81.

TAJBER, L., CORRIGAN, D. O., CORRIGAN, O. I. & HEALY, A. M. 2009a. Spray drying of budesonide, formoterol fumarate and their composites-I. Physicochemical characterisation. *International Journal of Pharmaceutics,* 367**,** 79-85.

TAJBER, L., CORRIGAN, O. I. & HEALY, A. M. 2009b. Spray drying of budesonide, formoterol furnarate and their composites-II. Statistical factorial design and in vitro deposition properties. *International Journal of Pharmaceutics,* 367**,** 86-96.

TAKI, M., AHMED, S., MARRIOTT, C., ZENG, X. M. & MARTIN, G. P. The 'stage-by-stage' deposition of drugs from commercial single-active and combination dry powder inhaler formulations. *European Journal of Pharmaceutical Sciences,* 43**,** 225-235.

TELKO, M. J. & HICKEY, A. J. 2005. Dry powder inhaler formulation. *Respiratory care,* 50**,** 1209-27.

TONG.H. H. Y & CHOW.A. H. L 2006. Control of Physical Forms of Drug Particles for Pulmonary Delivery by Spray Drying and Supercritical Fluid Processing. *KONA,* 24**,** 27-40.

TOROPAINEN, T., VELAGA, S., HEIKKILA, T., MATILAINEN, L., JARHO, P., CARLFORS, J., LEHTO, V. P., JARVINEN, T. & JARVINEN, K. 2006. Preparation of budesonide/gamma-cyclodextrin complexes in supercritical fluids with a novel SEDS method. *Journal of Pharmaceutical Sciences,* 95**,** 2235-2245.

USMANI, O. S., BIDDISCOMBE, M. F., NIGHTINGALE, J. A., UNDERWOOD, S. R. & BARNES, P. J. 2003. Effects of bronchodilator particle size in asthmatic patients using monodisperse aerosols. *Journal of Applied Physiology,* 95**,** 2106-2112.

VAN ANDEL, A. E., REISNER, C., MENJOGE, S. S. & WITEK, T. J. 1999. Analysis of inhaled corticosteroid and oral theophylline use among patients with stable COPD from 1987 to 1995. *Chest,* 115**,** 703-707.

VAN EERDENBRUGH, B., VAN DEN MOOTER, G. & AUGUSTIJNS, P. 2008. Top-down production of drug nanocrystals: Nanosuspension stabilization, miniaturization and transformation into solid products. *International Journal of Pharmaceutics,* 364**,** 64-75.

VERMA, S., HUEY, B. D. & BURGESS, D. J. 2009. Scanning Probe Microscopy Method for Nanosuspension Stabilizer Selection. *Langmuir,* 25**,** 12481-12487.

VESTBO, J., SORENSEN, T., LANGE, P., BRIX, A., TORRE, P. & VISKUM, K. 1999. Long-term effect of inhaled budesonide in mild and moderate chronic obstructive pulmonary disease: a randomised controlled trial. *Lancet,* 353**,** 1819-1823.

VIRONE, C., KRAMER, H. J. M., VAN ROSMALEN, G. M., STOOP, A. H. & BAKKER, T. W. 2006. Primary nucleation induced by ultrasonic cavitation. *Journal of Crystal Growth,* 294**,** 9-15.

WESTMEIER, R. & STECKEL, H. 2008. Combination particles containing salmeterol xinafoate and fluticasone propionate: Formulation and aerodynamic assessment. *Journal of Pharmaceutical Sciences,* 97**,** 2299-2310.

WIKIPEDIA. 2012. *Fractional factorial design* [Online]. Available: http://en.wikipedia.org/wiki/Fractional_factorial_design [Accessed].

WINKLER, J., HOCHHAUS, G. & DERENDORF, H. 2004. How the lung handles drugs: pharmacokinetics and pharmacodynamics of inhaled corticosteroids. *Proc Am Thorac Soc,* 1**,** 356-63.

WOUTERS, E. F. M., POSTMA, D. S., FOKKENS, B., HOP, W. C. J., PRINS, J., KUIPERS, A. F., PASMA, H. R., HENSING, C. A. J., CREUTZBERG, E. C. & GRP, C. S. 2005. Withdrawal of fluticasone propionate from combined salmeterol/fluticasone treatment in patients

with COPD causes immediate and sustained disease deterioration: a randomised controlled trial. *Thorax,* 60**,** 480-487.

XIA, D., OUYANG, M., WU, J. X., JIANG, Y., PIAO, H., SUN, S., ZHENG, L., RANTANEN, J., CUI, F. & YANG, M. 2012. Polymer-Mediated Anti-solvent Crystallization of Nitrendipine: Monodispersed Spherical Crystals and Growth Mechanism. *Pharmaceutical Research,* 29**,** 158-169.

YANG, J. Z., YOUNG, A. L., CHIANG, P.-C., THURSTON, A. & PRETZER, D. K. 2008. Fluticasone and Budesonide Nanosuspensions for Pulmonary Delivery: Preparation, Characterization, and Pharmacokinetic Studies. *Journal of Pharmaceutical Sciences,* 97**,** 4869-4878.

YEH, H. C., PHALEN, R. F. & RAABE, O. G. 1976. Factors influencing deposition of inhaled particles

Environmental Health Perspectives, 15**,** 147-156.

YORK P., KOMPELLA U. B. & SHEKUNOV B. Y. 2004. *Supercritical fluid technology for drug product development*. New York, M. Dekker.

ZANEN, P., GO, L. T. & LAMMERS, J. W. J. 1996. Optimal particle size for beta(2) agonist and anticholinergic aerosols in patients with severe airflow obstruction. *Thorax,* 51**,** 977-980.

Appendix

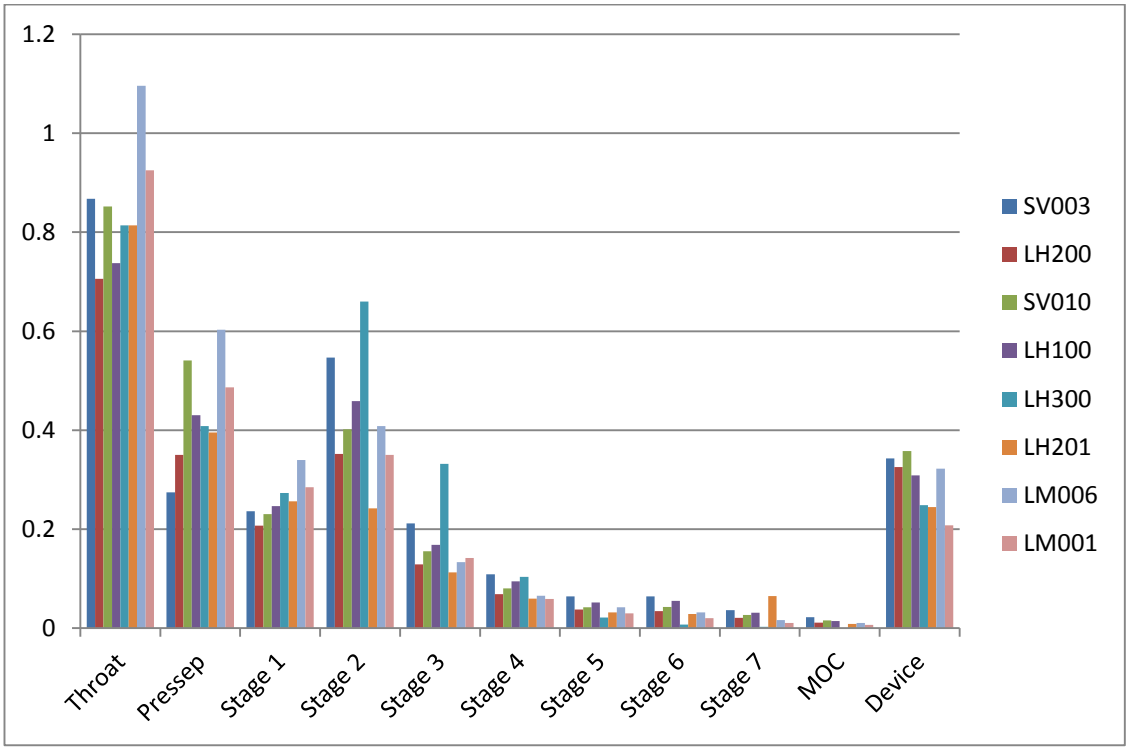

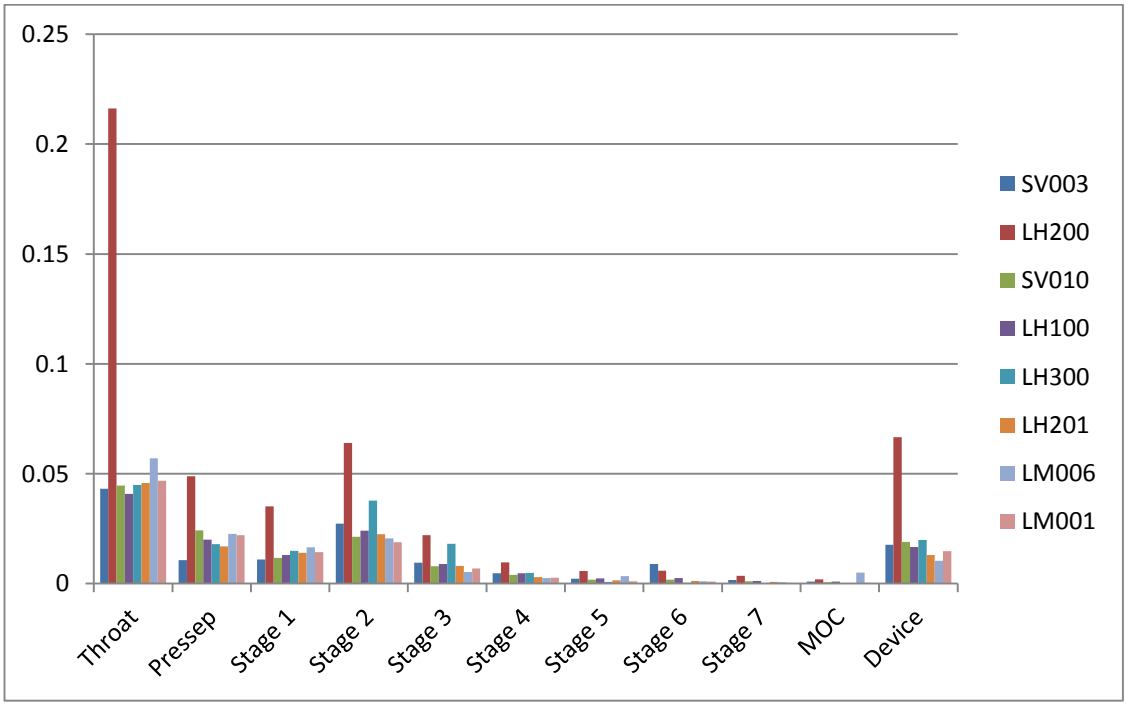

Figure A1 NGI result of powders mixed with different grade of lactose (ultrasonic sample TB002 and spray dry TB003)

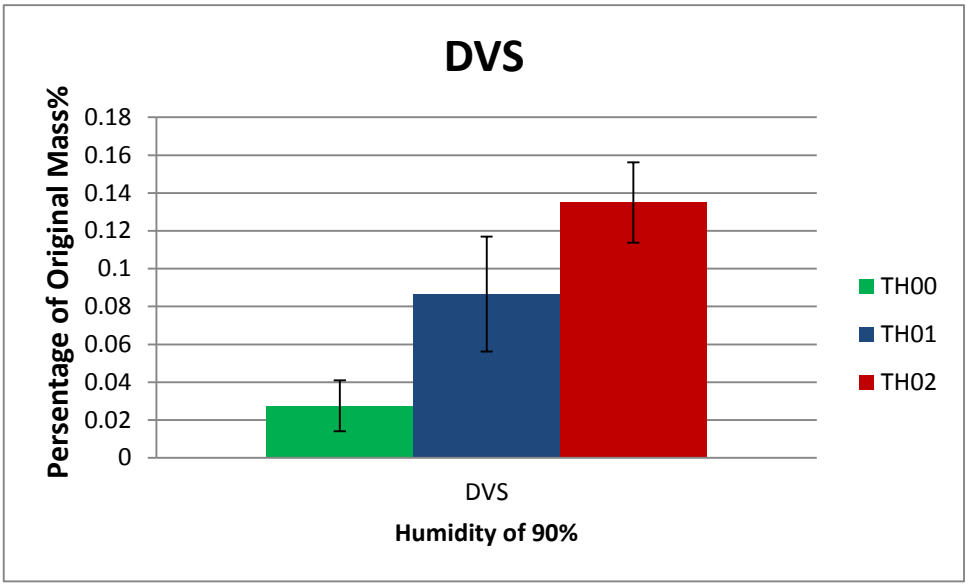

A

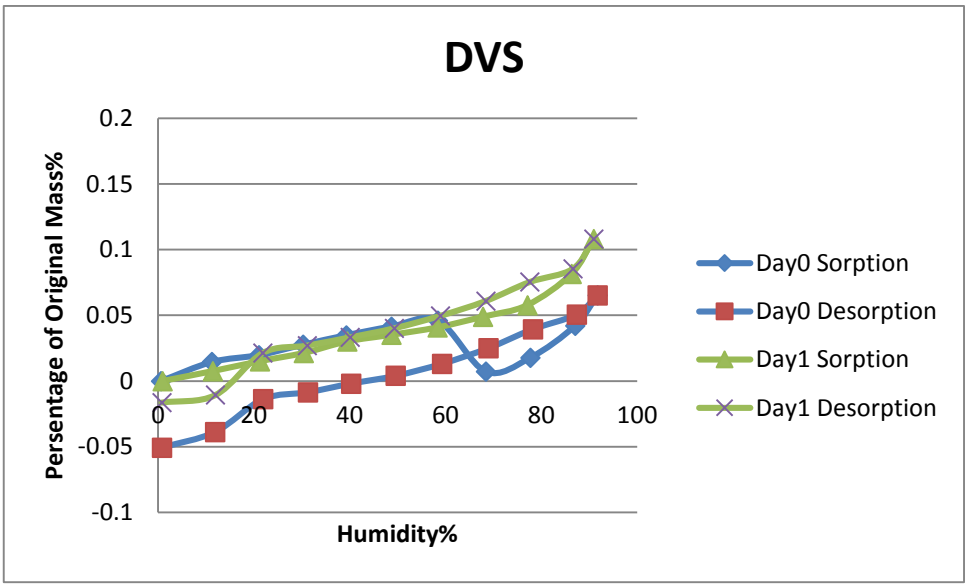

B

Figure A2 DVS profiles of TH00, TH01 and TH02. A: the weight changes of theophyllines at RH=90%; B: sorption-desorption curve of TH01 at day0 and day1. TH00: raw material; TH01: jet milled sample produced by low feed rate; TH02: jet milled sample produced by high feed rate

a.TB001 was spray dried from TH/BU=20/1solution (non excipients)

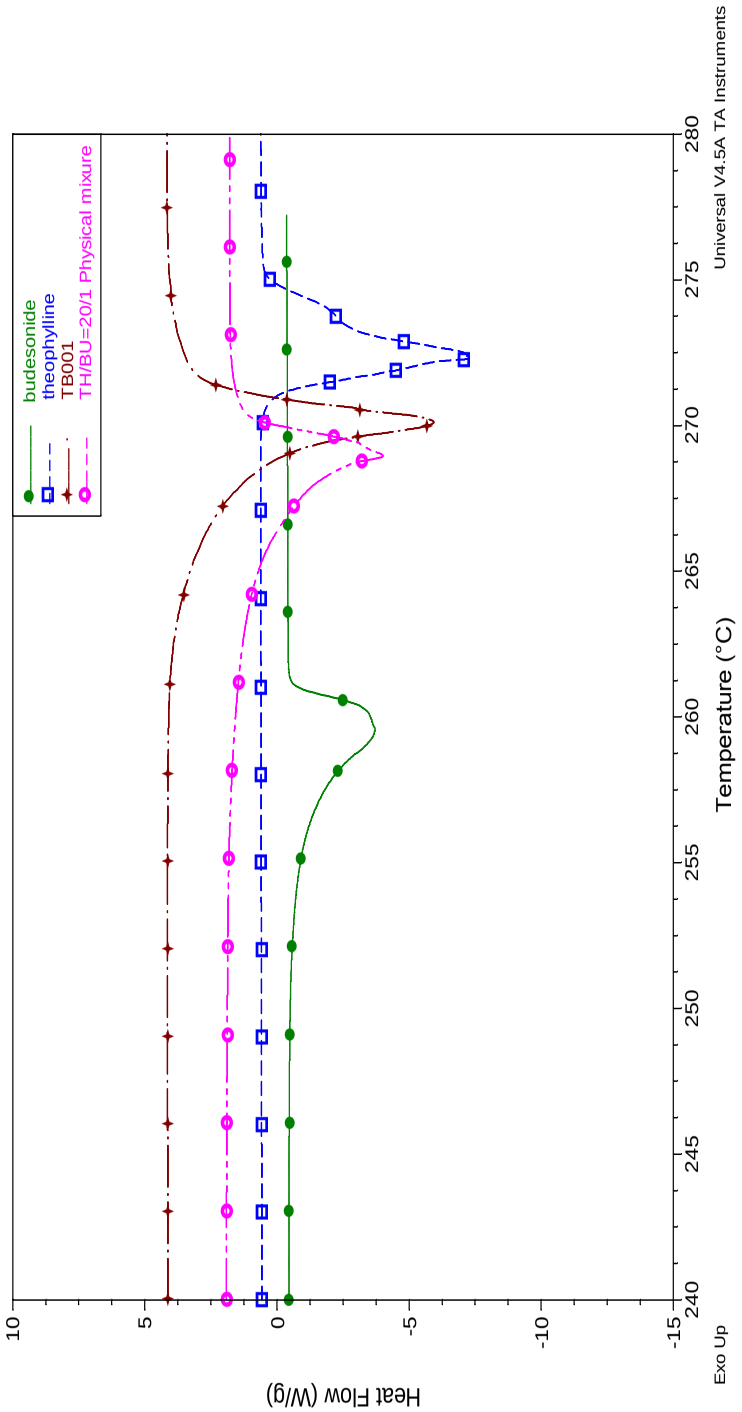

b. TB002 was spray dried from ultrasonic sample TB05 (TH/BU=20/1, HPMC=0.25%, PVP=0.05%)

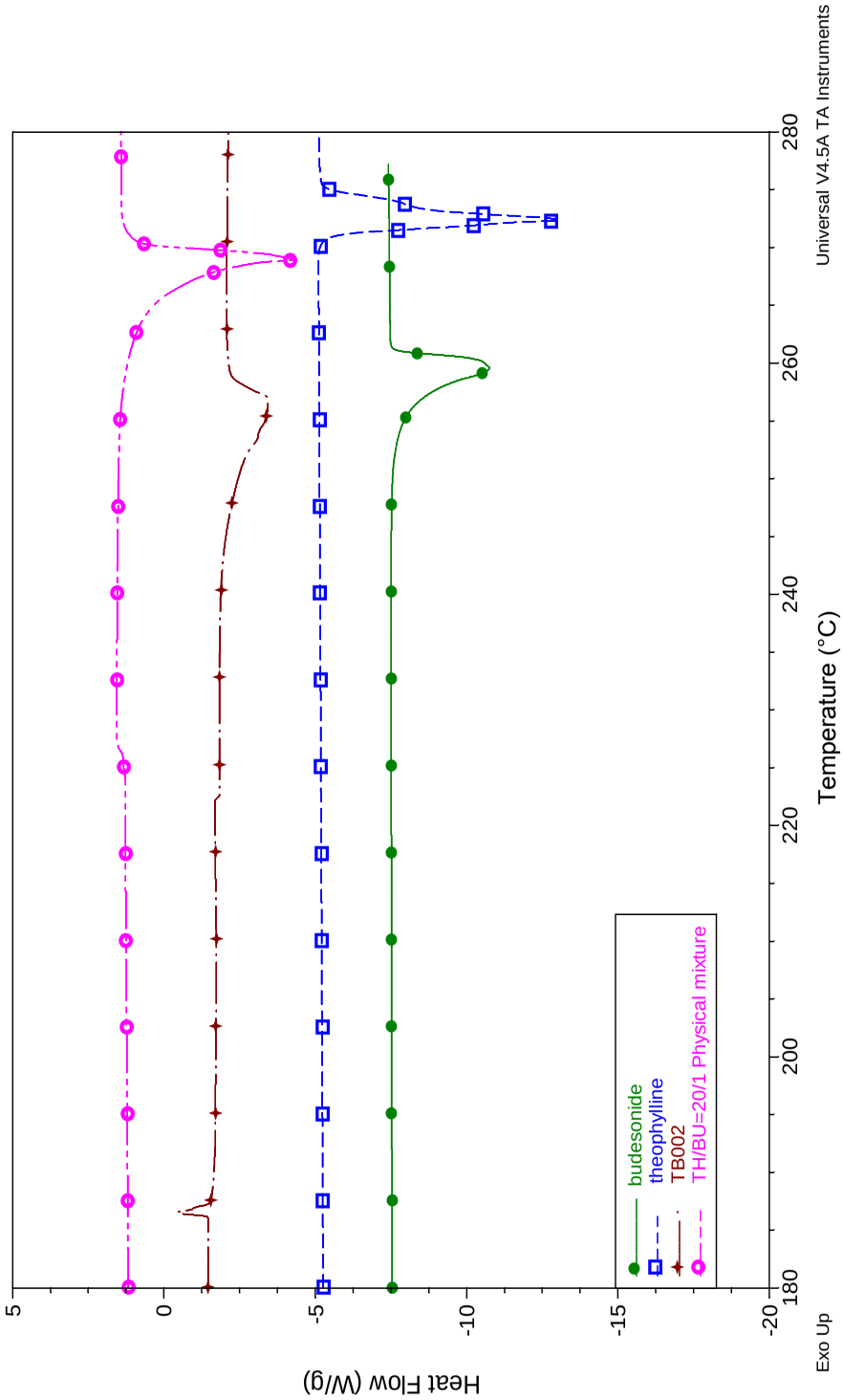

c. TB003 was spray dried from solution containing

TH/BU=20/1, HPMC=0.25% and PVP=0.05%

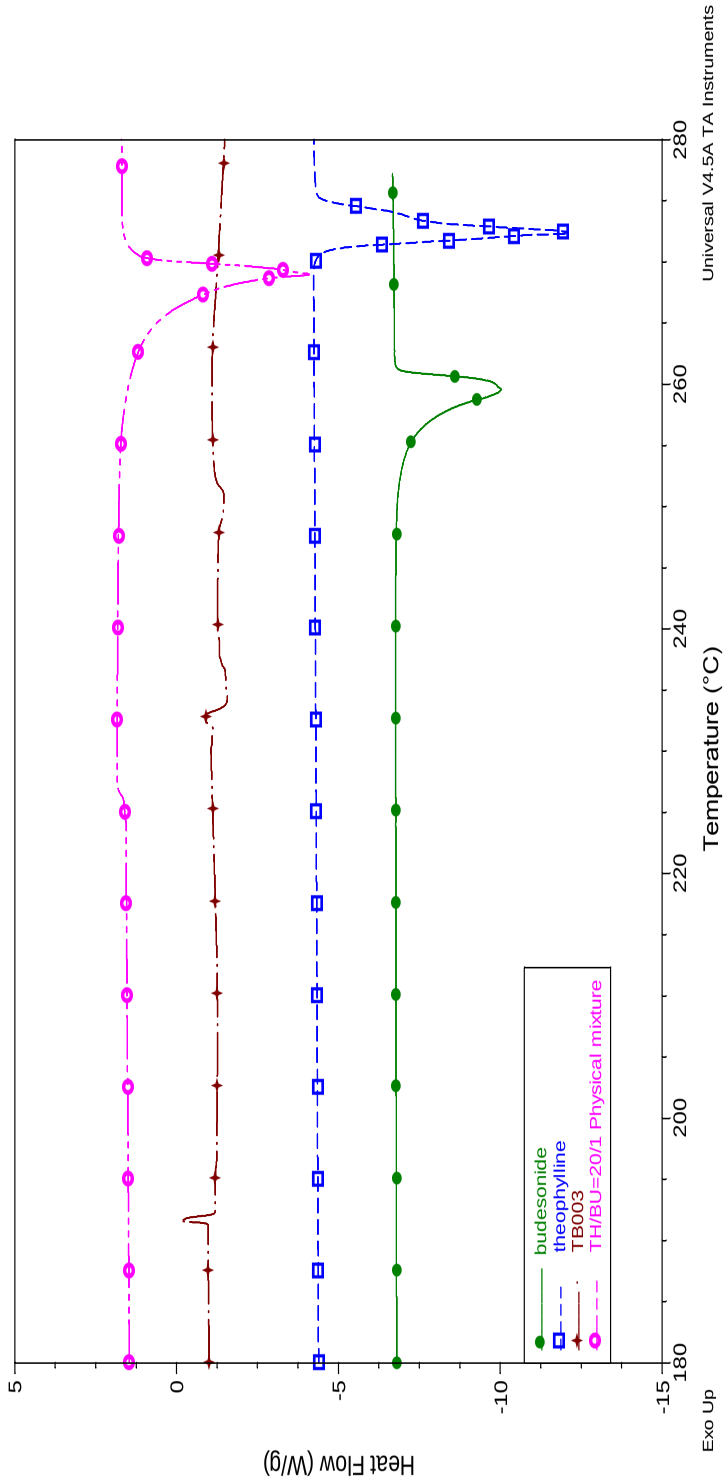

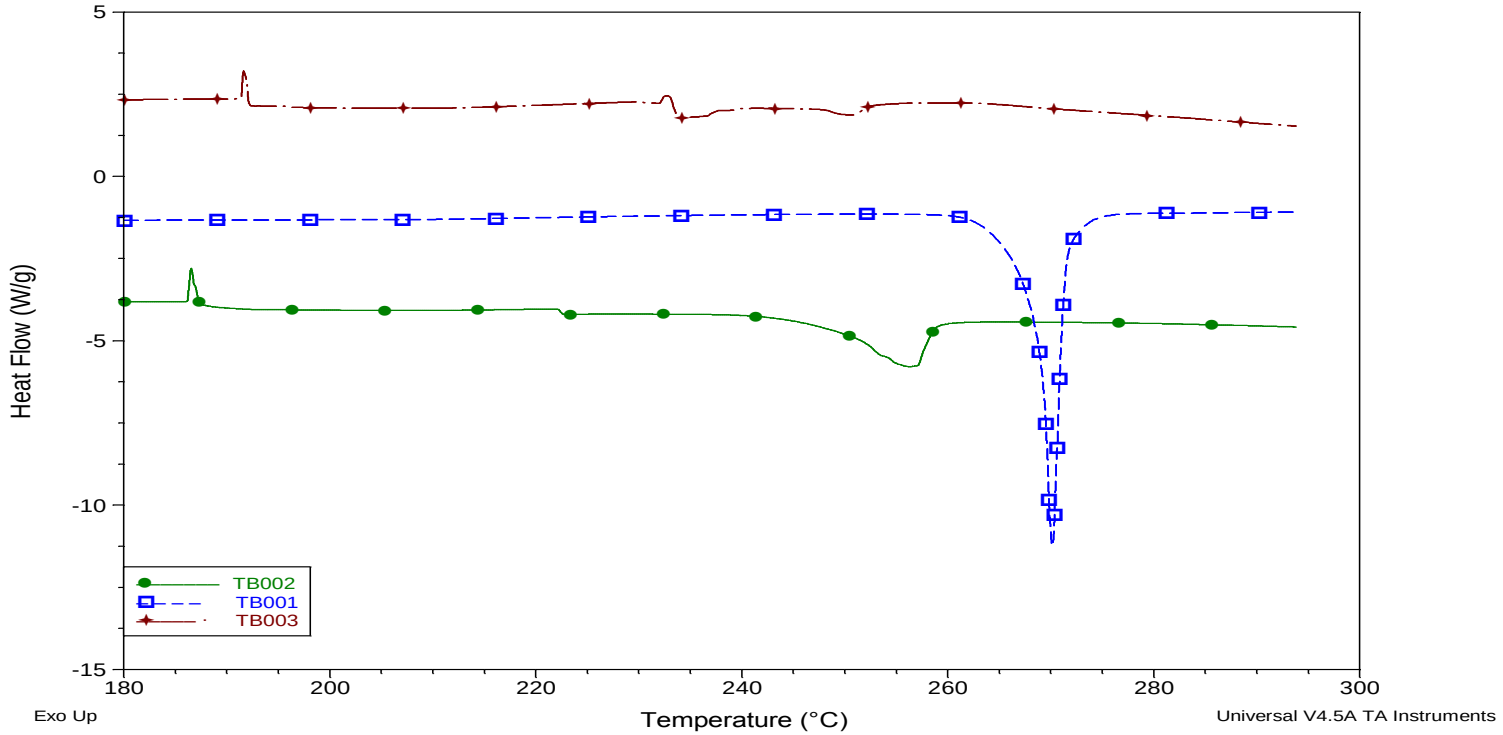

Figure A3 DSC of spray dried samples in Chapter 4

TB-1

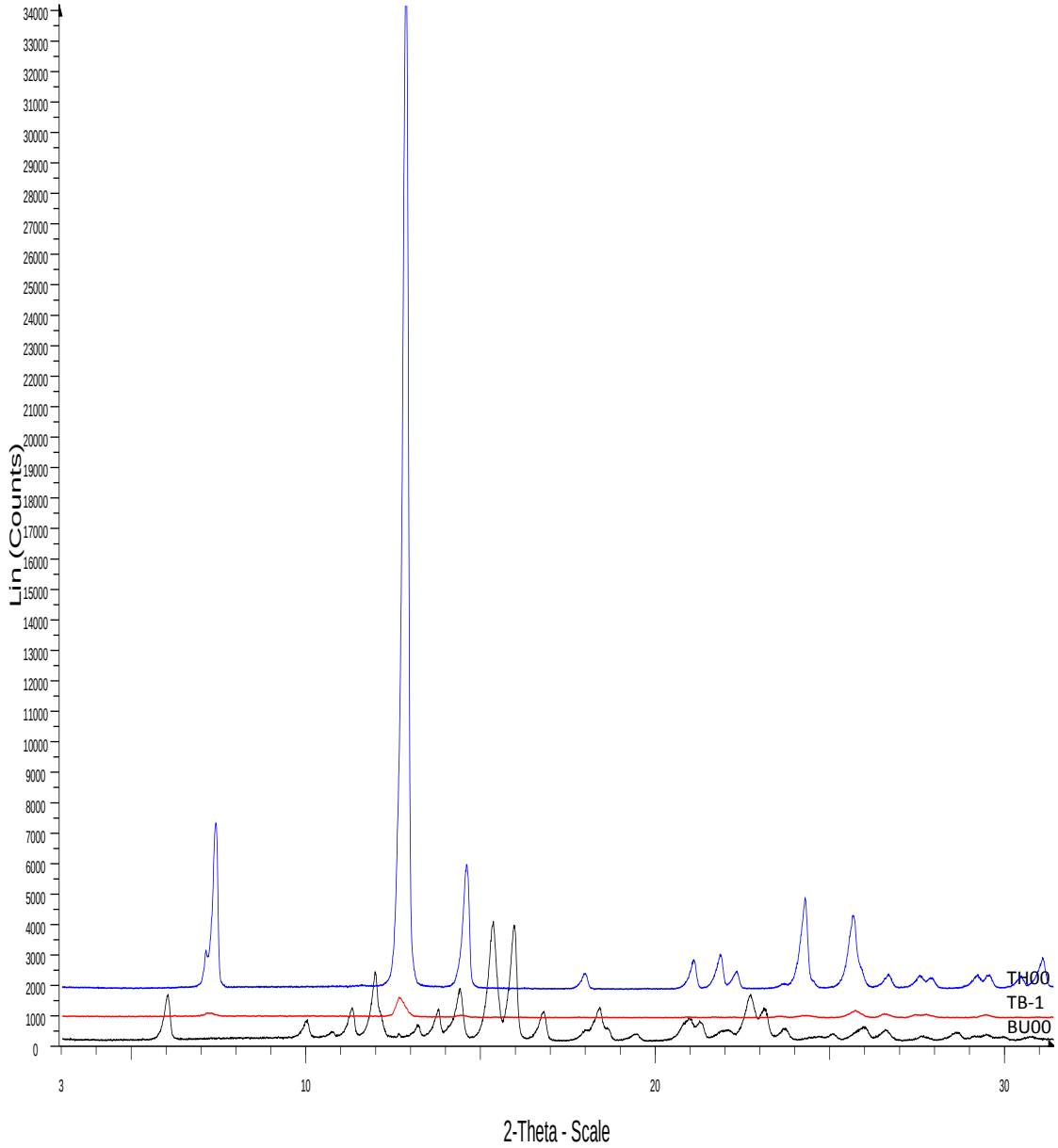

TB01 - File: TB-1.raw - Type: 2Th/Th locked - Start: 3.000 ° - End: 35.000 ° - Step: 0.020 ° - Step time: 1. s - Temp.: 25 °C (Room) - Time Started: 14 s - 2-Theta: 3.000 ° - Theta: 1.500 ° - Chi: 0.00 ° - Phi: 0.00 ° - X: 0.0 mm - Y: 0.0
Operations: Y Scale Add 859 | Import

budesonide - File: Budesonide-121110-01.raw - Type: 2Th/Th locked - Start: 3.000 ° - End: 50.000 ° - Step: 0.010 ° - Step time: 1. s - Temp.: 25 °C (Room) - Time Started: 13 s - 2-Theta: 3.000 ° - Theta: 1.500 ° - Chi: 0.00 ° - Phi: 0.
Operations: Import

theophylline - File: theophylline-121110-01.raw - Type: 2Th/Th locked - Start: 3.000 ° - End: 50.000 ° - Step: 0.010 ° - Step time: 1. s - Temp.: 25 °C (Room) - Time Started: 10 s - 2-Theta: 3.000 ° - Theta: 1.500 ° - Chi: 0.00 ° - Phi: 0
Operations: Y Scale Add 1771 | Import

TB-1: HPMC=0%; PVP=0%

TB-2

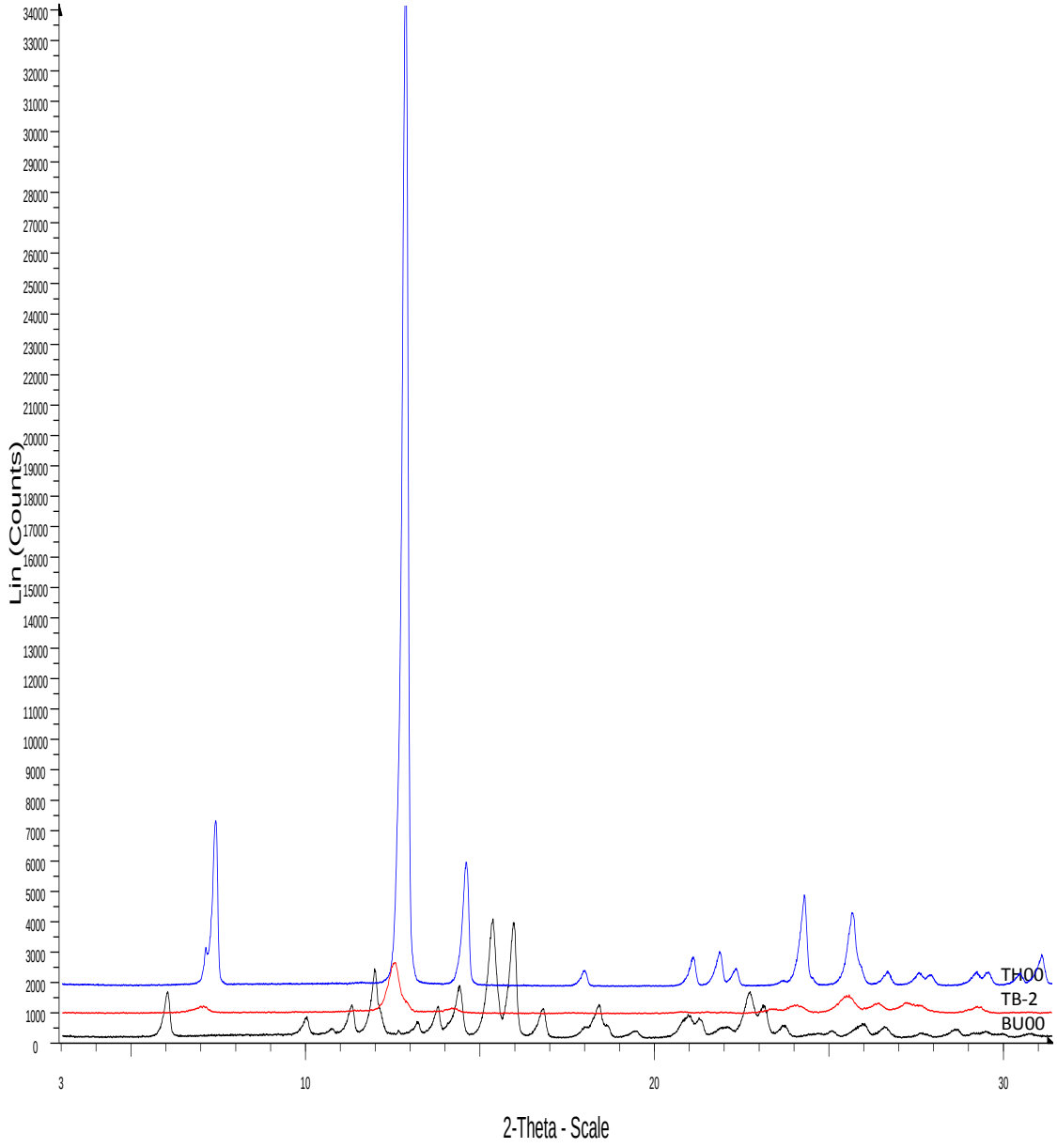

TB-2: HPMC=0%; PVP=0.05%

TB-3

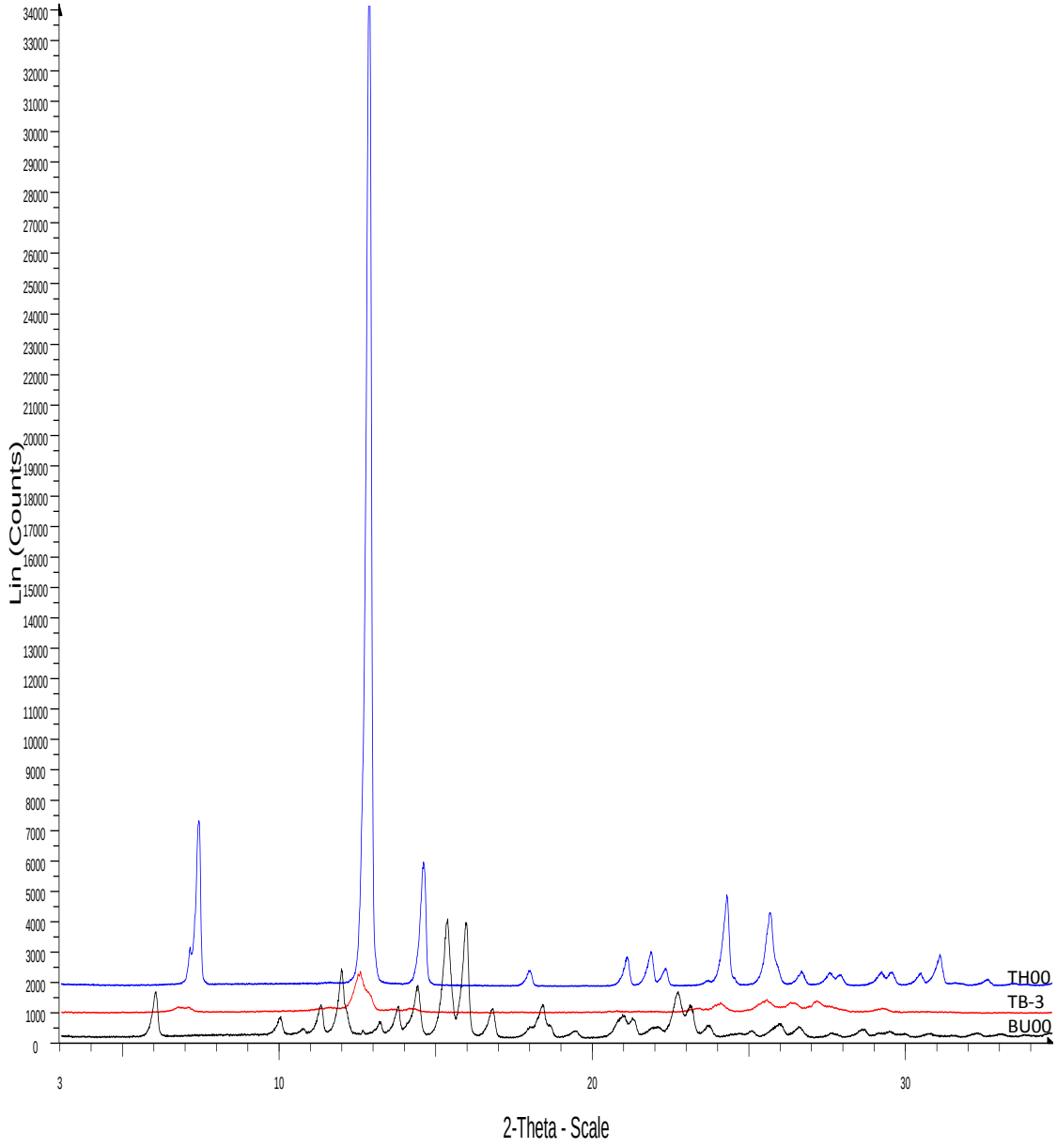

TB-3: HPMC=0%; PVP=0.1%

TB-4

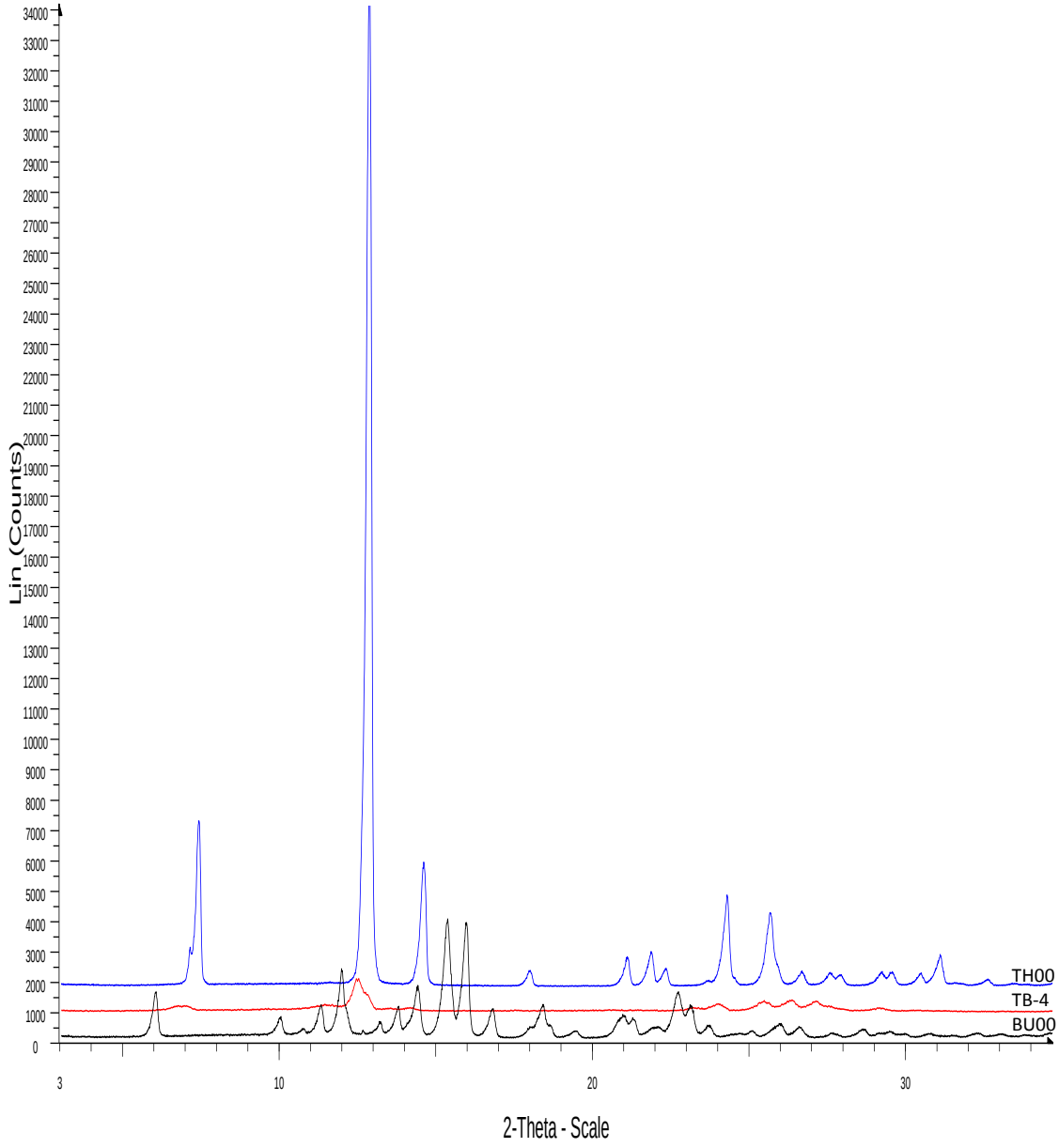

TB-4: HPMC=0.25%; PVP=0%

TB-5

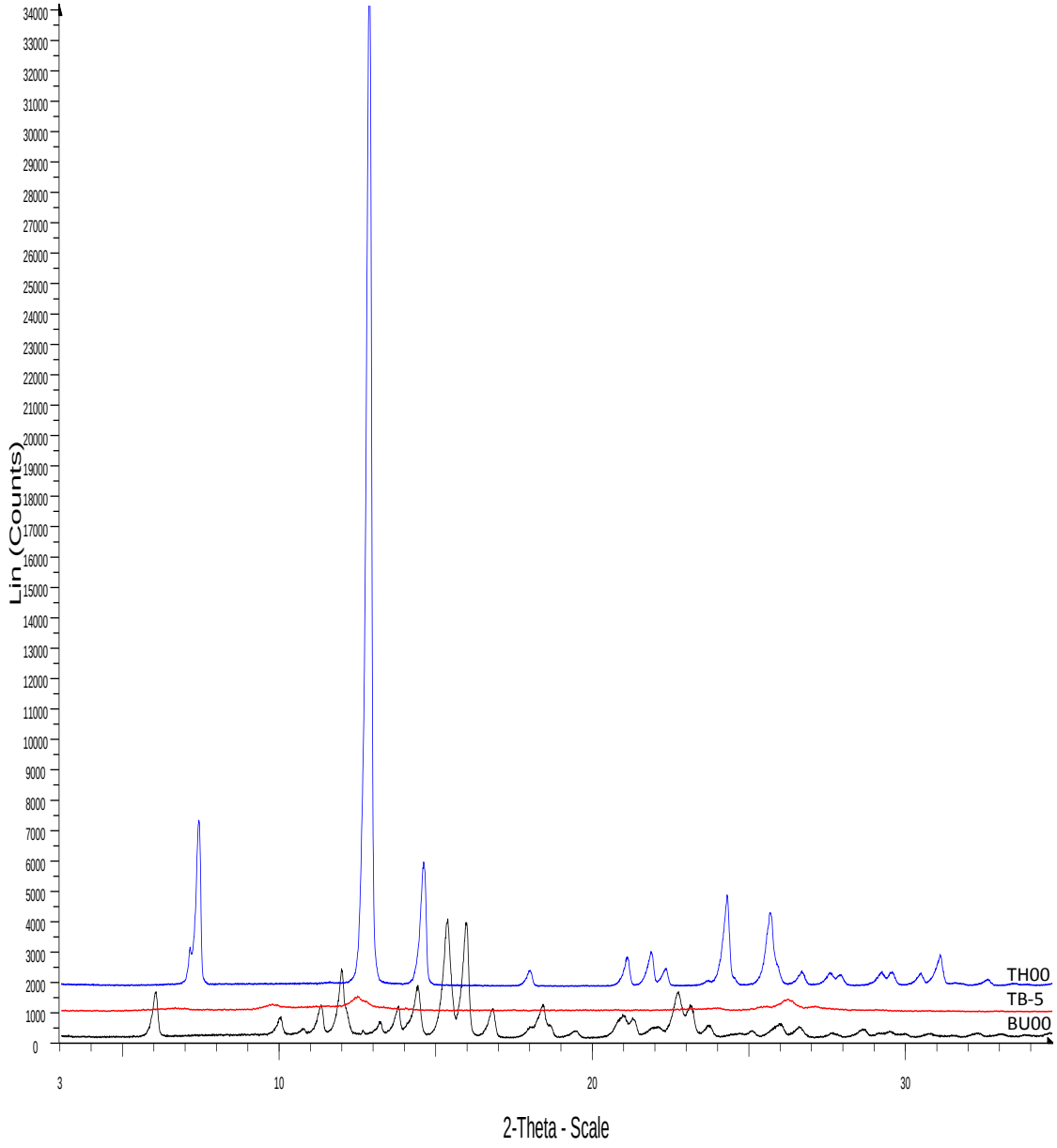

TB-5: HPMC=0.25%; PVP=0.05%

TB-6

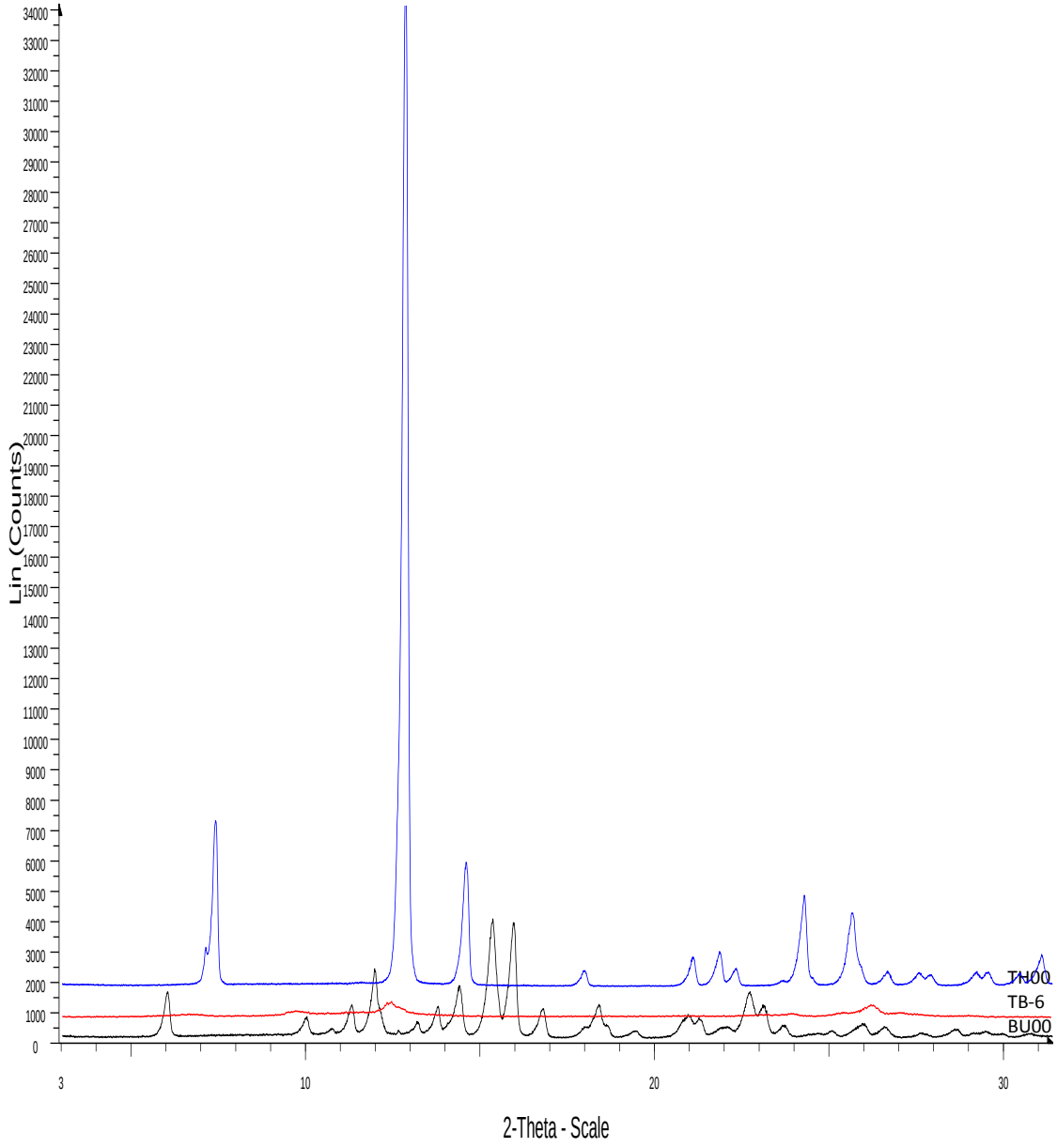

TB-6: HPMC=0.25%; PVP=0.1%

TB-7

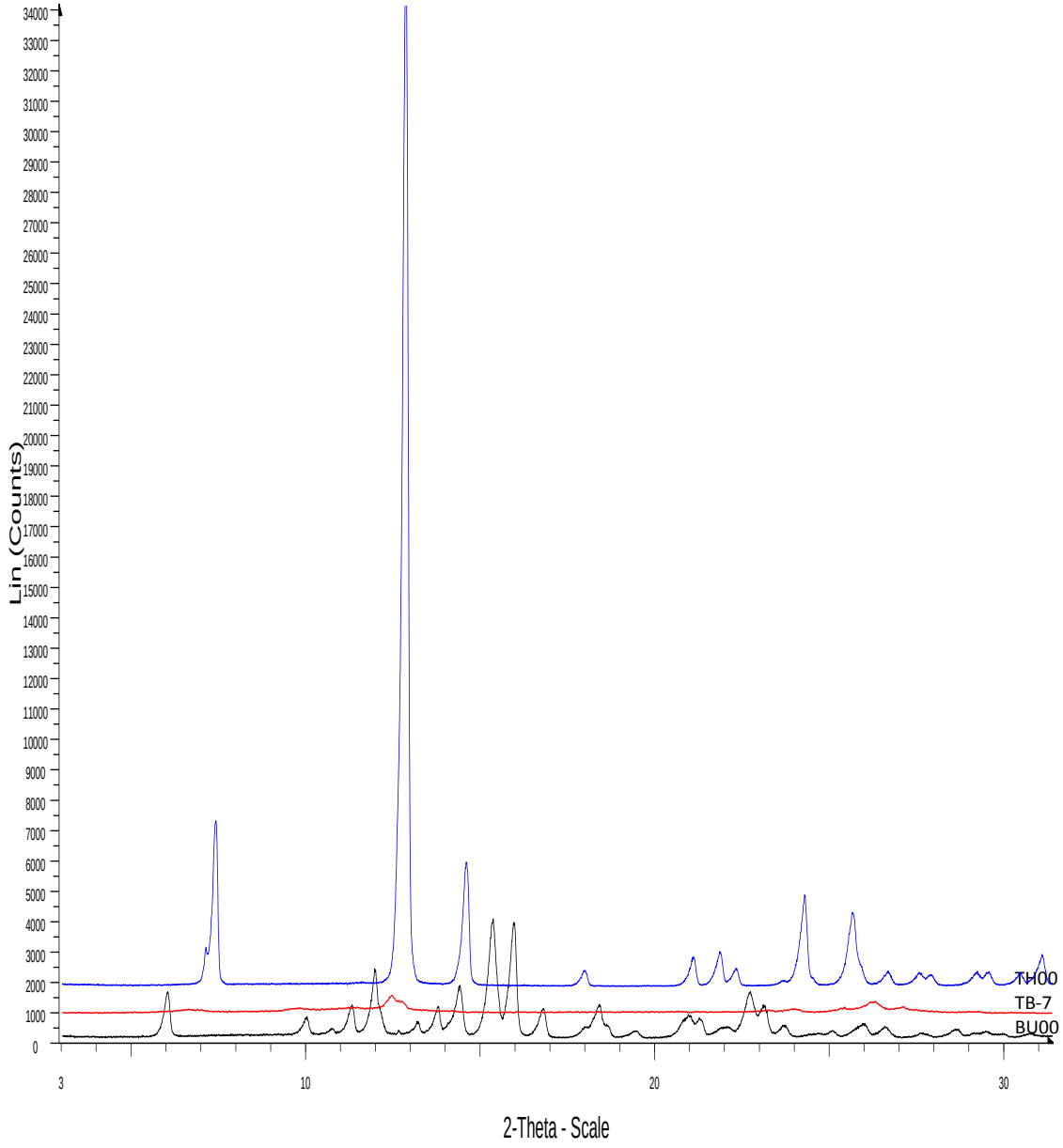

TB-7: HPMC=0.5%; PVP=0%

TB-8

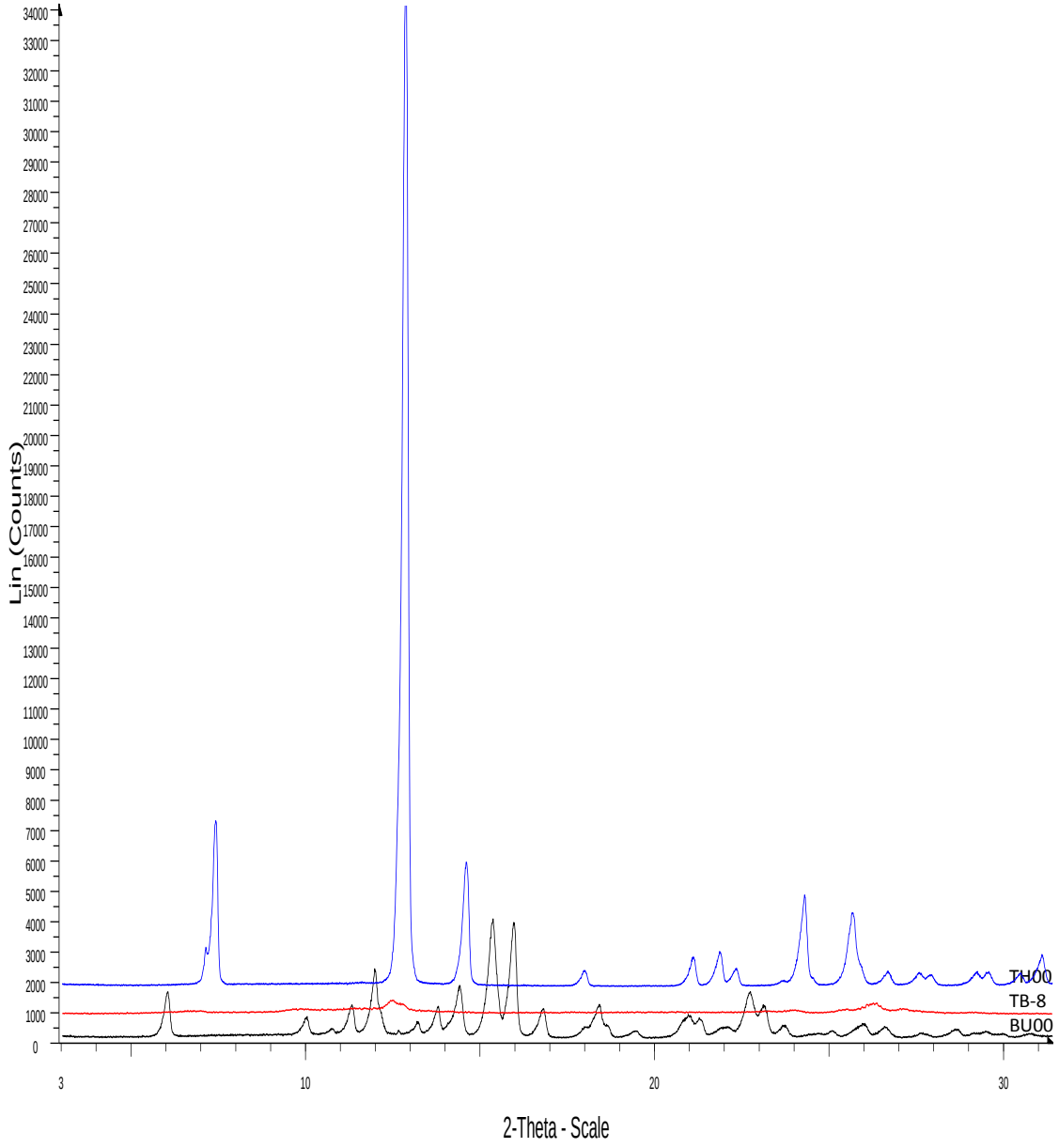

TB-8: HPMC=0.5%; PVP=0.05%

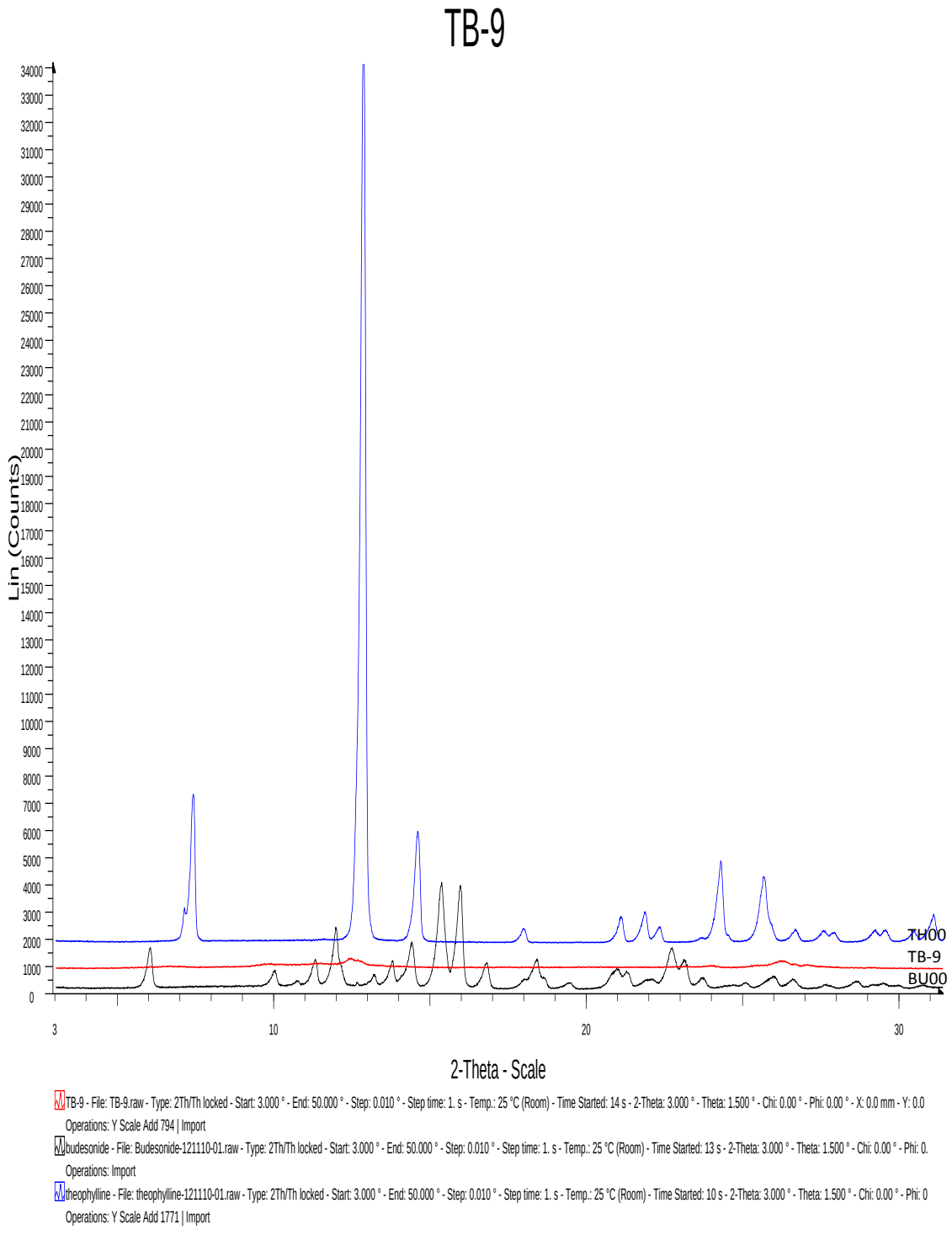

TB-9: HPMC=0.5%; PVP=0.1%

Figure A4 spray dried samples in Chapter 4

Table A1 observed result of spray drying. IT: inlet temperature, FR: feed rate, A: atomization, AS: air flow rate, size: particle size, Ratio: ratio between theophylline and budesonide in particles.

HMPC	PVP	IT	FR	A	AS	Size(μm)	stv	ratio	stv
-1	-1	-1	-1	-1	-1	19.11	±2.72	14.2	±3.67
-1	-1	-1	-1	-1	1	11.56	±1.23	14.89	±4.21
-1	-1	-1	-1	1	-1	11.01	±3.10	14.72	±1.43
-1	-1	-1	-1	1	1	8.19	±2.80	14.9	±3.33
-1	-1	-1	1	-1	-1	16.24	±1.32	16.32	±1.24
-1	-1	-1	1	-1	1	10.98	±2.46	14.24	±4.20
-1	-1	-1	1	1	-1	13.12	±4.23	15.98	±2.42
-1	-1	-1	1	1	1	11.52	±2.43	13.89	±0.98
-1	-1	1	-1	-1	-1	14.52	±3.12	14.02	±6.21
-1	-1	1	-1	-1	1	10.32	±0.52	14.98	±1.75
-1	-1	1	-1	1	-1	10.58	±1.89	15.92	±3.11
-1	-1	1	-1	1	1	11.8	±3.63	14.21	±1.92
-1	-1	1	1	-1	-1	11.22	±1.83	15.26	±3.10
-1	-1	1	1	-1	1	9.72	±2.51	14.52	±4.21
-1	-1	1	1	1	-1	11.63	±2.72	15.21	±3.71
-1	-1	1	1	1	1	12.2	±1.52	14.74	±2.03
-1	1	-1	-1	-1	-1	15.54	±3.61	16.14	±3.16
-1	1	-1	-1	-1	1	11.54	±1.53	15.92	±4.2
-1	1	-1	-1	1	-1	11.99	±1.36	14.78	±3.89
-1	1	-1	-1	1	1	15.62	±2.36	16.94	±2.32
-1	1	-1	1	-1	-1	15.9	±2.74	17.23	±3.77
-1	1	-1	1	-1	1	8.09	±1.47	16.32	±5.21
-1	1	-1	1	1	-1	10.2	±4.12	19.23	±2.22
-1	1	-1	1	1	1	11.9	±2.83	16.92	±1.62
-1	1	1	-1	-1	-1	13.23	±3.21	16.34	±4.67
-1	1	1	-1	-1	1	15.8	±1.55	15.78	±0.87
-1	1	1	-1	1	-1	13.92	±0.92	16.77	±3.60
-1	1	1	-1	1	1	14.03	±3.18	18.9	±1.63
-1	1	1	1	-1	-1	13.27	±1.06	16.91	±5.82
-1	1	1	1	-1	1	10.13	±2.77	15.89	±2.17
-1	1	1	1	1	-1	13.48	±3.12	16.92	±4.09
-1	1	1	1	1	1	13.8	±4.00	14.92	±2.72
1	-1	-1	-1	-1	-1	10.78	±5.22	18.29	±4.21
1	-1	-1	-1	-1	1	10.04	±3.99	16.98	±3.82
1	-1	-1	-1	1	-1	7.23	±3.16	18.55	±3.01
1	-1	-1	-1	1	1	8.99	±0.33	19.4	±1.61
1	-1	-1	1	-1	-1	10.1	±3.41	17.09	±3.11
1	-1	-1	1	-1	1	6.89	±2.98	18.67	±4.02
1	-1	-1	1	1	-1	8.03	±1.63	21.09	±2.98
1	-1	-1	1	1	1	7.53	±2.11	19.65	±0.97

1	-1	1	-1	-1	-1	11.03	±1.42	20.94	±2.13
1	-1	1	-1	-1	1	10.78	±3.16	17.98	±1.36
1	-1	1	-1	1	-1	10.55	±1.32	19.87	±3.26
1	-1	1	-1	1	1	9.03	±2.15	18.99	±2.86
1	-1	1	1	-1	-1	10.11	±5.21	17.53	±1.54
1	-1	1	1	-1	1	10.93	±2.74	18.32	±3.22
1	-1	1	1	1	-1	7.49	±1.59	20.51	±3.90
1	-1	1	1	1	1	7.99	±2.61	18.42	±2.92
1	1	-1	-1	-1	-1	9.78	±4.21	21.04	±1.09
1	1	-1	-1	-1	1	7.88	±2.3	19.63	±2.11
1	1	-1	-1	1	-1	8.06	±1.90	23.58	±1.89
1	1	-1	-1	1	1	5.76	±0.63	20.1	±2.16
1	1	-1	1	-1	-1	8.13	±3.26	18.99	±1.14
1	1	-1	1	-1	1	6.29	±2.11	18.26	±2.31
1	1	-1	1	1	-1	6.06	±1.52	18.09	±1.09
1	1	-1	1	1	1	6.9	±3.56	20.85	±3.26
1	1	1	-1	-1	-1	9.05	±2.75	19.52	±1.08
1	1	1	-1	-1	1	10.07	±3.17	20.96	±2.51
1	1	1	-1	1	-1	8.42	±4.02	18.93	±1.44
1	1	1	-1	1	1	7.9	±2.63	19.03	±1.96
1	1	1	1	-1	-1	10.63	±1.99	19.95	±3.41
1	1	1	1	-1	1	6.68	±3.86	19.03	±2.91
1	1	1	1	1	-1	7.11	±3.32	18.99	±2.90
1	1	1	1	1	1	6.97	±2.29	19.54	±3.01

Table A2 Regression (dependent: size)

Model		Unstandardized Coefficients		Standardized Coefficients	t	Sig.	95.0% Confidence Interval for B	
		B	Std. Error	Beta			Lower Bound	Upper Bound
1	(Constant)	10.552	.235		44.984	.000	10.083	11.022
	HPMC	-2.015	.235	-.702	-8.590	.000	-2.485	-1.545
	PVP	-.111	.235	-.039	-.472	.639	-.581	.359
	IT	.210	.235	.073	.895	.375	-.260	.680
	FR	-.514	.235	-.179	-2.189	.033	-.983	-.044
	A	-.583	.235	-.203	-2.486	.016	-1.053	-.114
	AS	-.620	.235	-.216	-2.644	.011	-1.090	-.150

a. Dependent Variable: size

Table A3 regression (dependent: ratio TH/BU)

Model		Unstandardized Coefficients		Standardized Coefficients	t	Sig.	95.0% Confidence Interval for B	
		B	Std. Error	Beta			Lower Bound	Upper Bound
1	(Constant)	17.542	.142		123.222	.000	17.257	17.827
	HPMC	1.795	.142	.806	12.607	.000	1.510	2.080
	PVP	.658	.142	.296	4.623	.000	.373	.943
	IT	-.048	.142	-.022	-.338	.737	-.333	.237
	FR	-.058	.142	-.026	-.408	.685	-.343	.227
	A	.288	.142	.129	2.020	.048	.002	.573
	AS	-.237	.142	-.106	-1.662	.102	-.522	.049

a. Dependent Variable: ratio

Table A4 ANOVA analysis (dependent size)

Tests of Between-Subjects Effects

Dependent Variable:size

Source	Type III Sum of Squares	df	Mean Square	F	Sig.
Corrected Model	527.151[a]	62	8.502	23.717	.162
Intercept	7126.525	1	7126.525	19878.645	.005
HPMC	259.895	1	259.895	724.947	.024
PVP	.785	1	.785	2.191	.378
IT	2.818	1	2.818	7.861	.218
FR	16.882	1	16.882	47.090	.092
AS	24.614	1	24.614	68.658	.076
A	21.774	1	21.774	60.736	.081
AS * A	27.812	1	27.812	77.580	.072
FR * A	5.388	1	5.388	15.030	.161
HPMC * A	2.628	1	2.628	7.332	.225
IT * A	4.075	1	4.075	11.368	.184
PVP * A	4.813	1	4.813	13.424	.170
FR * AS	1.185	1	1.185	3.306	.320
HPMC * AS	3.915	1	3.915	10.922	.187
IT * AS	8.636	1	8.636	24.090	.128
PVP * AS	1.229	1	1.229	3.429	.315
HPMC * FR	.072	1	.072	.201	.731
IT * FR	.095	1	.095	.266	.697
PVP * FR	2.735	1	2.735	7.629	.221
HPMC * IT	5.730	1	5.730	15.983	.156
HPMC * PVP	20.851	1	20.851	58.161	.083
PVP * IT	4.136	1	4.136	11.537	.182
FR * AS * A	2.628	1	2.628	7.332	.225
HPMC * AS * A	10.441	1	10.441	29.124	.117
IT * AS * A	8.888	1	8.888	24.792	.126
PVP * AS * A	.159	1	.159	.444	.626
HPMC * FR * A	3.511	1	3.511	9.793	.197
IT * FR * A	.468	1	.468	1.304	.458
PVP * FR * A	1.437	1	1.437	4.008	.295

HPMC * IT * A	6.976	1	6.976	19.459	.142
HPMC * PVP * A	2.469	1	2.469	6.887	.232
PVP * IT * A	1.349	1	1.349	3.761	.303
HPMC * FR * AS	.110	1	.110	.306	.678
IT * FR * AS	.022	1	.022	.062	.845
PVP * FR * AS	4.280	1	4.280	11.938	.179
HPMC * IT * AS	3.906	1	3.906	10.894	.187
HPMC * PVP * AS	6.357	1	6.357	17.731	.148
PVP * IT * AS	.905	1	.905	2.524	.358
HPMC * IT * FR	.051	1	.051	.143	.770
HPMC * PVP * FR	3.827	1	3.827	10.675	.189
PVP * IT * FR	.803	1	.803	2.241	.375
HPMC * PVP * IT	4.500	1	4.500	12.551	.175
HPMC * FR * AS * A	.603	1	.603	1.681	.418
IT * FR * AS * A	.356	1	.356	.992	.501
PVP * FR * AS * A	5.935	1	5.935	16.556	.153
HPMC * IT * AS * A	1.635	1	1.635	4.561	.279
HPMC * PVP * AS * A	.028	1	.028	.077	.828
PVP * IT * AS * A	1.116	1	1.116	3.112	.328
HPMC * IT * FR * A	2.702	1	2.702	7.537	.222
HPMC * PVP * FR * A	2.980	1	2.980	8.312	.213
PVP * IT * FR * A	3.335	1	3.335	9.303	.202
HPMC * PVP * IT * A	2.013	1	2.013	5.615	.254
HPMC * IT * FR * AS	.024	1	.024	.068	.837
HPMC * PVP * FR * AS	4.542	1	4.542	12.670	.174
PVP * IT * FR * AS	3.023	1	3.023	8.433	.211
HPMC * PVP * IT * AS	.630	1	.630	1.757	.411
HPMC * PVP * IT * FR	.622	1	.622	1.735	.413
HPMC * IT * FR * AS * A	.024	1	.024	.068	.837
HPMC * PVP * FR * AS * A	.383	1	.383	1.068	.490
PVP * IT * FR * AS * A	.963	1	.963	2.686	.349
HPMC * PVP * IT * AS * A	7.583	1	7.583	21.152	.136
HPMC * PVP * IT * FR * A	.817	1	.817	2.278	.373
HPMC * PVP * IT * FR * AS	4.682	1	4.682	13.059	.172

Error	.359	1	.359		
Total	7654.035	64			
Corrected Total	527.510	63			

a. R Squared = .999 (Adjusted R Squared = .957)

Table A5 ANOVA analysis (dependent ration between theophylline and budesonide in particles)

Tests of Between-Subjects Effects

Dependent Variable:ratio

Source	Type III Sum of Squares	df	Mean Square	F	Sig.
Corrected Model	317.019[a]	62	5.113	798.940	.028
Intercept	19693.912	1	19693.912	3077173.785	.000
HPMC	206.138	1	206.138	32209.032	.004
PVP	27.720	1	27.720	4331.285	.010
IT	.148	1	.148	23.160	.130
FR	.216	1	.216	33.785	.108
AS	3.582	1	3.582	559.618	.057
A	5.290	1	5.290	826.562	.062
AS * A	.002	1	.002	.282	.189
FR * A	.093	1	.093	14.535	.163
HPMC * A	.644	1	.644	100.626	.363
IT * A	1.729	1	1.729	270.191	.239
PVP * A	.429	1	.429	67.035	.097
FR * AS	.788	1	.788	123.071	.157
HPMC * AS	.011	1	.011	1.723	.114
IT * AS	.002	1	.002	.353	.259
PVP * AS	.620	1	.620	96.899	.164
HPMC * FR	3.019	1	3.019	471.704	.129
IT * FR	1.334	1	1.334	208.441	.344
PVP * FR	1.243	1	1.243	194.254	.246
HPMC * IT	.003	1	.003	.431	.630
HPMC * PVP	2.933	1	2.933	458.228	.030
PVP * IT	1.051	1	1.051	164.160	.450
FR * AS * A	.522	1	.522	81.563	.170
HPMC * AS * A	.000	1	.000	.035	.082
IT * AS * A	.089	1	.089	13.829	.167
PVP * AS * A	1.216	1	1.216	189.923	.146
HPMC * FR * A	1.544	1	1.544	241.220	.341
IT * FR * A	.137	1	.137	21.391	.136
PVP * FR * A	.260	1	.260	40.641	.399

HPMC * IT * A	3.106	1	3.106	485.376	.229
HPMC * PVP * A	2.504	1	2.504	391.298	.132
PVP * IT * A	.270	1	.270	42.250	.197
HPMC * FR * AS	8.556	1	8.556	1336.816	.117
IT * FR * AS	.047	1	.047	7.392	.224
PVP * FR * AS	.089	1	.089	13.829	.167
HPMC * IT * AS	.060	1	.060	9.379	.201
HPMC * PVP * AS	.024	1	.024	3.754	.303
PVP * IT * AS	.842	1	.842	131.532	.055
HPMC * IT * FR	1.939	1	1.939	302.978	.137
HPMC * PVP * FR	1.507	1	1.507	235.431	.441
PVP * IT * FR	.483	1	.483	75.473	.473
HPMC * PVP * IT	.693	1	.693	108.290	.061
HPMC * FR * AS * A	.078	1	.078	12.250	.177
IT * FR * AS * A	6.250E-6	1	6.250E-6	.001	.280
PVP * FR * AS * A	.907	1	.907	141.759	.153
HPMC * IT * AS * A	.000	1	.000	.016	.921
HPMC * PVP * AS * A	.090	1	.090	14.063	.166
PVP * IT * AS * A	.025	1	.025	3.876	.299
HPMC * IT * FR * A	2.038	1	2.038	318.399	.336
HPMC * PVP * FR * A	.439	1	.439	68.579	.277
PVP * IT * FR * A	.416	1	.416	65.004	.679
HPMC * PVP * IT * A	.056	1	.056	8.813	.207
HPMC * IT * FR * AS	2.265	1	2.265	353.910	.134
HPMC * PVP * FR * AS	.585	1	.585	91.441	.566
PVP * IT * FR * AS	3.413	1	3.413	533.321	.128
HPMC * PVP * IT * AS	1.677	1	1.677	262.035	.439
HPMC * PVP * IT * FR	7.196	1	7.196	1124.345	.119
HPMC * IT * FR * AS * A	.403	1	.403	63.004	.480
HPMC * PVP * FR * AS * A	13.506	1	13.506	2110.254	.114
PVP * IT * FR * AS * A	.439	1	.439	68.579	.477
HPMC * PVP * IT * AS * A	.245	1	.245	38.285	.102
HPMC * PVP * IT * FR * A	1.645	1	1.645	257.001	.140
HPMC * PVP * IT * FR * AS	.714	1	.714	111.566	.460

Error	.006	1	.006		
Total	20010.938	64			
Corrected Total	317.026	63			

a. R Squared = 1.000 (Adjusted R Squared = .999)